Working Examples In Geometric Optimal Control

Bernard Bonnard, Monique Chyba, Jérémy Rouot

Bernard Bonnard, Monique Chyba, Jérémy Rouot

Working Examples In Geometric Optimal Control

PRELIMINARY VERSION

November 10, 2015

Springer

Preface

This series of notes have their origin into accelerated course in optimal control given to multidisciplinary Phd students in Mathematics, Physics or Control Engineering and the purpose is to present the seminal results of this theory in view of applications to concrete problems. For that we choose to make the presentation using two real life applications which are the core of current research projects on the academic side and motivated by industrial applications. The purpose is to make the potential reader familiar with the techniques of optimal control whose peculiarity is to combine a large amount of methods which are not so familiar to recent applied mathematicians but were somehow in the culture of the ancient school of mathematicians with no separation between pure and applied mathematics who contribute to both sides, an example being H. Poincaré.

Following this tradition this was at the origin of the development in the seventies of geometric optimal control which under the impulses of R. Brockett, H. Sussmann and I. Kupka in particular, proving the interest to reintroduce modern geometry and recent singularity theory in this area in the spirit of contributors to dynamical systems like S. Lefschetz, V. Arnold. Also optimal control was at the origin developed by L. Pontryagin in view of engineering applications in space mechanics which is the originality of the birth of this discipline.

One further step being to use the progress in numerics and the applications towards recent developments in physics and chemistry like for instance molecular dynamics. Overall our desire is to use a wide range of techniques rather to concentrate on some tiny understanding of mathematics.

To succeed in our presentation we have chosen to restrict to seminal techniques and results, rather to fall in a debauchee of results. Also the different methodologies will be explained and developed in view of the motivating examples. For that we will concentrate our presentation to two recent and promising applications which let the road open to further researches and developments of our potential readers. Also such choices being motivated by a neat mathematical model suitable to the geometric analysis but also reasonable practical implementations.

The first example concerns the *swimming problem at low Reynolds number* which described accuratly the swimming methods of microorganisms like zooplanktons,

and can be easily observed in the nature but also reproduced using swimming of micro robots and with obvious medical applications. This case will serve as an introduction to geometric optimal control in view of applications to *sub-Riemannian geometry*, a non trivial extension of Riemannian geometry and a tribute in the eighties of control theory to geometry under the impulse of R. Brockett.

For this problem only the *weak maximum principle* is necessary hence it will be presented first the advantage being that the proof is simple but contains all the geometric ingredients of the general maximum principle (see the historical paper by R.V. Gamkrelidze about the discovery of the maximum principle [31]). Also in this case, using smoothness the second order conditions related to the concept of conjugate points and Jacobi equation can be easily explained and numerically implemented.

Using the SR-framework in optimal control the problem is written:

$$\frac{dx}{dt}(t) = \sum_{i=1,\ldots,m} u_i(t) F_i(x(t)), Min \rightarrow \int_0^T \sum_{i=1,\ldots,m} u_i^2(t) dt,$$

where $q \in M$(smooth manifold) and the $SR-$ metric is defined by the orthonormal sub-frame $\{F_1,\ldots,F_m\}$determining the so-called non-holonomic contraints on the set of curves: $q(t) \in D(q(t))$ where D is the distribution $Span\{F_1,\ldots,F_m\}$.

The relation with the swimming problem modeled by some of our earliest prominent mathematicians (e.g. Newton, Euler) and more recently (Stokes, Reynolds, Purcell) is straightforward in the framework of control. The state variable x of the system decomposes into (x_1,x_2) where x_1 represents the displacement of the swimmer and x_2 is the shape variable representing the periodic shape deformation of the swimmer body (called stroke) necessary to produce for a given stroke a net displacement. The law of swimming at low Reynolds number related the speed of the displacement of x_1 to the speed of the shape deformation x_2 thus defining the SR-constraints while the mechanical expended energy defined the metric (see for the details the encyclopaedic book Low Reynolds number hydrodynamics by J. Happel and Brenner for a general reference and the excellent survey article The hydrodynamics of swimming microorganisms by E. Lauga and T.R. Powers for the applications to swimming of microorganisms [36], [48]). Also this lead to experimental experiments (see for instance: Experimental Demonstration of the Dynamics and Stability of a Low Reynolds Number Swimmer Near a Plane Wall by S. Zhang, Y. Or, and R.M. Murray [56]).

Our objective is to provide a self-contained presentation of the model, the underlying concepts of SR-geometry and techniques needed to make the mathematical analysis. The application of the optimization techniques to the problem is only very recent and only preliminary results were obtained.

We discuss two specific examples. First of all we consider the *Purcell swimmer*, a three links model where the shape variables are the two extremities links and the the displacement is modeled by both the position and the orientation of the central link representing the body of the swimmer. To make a more complete analysis in the framework of geometric control we use a simplified model due to D. Takagi

called the *copepod swimmer* where only line displacement are considered using symmetric shape links and which is also the model of swimming of a abundant variety of zooplanktons (copepods).

The second example concerns optimal control of systems in *Nuclear Magnetic Resonance* (NMR) and *Magnetic resonance Imaging* (MRI). The dynamics is modeled using the *Bloch equation* (1946) describing at the macroscopic scale the evolution of the magnetization vector of a spin 1/2 particle depending on two relaxation parameters T_1 and T_2 which are the chemical signatures of the chemical species (e.g; water, fat) and controlled by a Rf-magnetic pulse perpendicular to the strong polarizing field apply in the $z-$ axis direction (see Bloch Equations [10]). Optimal control was introduced very recently in the dynamics of such systems at the experimental level and in vitro situations and the objective is to replace the heuristic pulses used in the medical applications in real life in vivo MRI. This means to replace in a near future the standard industrial softwares by a new generation of softwares producing a double gain: better image in shorter time.

In our opinion this framework is a one of the most challenging application of optimal control because the Bloch equations are describing with great accuracy the evolution of the dynamics of the process and the computed control laws can be implemented quite easily . Geometric control has to be developed to handle the mathematical problems and in parallel a new generation of specific softwares dedicated to optimal control (`HamPath`, `Bocop`, `GloptiPoly`) have to be used.

Having this optic in mind we shall introduce the reader to two important problems in NMR and MRI.

The first one is simply to *saturate in minimum time* the magnetization vector, that is to drive its amplitude to zero. For this problem one must first introduce the most general maximum principle, since the applied Rf-magnetic field is of bounded amplitude. The second step is to compute with geometric techniques the structure of the optimal law as a closed loop function, this corresponds to the concept of optimal synthesis.

The second problem is the *contrast problem in MRI* where we must distinguish in the image two possible species distributed in the image, e.g. healthy and cancer cells and characterized thanks to Bloch equation by different responses to the same Rf-field, due to different relaxation parameters. The actual technology in MRI replaces this observation problem of the parameters by and optimal control problem of the Mayer form:

$$\frac{\mathrm{d}x}{\mathrm{d}t} = f(x,u), |\, u \,| \leq M, \ \mathrm{Min} \rightarrow c(x(t_f)),$$

where t_f is a fixed transfer time related directly to the image processing time and the cost function modeled the contrast, while the dynamics is the coupling of the two Bloch equations controlled by the same Rf-field and with respective parameters associated to the two species to be distinguished and which can be easily computed in a simple experiment.

Also for the purpose of numerical computations using for instance the Hampath code the Mayer problem has to be regularized into a Bolza problem:

$$\text{Min} \rightarrow c(x(t_f)) + \int_0^{t_f} f_0(u)dt,$$

where the applied control is penalized in a suitable way.

Again the necessary conditions are deduced from the general maximum principle and furthermore really understood using the geometric framework of the maximum principle. The second step is to use geometric optimal control to analyze the contrast problem in MRI in relation with Lie brackets computations which is the essence of geometric control. The final step being to solve numerically the problem based on the geometric computations.

Dijon, August 2015 *Bernard Bonnard and Jérémy Rouot*
Hawaii *Monique Chyba*

Acknowledgements

- M. Chyba is partially supported by the National Science Foundation (NSF) Division of Mathematical Sciences, award #1109937, J. Rouot is supported by the French Space Agency CNES, R&T action R-S13/BS-005-012 and by the région Provence-Alpes-Côte d'Azur, B. Bonnard is partially supported by the ANR Project - DFG Explosys (Grant No. ANR-14-CE35-0013-01;GL203/9-1).
- The authors are indebted to Alain Jacquemard and Zou Rong.

Contents

Chapter 1
Historical part - Calculus of variations

The calculus of variations is an old mathematical discipline. Historically its foundation is the brachistochrone curve problem raised by Johann Bernoulli (1696) and we briefly introduce the reader to the main results. The first one is the fundamental formula in the classical of the classical calculus of variations and we follow the presentation by Gelfand Fomin, Calculus of variations. The originality is to have a general formula rather to start with the standard Euler-Lagrange formula derivation and to deal with general variations. From this we can derive has an exercise the standard first order necessary conditions : Euler-Lagrange equation, tranversality conditions, Erdmann-Weierstrass conditions for a broken extremal and the Hamilton Jacobi equation. The second point is to derive the second order necessary conditions in relation with the concept of conjugate point and Jacobi equation. The main concept is to introduce the so-called accessory problem replacing the positivity test of the second order derivative by a minimization problem of the associated quadratic form. The modern interpretation in terms of the spectral theory of the associated self-adjoint operator (Morse theory) is finally stated.

1.1 Statement of the Problem in the Holonomic Case

We consider the set $\mathscr{C}$ of all curves $x : [t_0, t_1] \to \mathbb{R}^n$ of class C^2, the initial and final times t_0, t_1 being not fixed and the problem of minimizing a functional on $\mathscr{C}$:

$$C(x) = \int_{t_0}^{t_1} L(t, x(t), \dot{x}(t))dt$$

where L is C^2. Moreover, we can impose extremities conditions: $x(t_0) \in M_0, x(t_1) \in M_1$ where M_0, M_1 are C^1-submanifolds of $\mathbb{R}^n$. The distance between the curves $x(t), x^*(t)$ is

$$\rho(x, x^*) = \max_t \|x(t) - x^*(t)\| + \max_t \|\dot{x}(t) - \dot{x}^*(t)\| + d(P_0, P_0^*) + d(P_1, P_1^*)$$

where $P_0 = (t_0, x_0)$ and $P_1 = (t_1, x_1)$ and $\|\cdot\|$ is any norm on $\mathbb{R}^n$ and d is the usual distance mapping on $\mathbb{R}^{n+1}$. Note that a curve is interpreted in the time extended space (t,x). The two curves $x(\cdot), x^*(\cdot)$ being not defined on the same interval they are by convention C^2-extended on the union of both intervals.

Proposition 1 ***(Fundamental formula of the classical calculus of variations)*** *We adopt the standard notation of classical calculus of variations, see [32]. Let $\gamma(\cdot)$ be a reference curve with extremities $(t_0,x_0),(t_1,x_1)$ and let $\underline{\gamma}(\cdot)$ be any curve with extremities $(t_0+\delta t_0, x_0+\delta x_0),(t_1+\delta t_1, x_1+\delta x_1)$. We denote by $h(\cdot)$ the variation: $h(t) = \underline{\gamma}(t) - \gamma(t)$. Then, if we set $\Delta C = C(\underline{\gamma}) - C(\gamma)$, we have*

$$\Delta C = \int_{t_0}^{t_1} \left(\frac{\partial L}{\partial x} - \frac{d}{dt}\frac{\partial L}{\partial \dot{x}} \right)_{|\gamma} .h(t)dt + \left[\frac{\partial L}{\partial \dot{x}_{|\gamma}} .\delta x \right]_{t_0}^{t_1} + \left[(L - \frac{\partial L}{\partial \dot{x}} .\dot{x})_{|\gamma} \delta t \right]_{t_0}^{t_1} + o(\rho(\underline{\gamma}, \gamma)) \tag{1.1}$$

where . denotes the scalar product in $\mathbb{R}^n$.

Proof. We write

$$\begin{aligned}
\Delta C &= \int_{t_0+\delta t_0}^{t_1+\delta t_1} L(t, \gamma(t)+h(t), \dot{\gamma}(t)+\dot{h}(t))dt - \int_{t_0}^{t_1} L(t,\gamma(t),\dot{\gamma}(t))dt \\
&= \int_{t_0}^{t_1} L(t, \gamma(t)+h(t), \dot{\gamma}(t)+\dot{h}(t))dt - \int_{t_0}^{t_1} L(t,\gamma(t),\dot{\gamma}(t))dt \\
&+ \int_{t_1}^{t_1+\delta t_1} L(t, \gamma(t)+h(t), \dot{\gamma}(t)+\dot{h}(t))dt - \int_{t_0}^{t_0+\delta t_0} L(t, \gamma(t)+h(t), \dot{\gamma}(t)+\dot{h}(t))dt
\end{aligned}$$

We develop this expression using the Taylor expansions keeping only the linear terms in $h, \dot{h}, \delta x, \delta t$. We get

$$\Delta C = \int_{t_0}^{t_1} \left(\frac{\partial L}{\partial x_{|\gamma}} .h(t) + \frac{\partial L}{\partial \dot{x}_{|\gamma}} .\dot{h}(t) \right) + [L(t,\gamma,\dot{\gamma})\delta t]_{t_0}^{t_1} + o(h,\dot{h},\delta t).$$

The derivative of the variation $\dot{h}$ is depending on h, integrating by parts we obtain

$$\Delta C \sim \int_{t_0}^{t_1} \left(\frac{\partial L}{\partial x} - \frac{d}{dt}\frac{\partial L}{\partial \dot{x}} \right)_{|\gamma} .h(t)dt + \left[\frac{\partial L}{\partial \dot{x}_{|\gamma}} .h(t) \right]_{t_0}^{t_1} + \left[L_{|\gamma} \delta t \right]_{t_0}^{t_1}$$

We observe that $h, \delta x, \delta t$ are not independent at the extremities and we have for $t = t_0$ or $t = t_1$ the relation

$$h(t+\delta t) \sim h(t) \sim \delta x - \dot{x}\delta t$$

Hence, we obtain the following approximation:

$$\Delta C \sim \int_{t_0}^{t_1} \left(\frac{\partial L}{\partial x} - \frac{d}{dt}\frac{\partial L}{\partial \dot{x}} \right)_{|\gamma} .h(t)dt + \left[\frac{\partial L}{\partial \dot{x}_{|\gamma}} .\delta x \right]_{t_0}^{t_1} + \left[(L - \frac{\partial L}{\partial \dot{x}} \dot{x})_{|\gamma} \delta t \right]_{t_0}^{t_1}$$

where all the quantities are evaluated along the reference trajectory $\gamma(\cdot)$. In this formula $h, \delta x, \delta t$ can be taken independent because in the integral the values $h(t_0), h(t_1)$ do not play any special role.

From 1.1, we deduce that the standard first-order necessary conditions of the calculus of variations.

Corollary 1 *Let us consider the minimization problem where the extremities $(t_0, x_0), (t_1, x_1)$ are fixed. Then a minimizer $\gamma(\cdot)$ satisfies the Euler-Lagrange equation*

$$\frac{\partial L}{\partial x} - \frac{d}{dt}\frac{\partial L}{\partial \dot{x}_{|\gamma}} = 0 \tag{1.2}$$

Proof. Since the extremities are fixed we set in (1.1) $\delta x = 0$ and $\delta t = 0$ at $t = t_0$ and $t = t_1$. Hence

$$\Delta C = \int_{t_0}^{t_1} \left(\frac{\partial L}{\partial x} - \frac{d}{dt}\frac{\partial L}{\partial \dot{x}} \right)_{|\gamma} .h(t)dt + o(h, \dot{h})$$

for each variation $h(\cdot)$ defined on $[t_0, t_1]$ such that $h(t_0) = h(t_1) = 0$. If $\gamma(\cdot)$ is a minimizer, we must have $\Delta C \geq 0$ for each $h(\cdot)$ and clearly by linearity, we have

$$\int_{t_0}^{t_1} \left(\frac{\partial L}{\partial x} - \frac{d}{dt}\frac{\partial L}{\partial \dot{x}} \right)_{|\gamma} .h(t)dt = 0$$

for each $h(\cdot)$. Since the mapping $t \mapsto (\frac{\partial L}{\partial x} - \frac{d}{dt}\frac{\partial L}{\partial \dot{x}})_{|\gamma}$ is continuous, it must be identically zero along $\gamma(\cdot)$ and the Ealer-Lagrange equation 1.2 is satisfied.

1.2 Hamiltonian Equations

The Hamiltonian formalism, which is the natural formalism to deal with the maximum principle, appears in the classical calculus of variations via the Legendre transformation.

Definition 1 *The Legendre transformation is defined by*

$$p = \frac{\partial L}{\partial \dot{x}}(t, x, \dot{x}) \tag{1.3}$$

and if the mapping $\varphi : (x, \dot{x}) \mapsto (x, p)$ is a diffeomorphism we can introduce the Hamiltonian:

$$H : (t, x, p) \mapsto p.\dot{x} - L(t, x, p). \tag{1.4}$$

Proposition 2 *The formula (1.1) takes the form*

$$\Delta C \sim \int_{t_0}^{t_1} \left(\frac{\partial L}{\partial x} - \frac{d}{dt}\frac{\partial L}{\partial \dot{x}} \right)_{|\gamma} .h(t)dt + \Big[p\delta x - H\delta t \Big]_{t_0}^{t_1} \tag{1.5}$$

and if $\gamma(\cdot)$ is a minimizer it satisfies the Euler-Lagrange equation in the Hamiltonian form

$$\dot{x}(t) = \frac{\partial H}{\partial p}(t, x(t), p(t)), \qquad \dot{p}(t) = -\frac{\partial H}{\partial x}(t, x(t), p(t)) \tag{1.6}$$

1.3 Hamilton-Jacobi-Bellman Equation

Definition 2 *A solution of the Euler-Lagrange equation is called an extremal. Let $P_0 = (t_0, x_0)$ and $P_1 = (t_1, x_1)$. The Hamilton-Jacobi-Bellman (HJB) function is the multivalued function defined by*

$$S(P_0, P_1) = \int_{t_0}^{t_1} L(t, \gamma(t), \dot{\gamma}(t))dt$$

where $\gamma(\cdot)$ is any extremal with fixed extremities x_0, x_1. If $\gamma(\cdot)$ is a minimizer, it is called the value function.

Proposition 3 *Assume that for each P_0, P_1 there exists a unique extremal joining P_0 to P_1 and suppose that the HJB function is C^1. Let P_0 be fixed and let $\bar{S} : P \mapsto S(P_0, P)$. Then $\bar{S}$ is a solution of the Hamilton-Jacobi-Bellman equation*

$$\frac{\partial S}{\partial t}(P_0, P) + H(t, x, \frac{\partial S}{\partial x}) = 0 \tag{1.7}$$

Proof. Let $P = (t, x)$ and $P + \delta P = (t + \delta t, x + \delta x)$. Denote by $\gamma(\cdot)$ the extremal joining P_0 to $P + \delta P$. We have

$$\Delta \bar{S} = \bar{S}(t + dt, x + dx) - \bar{S}(t, x) = C(\bar{\gamma}) - C(\gamma)$$

and from (2) it follows that:

$$\Delta \bar{S} = \Delta C \sim \int_{t_0}^{t} \left(\frac{\partial L}{\partial x} - \frac{d}{dt}\frac{\partial L}{\partial \dot{x}} \right)_{|\gamma} .h(t)dt + \Big[p\delta x - H\delta t \Big]_{t_0}^{t},$$

where $h(\cdot) = \bar{\gamma}(\cdot) - \gamma(\cdot)$. Since $\gamma(\cdot)$ is a solution of the Euler-Lagrange equation, the integral is zero and

$$\Delta \bar{S} = \Delta C \sim \Big[p\delta x - H\delta t \Big]_{t_0}^{t}$$

In other words, we have

$$d\bar{S} = pdx - Hdt.$$

Identifying, we obtain

$$\frac{\partial \bar{S}}{\partial t} = -H, \qquad \frac{\partial \bar{S}}{\partial x} = p. \tag{1.8}$$

Hence we get the HJB equation. Moreover p is the gradient to the level sets $\{x \in \mathbb{R}^n; \bar{S}(t,x) = c\}$.

Another consequence of the general formula are the so-called transversality conditions and Erdmann Weierstrass (1877). They are presented in exercises.

Exercise 1.1. Consider the following problem: among all smooth curves $t \to x(t)$ whose extremity point $P_1 = (t_1, x_1)$ lies on a curve $y(t) = \Psi(t)$ find the curve for which the functional $\int_{t_0}^{t_1} L(t,x,\dot{x})dt$ has an extremum. Deduce from the general formula the transversality conditions

$$L + L_{\dot{x}}(\dot{\Psi} - \dot{x}) = 0 \text{ at } t = t_1.$$

Exercise 1.2. Let $t \to x(t)$ be a minimizing solution of $\int_{t_0}^{t_1} L(t,x,\dot{x})dt$ with fixed extremities. Assume that $t \to x(t)$ is a broken curve with a corner at $t = 0 \in]t_0, t_1[$. Prove the Erdmann Weierstrass condition

$$\begin{aligned} &L_{\dot{x}}(c-) = L_{\dot{x}}(c+), \\ &[L - L_{\dot{x}}\dot{x}](c-) = [L - L_{\dot{x}}\dot{x}](c+) \end{aligned}$$

Give an interpretation using Hamiltonian formalism.

1.4 Second Order Conditions

The Euler-Lagrange equation has been derived using the linear terms in the Taylor expansion of ΔC. Using the quadratic terms we can get necessary and sufficient second order condition. For the sake of simplicity, from now on we assume that the curves $t \mapsto x(t)$ belongs to $\mathbb{R}$, and we consider the problem with fixed extremities: $x(t_0) = x_0, x(t_1 = x_1)$. If the map L is taken C^3, the second derivative is computed as follows:

$$\begin{aligned} \Delta C &= \int_{t_0}^{t_1} \Big(L(t), \gamma(t) + h(t), \dot{\gamma}(t) + \dot{h}(t) - L(t, \gamma(t), \dot{\gamma(t)}) \Big) dt \\ &= \int_{t_0}^{t_1} \left(\frac{\partial L}{\partial x} - \frac{d}{dt}\frac{\partial L}{\partial \dot{x}} \right)_{|\gamma} .h(t)dt + \frac{1}{2}\int_{t_0}^{t_1} \Big((\frac{\partial^2 L}{\partial x^2})_{|\gamma} h^2(t) + 2(\frac{\partial^2 L}{\partial x \partial \dot{x}})_{|\gamma} h(t)\dot{h}(t) \\ &+ (\frac{\partial^2 L}{\partial \dot{x}^2})_{|\gamma} \dot{h}^2(t) \Big) dt + o(h, \dot{h})_2 \end{aligned}$$

If $\gamma(t)$ is an extremal, the first integral is zero and the second integral corresponds to the intrinsic second-order derivative $\delta^2 C$, that is:

$$\delta^2 C = \frac{1}{2}\int_{t_0}^{t_1} \Big((\frac{\partial^2 L}{\partial x^2})_{|\gamma} h^2(t) + 2(\frac{\partial^2 L}{\partial x \partial \dot{x}})_{|\gamma} h(t)\dot{h}(t) + (\frac{\partial^2 L}{\partial \dot{x}^2})_{|\gamma} \dot{h}^2(t) \Big) dt \tag{1.9}$$

Using $h(t_0) = h(t_1) = 0$, it can be written after an integration by parts as

$$\delta^2 C = \int_{t_0}^{t_1} \Big(P(t)\dot{h}^2(t) + Q(t)h^2(t) \Big) dt \tag{1.10}$$

where

$$P = \frac{1}{2}(\frac{\partial^2 L}{\partial \dot{x}^2})_{|\gamma}, \qquad Q = \frac{1}{2}\left(\frac{\partial^2 L}{\partial x^2} - \frac{d}{dt}\frac{\partial^2 L}{\partial x \partial \dot{x}} \right)_{|\gamma}.$$

Using the fact that in the integral (1.10) the term $P\dot{h}^2$ is dominating [32], we get the following proposition.

Proposition 4 *If $\gamma(\cdot)$ is a minimizing curve for the fixed extremities problem then it must satisfy the Legendre condition:*

$$(\frac{\partial^2 L}{\partial \dot{x}^2})_{|\gamma} \geq 0. \tag{1.11}$$

1.5 The Accessory Problem and the Jacobi Equation

The intrinsic second-order derivative is given by

$$\delta^2 C = \int_{t_0}^{t_1} \Big(P(t)\dot{h}^2(t) + Q(t)h^2(t) \Big) dt, \qquad h(t_0) = h(t_1) = 0,$$

where P, Q are as above. We write

$$\delta^2 C = \int_{t_0}^{t_1} \Big((P(t)\dot{h}(t))\dot{h}(t) + (Q(t)h(t))h(t) \Big) dt$$

and integrating by parts using $h(t_0) = h(t_1) = 0$, we obtain

$$\delta^2 C = \int_{t_0}^{t_1} \Big(Q(t)h(t) - \frac{d}{dt}(P(t)\dot{h}(t)) \Big) h(t) dt$$

Let us introduce the linear operator $D : h \mapsto Qh - \frac{d}{dt}(P\dot{h})$. Hence, we can write

$$\delta^2 C = (Dh, h) \tag{1.12}$$

where $(,)$ is the usual scalar product on $L^2([t_0,t_1])$. The linear operator D is called the Euler-Lagrange operator.

Definition 3 *From (1.12), $\delta^2 C$ is a quadratic operator on the set $\mathscr{C}_0$ of C^2-curves $h:[t_0,t_1]\to\mathbb{R}$ satisfying $h(t_0)=h(t_1)=0, h\neq 0$. Rather to study $\delta^C>0$ for each $h(\cdot)\in\mathscr{C}_0$ we can study the so-called accessory problem: $\min_{h\in\mathscr{C}_0}\delta^2 C$.*

Definition 4 *The Euler-Lagrange equation corresponding to the accessory problem is called the Jacobi equation and is given by*

$$Dh=0 \tag{1.13}$$

where D is the Euler-Lagrange operator: $Dh=Qh-\frac{d}{dt}(P\dot{h})$. It is a second-order linear differential operator.

Definition 5 *The strong Legendre condition is $P>0$ where $P=\frac{1}{2}(\frac{\partial^2 L}{\partial\dot{x}^2})_{|\gamma}$. If this condition is satisfied, the operator D is said to be nonsingular.*

1.6 Conjugate Point and Local Morse Theory

See also [34], [54].

Definition 6 *Let $\gamma(\cdot)$ be an extremal. A solution $J(\cdot)\in\mathscr{C}_0$ of $DJ=0$ on $[t_0,t_1]$ is called a Jacobi curve. If there exists a Jacobi curve along $\gamma(\cdot)$ on $[t_0,t_1]$ the point $\gamma(t_1)$ is said to be conjugate to $\gamma(t_0)$.*

Theorem 1 ***(Local Morse theory [54]).*** *Let t_0 be fixed and let us consider the Euler-Lagrange operator (indexed by $t>t_0$) D^t defined on the set $\mathscr{C}_0^t$ of curves on $[t_0,t]$ satisfying $h(t_0)=h(t_1)=0$. By definition, a Jacobi curve on $[t_0,t]$ corresponds to an eigenvector J^t associated to an eigenvalue $\lambda^t=0$ of D^t. If the strong Legendre condition is satisfied along an extremal $\gamma:[t_0,t]\to\mathbb{R}^n$, we have a precise description of the spectrum of D^t as follows. There exists $t_0<t_1<\cdots<t_s<T$ such that each $\gamma(t_i)$ is conjugate to $\gamma(t_0)$. If n_i corresponds to the dimension of the set of the Jacobi curves J^{t_i} associated to the conjugate point $\gamma(t_i)$, then for any $\widetilde{T}$ such that $t_0<t_1<\cdots<t_k<\widetilde{T}<t_{k+1}<\cdots<T$ we have the identity*

$$n^-_{\widetilde{T}}=\sum_{i=1}^{k} n_i \tag{1.14}$$

where $n^-_{\widetilde{T}}=dim\{$linear space of eigenvectors of $D^{\widetilde{T}}$ corresponding to strictly negative eigenvalues$\}$. In particular if $\widetilde{T}>t_1$ we have

$$\min_{h\in\mathscr{C}_0}\int_{t_0}^{\widetilde{T}}(Q(t)h^2(t)+P(t)\dot{h}^2(t))dt=-\infty \tag{1.15}$$

Chapter 2
Weak Maximum Principle and Application to Swimming at low Reynolds Number

2.1 Pre-requisite of Differential and Symplectic Geometry

We denote by M a smooth (C^∞ or C^ω) manifold of dimension n, connected and second countable. We denote by TM the fiber bundle and by T^*M the cotangent bundle. Let $V(M)$ be the set of smooth vector fields on M and $Diff(M)$ the set of smooth diffeomorphisms.

Definition 7 *Let $X \in V(M)$ and let f be a smooth function on M. The Lie derivative is defined as: $L_X f = df(X)$. If $X, Y \in V(M)$, the Lie bracket is given by*

$$ad\,X(Y) = [X,Y] = L_Y \circ L_X - L_X \circ L_Y.$$

If $x = (x^1, \cdots, x^n)$ are a local system of coordinates we have:

$$X(x) = \sum_{i=1}^{n} X_i(x) \frac{\partial}{\partial x^i}$$

$$L_X f(x) = \frac{\partial f}{\partial x} X(x)$$

$$[X,Y](x) = \frac{\partial X}{\partial x}(x) Y(x) - \frac{\partial Y}{\partial x}(x) X(x)$$

The mapping $(X,Y) \mapsto [X,Y]$ is $\mathbb{R}$-linear and skew-symmetric. Moreover, the Jacobi identity holds:

$$[X,[Y,Z]] + [Y,[Z,X]] + [Z,[X,Y]] = 0.$$

Definition 8 *Let $X \in V(M)$. We denote by $x(t,x_0)$ the maximal solution of the Cauchy problem $\dot{x}(t) = X(x(t))$, $x(0) = x_0$. This solution is defined on a maximal open interval J containing 0. We denote by $\exp tX$ the local one parameter group associated to X, that is: $\exp tX(x_0) = x(t,x_0)$. The vector field X is said to be complete if the trajectories can be extended over $\mathbb{R}$.*

Definition 9 *Let $X \in V(M)$ and $\varphi \in Diff(M)$. The image of X by φ is $\varphi * X = d\varphi(X \circ \varphi^{-1})$.*

We recall the following results.

Proposition 5 *if $X, Y \in V(M)$ and $\varphi \in Diff(M)$, we have:*

1. *The one parameter local group of $Z = -\varphi * X$ is given by:*

$$\exp tZ = \varphi \circ \exp tX \circ \varphi^{-1}$$

2. $\varphi * [X,Y] = [\varphi * X, \varphi * Y]$
3. *The Baker-Campbell-Hausdorf (BCH) formula is:*

$$\exp sX \exp tY = \exp \zeta(X,Y)$$

where $\zeta(X,Y)$ belongs to the Lie algebra generated by $[X,Y]$ with:

$$\zeta(X,Y) = sX + tY + \frac{st}{2}[X,Y] + \frac{st^2}{12}[[X,Y],Y] - \frac{s^2t}{12}[[X,Y],X]$$

$$-\frac{s^2t^2}{24}[X,[Y,[X,Y]]] + \cdots,$$

the series converging for s,t small enough in the analytic case.

4. *We have*

$$\exp tX \exp \varepsilon Y \exp -tX = \exp \eta(X,Y)$$

with $\eta(X,Y) = \varepsilon \sum_{k \geq 0} \frac{t^k}{k!} ad^k X(Y)$ and the series converging for ε, t small enough in the analytic case.

5. *The ad-formula is:*

$$\exp tX * Y = \sum_{k \geq 0} \frac{t^k}{k!} ad^k X(Y)$$

where the series is converging for t small enough.

Definition 10 *Let V be a $\mathbb{R}$-linear space of dimension $2n$. This space is said to be symplectic if there is exists an application $\omega : V \times V \to \mathbb{R}$ which is bilinear, skew-symmetric and nondegenerate, that is if $\omega(x,y) = 0$ for all $x \in V$ then $y = 0$. Let W be a linear subspace of V. We denote by $W^\perp$ the set*

$$W^\perp = \{x \in V;\ \omega(x,y) = 0\ \forall y \in W\}.$$

The space W is isotropic if $W \subset W^\perp$. An isotropic space is said to be Lagrangian if $dim W = dim \frac{V}{2}$. Let (V_1, ω_1), (V_2, ω_2) be two symplectic linear spaces. A linear mapping $f : V_1 \to V_2$ is symplectic if $\omega_1(x,y) = \omega_2(f(x), f(y))$ for each $x, y \in V_1$.

Proposition 6 *Let (V, ω) be a linear symplectic space. Then there exists a basis $\{e_1, ..., e_n, f_1, ..., f_n\}$ called canonical defined by $\omega(e_i, e_j) = \omega(f_i, f_j) = 0$ for $1 \leq$*

$i,j \leq n$ and $\omega(e_i,f_j)=\delta_{ij}$ (Kronecker symbol). If J is the matrix $\begin{pmatrix} 0 & I \\ -I & 0 \end{pmatrix}$ where I is the identity matrix of order n, then we can write $\omega(x,y)=\langle Jx,y\rangle$ where $\langle,\rangle$ is the scalar product (in the basis (e_i,f_j)). In the canonical basis, the set of all linear symplectic transformations is represented as the symplectic group defined by $Sp(n,\mathbb{R})=\{S\in GL(2n,\mathbb{R}); S^{\intercal}JS=J\}$.

Definition 11 *Let M be a C^{∞}-manifold with dimension $2n$. A symplectic structure on M is defined by a 2-form ω such that $d\omega=0$ and ω is regular, that is $\forall x\in M, \omega_x$ is nondegenerate.*

Proposition 7 *For any C^{∞}-manifold with dimension n, the cotangent bundle T^*M admits a canonical symplectic structure defined by $\omega=d\alpha$ where α is the Liouville form. If $x=(x_1,...,x_n)$ is a coordinate system on M and (x,p) with $(p_1,...,p_n)$ the associated coordinates on T^*M , the Liouville form is written locally as $\alpha=\sum_{i=1}^n p_i dx_i$ and $\omega=d\alpha=\sum_{i=1}^n dp_i\wedge dx_i$.*

Proposition 8 (Darboux) *Let (M,ω) be a symplectic manifold. Then given any point of M, there exists a local system of coordinates called Darboux-coordinates, $(x_1,...,x_n,p_1,...,p_n)$ such that ω is given locally by $\sum_{i=1}^n dp_i\wedge dx_i$. (Hence the symplectic geometry is a geometry with no local invariant).*

Definition 12 *Let (M,ω) be a symplectic manifold and let X be a vector field on M. We note $i_X\omega$ the interior product defined by $i_X\omega(Y)=\omega(X,Y)$ for any vector field Y on M. Let $H:M\to\mathbb{R}$. The vector field denoted by $\overrightarrow{H}$ and defined by $i_{\overrightarrow{H}}(\omega)=-dH$ is the Hamiltonian vector field associated to H. If (x,p) is a Darboux-coordinates system, then the Hamiltonian vector field is expressed in these coordinates by*

$$\overrightarrow{H}=\sum_{i=1}^{n}\frac{\partial H}{\partial p_i}\frac{\partial}{\partial x_i}-\frac{\partial H}{\partial x_i}\frac{\partial}{\partial p_i}$$

Definition 13 *Let $F,G:M\to\mathbb{R}$ be two mappings. We denote by $\{F,G\}$ the Poisson-bracket of F,G defined by $\{F,G\}=dF(\overrightarrow{G})$.*

Proposition 9 (Properties of the Poisson-bracket)

1. *The mapping $(F,G)\mapsto\{F,G\}$ is bilinear and skew-symmetric.*
2. *The Leibnitz identity holds:*

$$\{FG,H\}=G\{F,G\}+F\{G,H\}.$$

3. *In a Darboux-coordinates system, we have*

$$\{F,G\}=\sum_{i=1}^{n}\frac{\partial G}{\partial p_i}\frac{\partial F}{\partial x_i}-\frac{\partial G}{\partial x_i}\frac{\partial F}{\partial p_i}.$$

4. *If the Lie bracket is defined by $[\overrightarrow{F},\overrightarrow{G}]=\overrightarrow{G}\circ\overrightarrow{F}-\overrightarrow{F}\circ\overrightarrow{G}$, then its relation with the Poisson bracket is given by: $[\overrightarrow{F},\overrightarrow{G}]=\{\overrightarrow{F,G}\}$.*

5. The Jacobi identity is satisfied:

$$\{\{F,G\},H\}+\{\{G,H\},F\}+\{\{H,F\},G\}=0.$$

Definition 14 *Let $\overrightarrow{H}$ be a Hamiltonian vector field on (M,ω) and $F:M\to\mathbb{R}$. We say that F is a first integral for $\overrightarrow{H}$ if F is constant along any trajectory of $\overrightarrow{H}$, that is $dF(\overrightarrow{H})=\{F,H\}=0$.*

Definition 15 *Let (x,p) be a Darboux-coordinates system and $H:M\to\mathbb{R}$. The coordinate x_1 is said to be cyclic if $\frac{\partial H}{\partial x_1}=0$. Hence $F:(x,p)\mapsto p_1$ is a first integral.*

Definition 16 *Let M be a $n-$dimensional manifold and let (x,p) be Darboux-coordinates on T^*M. For any vector field X on M we can define a Hamiltonian vector field $\overrightarrow{H}_X$ on T^*M by $H(x,p)=\langle p,X(x)\rangle$; $\overrightarrow{H}_X$ is called the Hamiltonian lift and $\overrightarrow{H}_X=X\frac{\partial}{\partial x}-\frac{\partial X}{\partial x}^{\intercal}p\frac{\partial}{\partial p}$. Each diffeomorphism φ on M can be lifted into a symplectic diffeomorphism $\overrightarrow{\varphi}$ on T^*M defined in a local system of coordinates as follows. If $x=\varphi(y)$, then $\overrightarrow{\varphi}:(y,q)\mapsto(x,p)=\left(\varphi(y),\frac{\partial\varphi^{-1}}{\partial y}^{\intercal}q\right)$.*

Theorem 2.1 (Noether). *Let (x,p) be Darboux-coordinates on T^*M, X a vector field on M and $\overrightarrow{H}_X$ its Hamiltonian lift. We assume $\overrightarrow{H}_X$ to be a complete vector field and we denote by φ_t the associated one parameter group. Let $F:T^*M\to\mathbb{R}$ and let us assume that $F\circ\varphi_t=F$ for all $t\in\mathbb{R}$. Then H_X is a first integral for $\overrightarrow{F}$.*

Definition 17 *Let M be a manifold of dimension $2n+1$ and let ω be a 2-form on M. Then for all $x\in M$, ω_x is bilinear , skew-symmetric and its rank is $\leq 2n$. If for each x, the rank is $2n$, we say that ω is regular. In this case $\ker\omega$ is of rank one and is generated by an unique vector field X up to a scalar. If α is a $1-$form such that $d\alpha$ is of rank $2n$, the vector field associated with $d\alpha$ is called the characteristic vector field of α and the trajectories of X are called the characteristics.*

Proposition 10 *On the space $T^*M\times\mathbb{R}$ with coordinates (x,p,t) the characteristics of the $1-$form $\sum_{i=1}^{n}(p_idx_i-Hdt)$ project onto solutions of the Hamilton equations:*

$$\dot{x}(t)=\frac{\partial H}{\partial p}(x(t),p(t),t),\quad \dot{p}(t)=-\frac{\partial H}{\partial x}(x(t),p(t),t).$$

Definition 18 *Let $\varphi:(x,p,t)\mapsto(X,P,T)$ be a change of coordinates on $T^*M\times\mathbb{R}$. If there exists two functions $K(X,P,T)$ and $S(X,P,T)$ such that*

$$pdx-Hdt=PdX-KdT+dS$$

then the mapping φ is a canonical transformation and S is called the generating function of φ.

Proposition 11 *For a canonical transformation the equations*

$$\dot{x}(t)=\frac{\partial H}{\partial p}(x(t),p(t),t),\quad \dot{p}(t)=-\frac{\partial H}{\partial x}(x(t),p(t),t)$$

transform onto

$$\frac{dX}{dT}(T) = \frac{\partial K}{\partial P}(X(T),P(T),T), \quad \frac{dP}{dT}(T) = -\frac{\partial K}{\partial X}(X(T),P(T),T).$$

If $T = t$ and (x,X) forms a coordinate system, then we have

$$\frac{dX}{dt}(t) = \frac{\partial K}{\partial P}(X(t),P(t),t), \quad \frac{dP}{dt}(t) = -\frac{\partial K}{\partial X}(X(t),P(t),t).$$

with

$$p(t) = \frac{\partial S}{\partial x}(X(t),P(t),t), \quad P(t) = -\frac{\partial S}{\partial X}(X(t),P(t),t),$$
$$H(X(t),P(t),t) = K(X(t),P(t),t) - \frac{\partial S}{\partial t}(X(t),P(t),t).$$

Remark 2.1 (Integrability). Assume that the generating function S is not depending on t. If there exists coordinate such that $K(X,P) = H(x,p)$ is not depending on P, we have $\dot{X}(t) = 0$, $X(t) = X(0)$; hence $P(t) = P(0) + t\frac{\partial K}{\partial X}_{|X=X(0)}$. The equations are integrable. With $H(x,p) = K(X)$ we get

$$H(x, \frac{\partial S}{\partial x}) = K(X).$$

Since $X(t) = (X_1(0),...,X_n(0))$ is fixed, if we can integrate the previous equation we get solutions of Hamilton equations. A standard method is by separating the variables. This is called the Jacobi method to integrate the Hamilton equations. In particular, this leads to a classification of integrable mechanical systems in small dimension, see [45].

Definition 19 *A polysystem D is a family $\{V_i; i \in I\}$ of vector fields. We denote by the same letter the associated distribution, that is the mapping $x \mapsto Span\{V(x); V \in D\}$. The distribution D is said to be involutive if $[V_i,V_j] \subset D, \forall V_i,V_j \in D$.*

Definition 20 *Let D be a polysystem. We design by $D_{L.A.}$ the Lie algebra generated by D. By construction the associated distribution $D_{L.A.}$ is involutive. The Lie algebra $D_{L.A.}$ is constructed recursively as follows:*

$$\begin{aligned} D_1 &= Span\{D\}, \\ D_2 &= Span\{D_1 + [D_1,D_1]\}, \\ &\dots, \\ D_k &= Span\{D_{k-1} + [D_1,D_{k-1}]\} \end{aligned}$$

and $D_{L.A.} = \cup_{k\geq 1} D_k$. If $x \in M$, we associate the following sequence of integers: $n_k(x) = dim\, D_k(x)$.

Definition 21 *Consider a control system $\dot{x} = F(x,u)$, $u \in U$ on M. We can associate to this system the polysystem $D = \{f(\cdot,u); u$ constant $, u \in U$. We denote by $S_T(D)$*

the set

$$S_T(D) = \{\exp t_1 V_1 \cdots \exp t_k V_k;\ k \in \mathbb{N}, t_i \geq 0 \text{ and } \sum_{i=1}^{k} t_i = T, V_i \in D\}$$

and by $S(D)$ the local semi-group: $\cup_{T\geq 0} S_T(D)$. We denote by $G(D)$ the local group generated by $S(D)$, that is

$$G(D) = \{\exp t_1 V_1 \cdots \exp t_k V_k;\ k \in \mathbb{N}, t_i \in \mathbb{R}, V_i \in D\}.$$

Properties.

1. The accessibility set from x_0 in time T is:

$$A(x_0, T) = S_T(D)(x_0).$$

2. The accessibility set from x_0 is the orbit of the local semi-group:

$$A(x_0) = S(D)(x_0).$$

Definition 22 *We call the orbit of x_0 the set $O(x_0) = G(D)(x_0)$. The system is said to be weakly controllable if for every $x_0 \in M$, $O(x_0) = M$.*

2.2 Controllability Results

2.2.1 Sussmann-Nagano Theorem

See [62]. When the rank condition is satisfied (rankΔ = constant) we get from the Frobenius theorem a description of all the integral manifolds near x_0. If we only need to construct the leaf passing through x_0 the rank condition is clearly too strong. Indeed, if $D = \{X\}$ is generated by a single vector field X, there exists an integral curve through x_0. For a family of vector fields this result is still true if the vector fields are analytic.

Theorem 2 ***(Nagano-Sussman Theorem)*** *Let D be a family of analytic vector fields near $x_0 \in M$ and let p be the rank of $\Delta : x \mapsto D_{L.A.}(x)$ at x_0. Then through x_0 there exists locally an integral manifold of dimension p.*

Proof. Let p be the rank of Δ at x_0. Then there exists p vector fields of $D_{L.A.}$: $X_1, \cdots, X_p$ such that $Span\{X_1(x_0), \cdots, X_p(x_0)\} = \Delta(x_0)$. Consider the mapping

$$\alpha : (t_1, \cdots, t_p) \mapsto \exp t_1 X_1 \cdots \exp t_p X_p(x_0).$$

It is an immersion for $(t_1, \cdots, t_p) = (0, \cdots, 0)$. Hence the image denoted by N is locally a submanifold of dimension p. To prove that N is an integral manifold we must

check that for each $y \in N$ near x_0, we have $T_yN = \Delta(y)$. It is a direct consequence of the equalities

$$D_{L.A.}(\exp tX_i(x)) = \mathrm{d}\exp tX_i(D_{L.A.}(x)),\ i = 1, \cdots, p$$

and x near x_0, t small enough. To show that the previous equalities hold, let $V(x) \in D_{L.A.}(x)$ such that $V(x) = Y(x)$. By analycity and the ad-formula for t small enough we have

$$(\mathrm{d}\exp tX_i)(Y(x)) = \sum_{k\geq 0} \frac{t^k}{k!} ad^k X_i(Y)(\exp tX_i(x)).$$

Hence for t small enough, we have

$$(\mathrm{d}\exp tX_i)(D_{L.A.}(x)) \subset D_{L.A.}(\exp tX_i(x)).$$

Changing t to $-t$ we show the second inclusion.

C^∞-Counter Example

To prove the previous theorem we use the following geometric property. Let X, Y be two analytic vector fields and assume $X(x_0) \neq 0$. From the ad-formula, if all the vector fields are $ad^k X(Y), k \geq 0$ are collinear to X at x_0, then for t small enough the vector field Y is tangent to the integral curve $\exp tX(x_0)$.

Hence is is easy to construct a C^∞-counter example using flat C^∞-mappings. Indeed take $f : \mathbb{R} \mapsto \mathbb{R}$ a smooth mapping such that $f(x) = 0$ for $x \leq 0$ and $f(x) \neq 0$ for $x > 0$. Consider the two vector fields on $\mathbb{R}^2 : X = \frac{\partial}{\partial x}$ and $Y = f(x)\frac{\partial}{\partial y}$. At 0, $D_{L.A.}$ is of rank 1. Indeed, we have $[X,Y](x) = -f'(x)\frac{\partial}{\partial y} = 0$ at 0 and hence $[X,Y](0) = 0$. The same is true for all high order Lie brackets. In this example the rank $D_{L.A.}$ is not constant along $\exp tX(0)$, indeed for $x > 0$, the vector field Y is transverse to this vector field.

2.2.2 Chow Theorem

Theorem 3 ***(Chow).*** *Let D be a C^∞-polysystem on M. We assume that for each $x \in M, D_{L.A.}(x = T_xM)$. Then we have*

$$G(D)(x) = G(D_{L.A.}(x)) = M,$$

for each $x \in M$.

Proof. Since M is connected it is sufficient to prove the result locally. The proof is based on the BHC-formula. We assume $M = \mathbb{R}^3$ and $D = \{X, Y\}$ with rank $\{X, Y, [X,Y]\} = 3$ at x_0; the generalization is straightforward. Let λ be a real number and consider the mapping

$$\varphi_\lambda : (t_1,t_2,t_3) \mapsto \exp \lambda X \exp t_3 Y \exp -\lambda X \exp t_2 Y \exp t_1 X(x_0).$$

We prove that for λ small but nonzero, φ_λ is an immersion. Indeed using the BHC formula we have

$$\varphi_\lambda(t_1,t_2,t_3) = \exp(t_1 X + (t_2+t_3)Y + \frac{\lambda t_3}{2}[X,Y] + \cdots)(x_0),$$

hence

$$\frac{\partial \varphi_\lambda}{\partial t_1}(0,0,0) = X(x_0), \qquad \frac{\partial \varphi_\lambda}{\partial t_2}(0,0,0) = Y(x_0),$$
$$\frac{\partial \varphi_\lambda}{\partial t_3}(0,0,0) = Y(x_0) + \frac{\lambda}{2}[X,Y](x_0) + o(\lambda)$$

Since $X, Y, [X,Y]$ are linearly independent at x_0, the rank of φ_λ at 0 is 3 for $\lambda \neq 0$ small enough.

2.3 Weak Maximum Principle

We consider the autonomous control system

$$\dot{x}(t) = f(x(t),u(t)), \qquad x(t) \in \mathbb{R}^n, u(t \in \Omega) \tag{2.1}$$

where f is a C^1-mapping. Let the initial and target sets M_0, M_1 be given. We assume M_0, M_1 to be C^1-submanifolds of $\mathbb{R}^n$. The control domain is a given subset $\Omega \subset \mathbb{R}^m$. The class of admissible controls $\mathscr{U}$ is the set of bounded measurable mappings $u : [0,T(u)] \to \Omega$. Let $u(\cdot) \in \mathscr{U}$ and $x_0 \in \mathbb{R}^n$ be fixed. Then, by the Caratheodory theorem [50], there exists a unique trajectory of (2.1) denoted by $x(\cdot,x_0,u)$ such that $x(0) = x_0$. This trajectory is defined on a nonempty subinterval J of $[0,T(u)]$ on which $t \mapsto x(t,x_0,u)$ is an absolutely continuous function and is a solution of 2.1 almost everywhere.

To each $u(\cdot) \in \mathscr{U}$ defined on $[0,T]$ with response $x(\cdot,x_0,u)$ issued from $x(0) = x_0 \in M_0$ defined on $[0,T]$, we assign a cost

$$C(u) = \int_0^T f^0(x(t),u(t))dt \tag{2.2}$$

where f^0 is a C^1-mapping. An admissible control $u^*(\cdot)$ with corresponding trajectory $x^*(\cdot,x_0,u)$ defined on $[0,T^*]$ such that $x^*(0) \in M_0$ and $x^*(T^*) \in M_1$ is optimal if for each admissible control $u(\cdot)$ with response $x(\cdot,x_0,u)$ on $[0,T], x(0) \in M_0$ and $x(T) \in M_1$, then

$$C(u^*) \leq C(u).$$

The Augmented System

The following remark is straightforward but is geometrically very important to understand the maximum principle. Let us consider $\widehat{f} = (f, f_0)$ and the corresponding system on $\mathbb{R}^{n+1}$ defined by the equations $\dot{\widehat{x}} = \widehat{f}(\widehat{x}(t), u(t))$, *i.e.*:

$$\dot{x}(t) = f(x(t), u(t)), \tag{2.3}$$

$$\dot{x}^0(t) = f^0(x(t), u(t)), \tag{2.4}$$

This system is called the augmented system. Since $\widehat{f}$ is C^1, according to the Caratheodory theorem, to each admissible control $u(\cdot) \in \mathscr{U}$ there exists an admissible trajectory $\widehat{x}(t, \widehat{x}_0, u)$ such that $\widehat{x}_0 = (x_0, x^0(0)), x^0(0) = 0$ where the added coordinate $x^0(\cdot)$ satisfies $x^0(T) = \int_0^T f^0(x(t), u(t))dt$.

Let us denote by $\widehat{A}_{M_0}$ the accessibility set $\cup_{u(\cdot)\in\mathscr{U}} \widehat{x}(T, \widehat{x}_0, u)$ from $M_0 = (M_0, 0)$ and let $\widehat{M}_1 = M_1 \times \mathbb{R}$. Then, we observe that an optimal control $u^*(\cdot)$ corresponds to a trajectory $\widehat{x}^*(\cdot)$ such that $\widehat{x}^* \in \widehat{M}_0$ and intersecting $\widehat{M}_1$ at a point $\widehat{x}^*(T^*)$ where x^0 is minimal. In particular $\widehat{x}^*(T)$ belongs to the boundary of the Accessibility set $\widehat{A}_{M_0}$.

Related Problems

Our framework is a general setting to deal with a large class of problems. Examples are the following:

1. Nonautonomous systems:

$$\dot{x}(t) = f(t, x(t), u(t)).$$

   We add the variable t to the state space by setting $\frac{dt}{ds} = 1, t(s_0) = s_0$.
2. Fixed time problem. If the time domain $[0, T(u)]$ is fixed ($T(u) = T$ for all $u(\cdot)$) we add the variable t to the state space by setting $\frac{dt}{ds} = 1, t(s_0) = s_0$ and we impose the following state constraints on $t : t = 0$ at $s = 0$ and $t = T$ at the free terminal time s.

Some specific problems important for applications are the following.

1. If $f^0 \equiv 1$, then $\min \int_0^T f^0(x(t), u(t))dt = \min T$ and we minimize the time of global transfer.
2. If the system is of the form: $\dot{x}(t) = f(t, x(t), u(t)), f(t, x, u) = A(t)x(t) + B(t)u(t)$, where $A(t), B(t)$ are matrices and $C(u) = \int_0^T L(t, x(t), u(t))dt$ where $L(x, u, \cdot)$ is a quadratic form for each t, T being fixed, the problem is called a linear quadratic problem (LQ-problem).

Singular Trajectories and the Weak Maximum Principle

Definition 23 *Consider a system of $\mathbb{R}^n : \dot{x}(t) = f(x(t),u(t))$ where f is a C^∞-mapping from $\mathbb{R}^n \times \mathbb{R}^m$ into $\mathbb{R}^n$. Fix $x_0 \in \mathbb{R}^n$ and $T > 0$. The end-point mapping (for fixed x_0, T) is the mapping $E^{x_0,T} : u(\cdot) \in \mathscr{U} \mapsto x(T,x_0,u)$. If $u(\cdot)$ is a control defined on $[0,T]$ such that the corresponding trajectory $x(\cdot,x_0,u)$ is defined on $[0,T]$, then $E^{x_0,T}$ is defined on a neighborhood V of $u(\cdot)$ for the $L^\infty([0,T])$ norm.*

First and Second Variations of $E^{x_0,T}$

It is a standard result, see for instance [61], that the end-point mapping is a C^∞-mapping defined on a domain of the Banach space $L^\infty([0,T])$. The formal computation of the successive derivatives uses the concept of Gâteaux derivative. Let us explain in details the process to compute the first and second variations.

Let $v(\cdot) \in L^\infty([0,T])$ be a variation of the reference control $u(\cdot)$ and let us denote by $x(\cdot)+\xi(\cdot)$ the response corresponding to $u(\cdot)+v(\cdot)$ issued from x_0. Since f is C^∞, it admits a Taylor expansion for each fixed t:

$$f(x+\xi,u+v) = f(x,u) + \frac{\partial f}{\partial x}(x,u)\xi + \frac{\partial f}{\partial u}(x,u)v + \frac{\partial^2 f}{\partial x \partial u}(x,u)(\xi,v) + \frac{1}{2}\frac{\partial^2 f}{\partial x^2}(\xi,\xi) + \frac{1}{2}\frac{\partial^2 f}{\partial u}(v,v) + \cdots$$

Using the differential equation we get

$$\dot{x}(t) + \dot{\xi}(t) = f(x(t)+\xi(t), u(t)+v(t)).$$

Hence we can write ξ on the form: $\delta_1 x + \delta_2 x + \cdots$ where $\delta_1 x$ is linear in v, $\delta_2 x$ is quadratic, etc. and are solutions of the following differential equations:

$$\dot{\delta_1 x} = \frac{\partial f}{\partial x}(x,u)\delta_1 x + \frac{\partial f}{\partial u}(x,u)v \tag{2.5}$$

$$\begin{aligned}\dot{\delta_2 x} = \frac{\partial f}{\partial x}(x,u)\delta_2 x + \frac{\partial^2 f}{\partial x \partial u}(x,u)(\delta_1 x, v) \\ + \frac{1}{2}\frac{\partial^2 f}{\partial x^2}(x,u)(\delta_1 x, \delta_2 x) + \frac{1}{2}\frac{\partial^2 f}{\partial u^2}(x,u)(v,v)\end{aligned} \tag{2.6}$$

Using $\xi(0) = 0$, these differential equations have to be integrated with the initial conditions

$$\delta_1 x(0) = \delta_2 x(0) = 0 \tag{2.7}$$

Let us introduce the following notations:

$$A(t) = \frac{\partial f}{\partial x}(x(t),u(t)), \qquad B(t) = \frac{\partial f}{\partial u}(x(t),u(t))$$

Definition 24 *The system*

$$\dot{\delta x}(t) = A(t)\delta x(t) + B(t)\delta u(t)$$

is called the linearized system along $(x(\cdot),u(\cdot))$.

Let $M(t)$ be the fundamental matrix on $[0,T]$ solution almost everywhere of

$$\dot{M}(t) = A(t)M(t), \qquad M(0) = identity.$$

Integrating 2.5 with $\delta_1 x(0) = 0$ we get the following expression for $\delta_1 x$:

$$\delta_1 x(T) = M(T)\int_0^T M^{-1}(t)B(t)v(t)dt \tag{2.8}$$

This implies the following lemma.

Lemma 1 *The Fréchet derivative of* $E^{x_0,T}$ *at* $u(\cdot)$ *is given by*

$$E'^{x_0,T}(v) = \delta_1 x(T) = M(T)\int_0^T M^{-1}(t)B(t)v(t)dt.$$

Definition 25 *The admissible control* $u(\cdot)$ *and its corresponding trajectory* $x(\cdot,x_0,u)$ *defined both on* $[0,T]$ *are said to be regular if the Fréchet derivative* $E'^{x_0,T}$ *is surjective. Otherwise they are called singular.*

Proposition 12 *Let* $A(x_0,T) = \cup_{u(\cdot)\in\mathscr{U}} x(T,x_0,u)$ *be the accessibility set at time* T *from* x_0. *If* $u(\cdot)$ *is a regular control on* $[0,T]$ *then there exists a neighborhood* U *of the end-point* $x(T,x_0,u)$ *contained in* $A(x_0,T)$.

Proof. Since $E'^{x_0,T}$ is surjective at $u(\cdot)$, we have using the open mapping theorem that $E^{x_0,T}$ is an open map.

Theorem 4 *Assume that the admissible control* $u(\cdot)$ *and its corresponding trajectory* $x(\cdot)$ *are singular on* $[0,T]$. *Then there exists a vector* $p(\cdot)\in\mathbb{R}^n\setminus\{0\}$ *absolutely continuous on* $[0,T]$ *such that* (x,p,u) *are solutions almost everywhere on* $[0,T]$ *of the following equations:*

$$\frac{dx}{dt}(t) = \frac{\partial H}{\partial p}(x(t),p(t),u(t)), \qquad \frac{dp}{dt} = -\frac{\partial H}{\partial x}(x(t),p(t),u(t)) \tag{2.9}$$

$$\frac{\partial H}{\partial u}(x(t),p(t),u(t)) = 0 \tag{2.10}$$

where $H(x,p,u) = \langle p, f(x,u)\rangle$ *is the pseudo-Hamiltonian,* $\langle,\rangle$ *being the standard inner product.*

Proof. We observe that the Fréchet derivative is a solution of the linear system

$$\dot{\delta x}(t) = A(t)\delta_1 x(t) + B(t)v(t).$$

Hence, if the pair $(x(\cdot), u(\cdot))$ is singular this system is not controllable on $[0,T]$. We use an earlier proof on controllability to get a geometric characterization of this property. The proof which is the heuristic basis of the maximum principle is given in detail. By definition, since $u(\cdot)$ is a singular control on $[0,T]$ the dimension of the linear space

$$\left\{ \int_0^T M(T)M^{-1}(t)B(t)v(t)dt;\, v(\cdot) \in L^\infty([0,T]) \right\}$$

is less than n. Therefore there exists a row vector $\underline{\mathrm{p}} \in \mathbb{R}^n \setminus \{0\}$ such that

$$\underline{\mathrm{p}} M(T)M^{-1}(t)B(t) = 0$$

for almost everywhere $t \in [0,T]$. We set

$$p(t) = \underline{\mathrm{p}} M(T)M^{-1}(t).$$

By construction $p(\cdot)$ is a solution of the adjoint system

$$\dot{p}(t) = -p(t)\frac{\partial f}{\partial x}(x(t), u(t)).$$

Moreover, it satisfies almost everywhere the following equality:

$$p(t)\frac{\partial f}{\partial u}(x(t), u(t)) = 0.$$

Hence we get the equations (2.9) and (2.10) if $H(x,p,u)$ denotes the scalar product $\langle p, f(x,u)\rangle$.

Geometric interpretation of the Adjoint Vector

In the proof of Theorem 4 we introduced a vector $p(\cdot)$. This vector is called an adjoint vector. We observe that if $u(\cdot)$ is singular on $[0,T]$, then for each $0 < t \leq T$, $u_{|_{[0,T]}}$ is singular and $p(t)$ is orthogonal to the image denoted $K(t)$ of $E^{\prime x_0,T}$ evaluated at $u_{|_{[0,T]}}$. If for each t, $K(t)$ is a linear space of codimension one then $p(t)$ is unique up to a factor.

The Weak Maximum Principle

Theorem 5 *Let $u(\cdot)$ be a control and $x(\cdot,x_0,u)$ the corresponding trajectory, both defined on $[0,T]$. If $x(T,x_0,u)$ belongs to the boundary of the accessibility set $A(x_0,T)$, then the control $u(\cdot)$ and the trajectory $x(\cdot,x_0,u)$ are singular.*

Proof. According to Proposition 12, if $u(\cdot)$ is a regular control on $[0,T]$ then $x(T)$ belongs to the interior of the accessibility set.

Corollary 2 *Consider the problem of maximizing the transfer time for system $\dot{x}(t) = f(x(t),u(t)), u(\cdot) \in \mathscr{U} = L^\infty$, with fixed extremities x_0, x_1. If $u^*(\cdot)$ and the corresponding trajectory are optimal on $[0,\tau^*]$, then $u^*(\cdot)$ is singular.*

Proof. If $u^*(\cdot)$ is maximizing then $x^*(T)$ must belong to the boundary of the accessibility set $A(x_0,T)$ otherwise there exists $\varepsilon > 0$ such that $x^*(T-\varepsilon) \in A(x_0,T)$ and hence can be reached by a solution $\underline{x}(\cdot)$ in time $T : x^*(T-\varepsilon) = \underline{x}(T)$. It follows that the point $x^*(T)$ can be joined in a time $\widehat{T} > T$. This contradicts the maximality assumption.

Corollary 3 *Consider the system $\dot{x}(t) = f(x(t),u(t))$ where $u(\cdot) \in \mathscr{U} = L^\infty([0,T])$ and the minimization problem: $\min_{u(\cdot)\in\mathscr{U}} \int_0^T L(x(t),u(t))dt$, where the extremities x_0, x_1 are fixed as well as the transfer time T. If $u^*(\cdot)$ and its corresponding trajectory are optimal on $[0,T]$ then $u^*(\cdot)$ is singular on $[0,T]$ for the augmented system: $\dot{x}(t) = f(x(t),u(t)), \dot{x}^0(t) = L(x(t),u(t))$. Therefore there exists $\widehat{p}^*(t) = (p(t),p_0) \in \mathbb{R}^{n+1} \setminus \{0\}$ such that $(\widehat{x}^*,\widehat{p}^*,u^*)$ satisfies*

$$\dot{\widehat{x}}(t) = \frac{\partial \widehat{H}}{\partial \widehat{p}}(\widehat{x}(t),\widehat{p}(t),u(t)), \qquad \dot{\widehat{p}}(t) = -\frac{\partial \widehat{H}}{\partial \widehat{x}}(\widehat{x}(t),\widehat{p}(t),u(t)) \qquad \frac{\partial \widehat{H}}{\partial u}(\widehat{x}(t),\widehat{p}(t),u(t)) = 0 \tag{2.11}$$

where $\widehat{x} = (x,x^0)$ and $\widehat{H}(\widehat{x},\widehat{p},u) = \langle p, f(x,u)\rangle + p_0 L(x,u)$. Moreover p_0 is a non-positive constant.

Proof. We have that $x^*(T)$ belongs to the boundary of the accessibility set $\widehat{A}(\widehat{x}_0,T)$. Applying (2.9), (2.10) we get the equations (2.11) where $\dot{p}_0 = -\frac{\partial \widehat{H}}{\partial x^0} = 0$ since $\widehat{H}$ is independent of x^0.

Abnormality

In the previous corollary, $\widehat{p}^*(\cdot)$ is defined up to a factor. Hence we can normalize p_0 to 0 or -1 and we have two cases:

1. *Case 1:* $u(\cdot)$ is regular for the system $\dot{x}(t) = f(x(t),u(t))$. Then $p_0 \neq 0$ and can be normalized to -1. This is called the normal case (in calculus of variations), see [23].

2. *Case 2:* $u(\cdot)$ is singular for the system $\dot{x}(t) = f(x(t), u(t))$. Then we can choose $p_0 = 0$ and the Hamiltonian $\widehat{H}$ evaluated along $(x(\cdot), p(\cdot), u(\cdot))$ doesn't depend on the cost $L(x,u)$. This case is called the abnormal case.

2.4 Second order conditions and conjugate points

In this section we make a brief introduction to the concept of conjugate point in optimal control, in relation with second order conditions, generalizing the similar concepts in calculus of variations presented in section 2.5.1.

The underlying geometric framework is neat and corresponds to the concept of Lagrangian manifold [55] and singularity of projection of Lagrangian manifold [4, 65]. They can be numerically computed using rank tests on Jacobi fields and this form one kernel of the Hampath code [29]. ALso this concept is well known related to zero eigenvalue of self-adjoint operators associated to the intrinsic second order derivative [41].

2.4.1 Lagrangian manifold and Jacobi equation

Definition 26 *Let (M, ω) be a (smooth) symplectic manifold of dimension $2n$. A regular submanifold L of M of dimension n is called Lagrangian if the restriction of ω to $T_xL \times T_xL$ is zero.*

Definition 27 *Let L be a Lagrangian submanifold of T^*M and let $\Pi : z = (x, p) \mapsto x$ be the canonical projection. A tangent non zero vector v of L is called vertical if $\mathrm{d}\Pi(v) = 0$. We call caustic the set of points x of L such that there exists at least one vertical field.*

Definition 28 *Let $\overrightarrow{H}$ be a (smooth) Hamiltonian vector field on T^*M, $\varphi_t = \exp t\overrightarrow{H}$ the associated one parameter group, L_0 the fiber T_xM and $L_t = \varphi_t(L_0)$. The set of caustics is called the set of conjugate loci of L.*

Definition 29 *Let $\overrightarrow{H}$ be a (smooth) Hamiltonian vector field on T^*M and let $z(t) = (x(t), p(t))$ be a reference trajectory of $\overrightarrow{H}$ defined on $[0,T]$. The variational equation*

$$\dot{\delta} z(t) = \frac{\partial \overrightarrow{H}}{\partial z}(z(t))\delta z(t)$$

is called Jacobi equation. We called Jacobi field $J(t) = (\delta x(t), \delta p(t))$ a non trivial solution of Jacobi equation. It is said vertical at time t if $\delta x(0) = 0$. A time t_c is called conjugated if there exists a Jacobi field vertical at times 0 and t_c and the point $x(t_c)$ is called geometrically conjugate to $x(0)$.

2.4.2 Numerical computation of the conjugate loci along a reference trajectory

Verticality test

Let $z(t) = (x(t), p(t))$ be a reference trajectory of $\overrightarrow{H}$ and $x_0 = x(0)$. The set of Jacobi fields forms a n-dimensional linear subspace. Let $(e_1, ..., e_n)$ be a basis of $T^*_{x_0}M$ and let $J_i(t) = (\delta x_i(t), \delta p_i(t)), i = 1, ..., n$ the set of Jacobi fields (vertical at $t = 0$), such that $\delta x_i(0) = 0, \delta p_i(0) = e_i$. Therefore the time t_c is geometrically conjugate if and only if the rank of

$$\mathrm{d}\Pi_{z(t_c)}(J_1(t_c), ..., J_n(t_c))$$

is strictly less than n.

2.5 Swimming problems at low Reynolds number.

2.5.1 Sub-Riemannian Geometry

In this section a crash introduction to sub-Riemannian geometry is presented which is the geometry framework of the swimming problem at low Reynolds number.

Sub-Riemannian manifold

Definition 30 *A sub-Riemannian manifold is a triple (M, D, S) where M is a smooth connected manifold, D is a smooth distribution of rank m on M and g is a riemannian metric on M.*

An *horizontal curve* is an absolutely continuous curve $t \to x(t)$, $t \in I$ such that $\dot{x}(t) \in D(x(t))$. The length of the curve γ is $l(\gamma) = \int_I g(\gamma(t))^{1/2} dt$ and the *energy* of the curve is $E(\gamma) = \frac{1}{2}\int_0^T g(\dot{x}(t))dt$ where one can choose $T = 1$.

Controllability

Let $D_1 = D$, $D_k = D_1 + [D_1, D_{k-1}]$. We assume that there exist for each $x \in M$ an integer $r(x)$ called the *degree of non holonomy* such that $D_{r(x)} = T_xM$. Moreover at a point $x \in M$, the distribution D is characterized by the *growth vector* $(n_1, n_2, ..., n_r)$ where $n_k = \dim\ D_k(x)$.

Distance

According to Chow theorem, for each pair $(x,y) \in M$, there exist an horizontal curve $x : [0,1] \mapsto M$ such that $x(0) = x,\ x(1) = y$. We denote by d the *sub-Riemannian distance*:

$$d(x,y) = \inf\{l(x);\ x \text{ is an horizontal curve joining } x \text{ to } y\}.$$

Geodesics equations

According to Maupertuis principle the length minimization problem is equivalent to the energy minimization problem. Also parametrizing the curves by arc-length the length minimization problem is equivalent to the time minimization problem.

To compute the geodesics equations it is convenient to minimize the energy $E(x)$. We proceed as follows. We choose a local orthonormal frame $\{F_1,...,F_m\}$ of D and we consider the problem

$$\frac{dx}{dt} = \sum_{i=1}^{m} u_i F_i, \qquad \min_{u(.)} \to \frac{1}{2}\int_0^1 \left(\sum_i u_i^2\right) dt$$

According to the weak maximum principle (control domain $U = \mathbb{R}^m$) introduce the pseudo-Hamiltonian:

$$H(x,p,u) = \sum_{i=1}^{m} u_i H_i(x,p) + p_0 \sum_{i=1}^{m} u_i^2$$

where $H_i = \langle p, F_i(x)\rangle$ is the Hamiltonian lift of F_i. By homogeneity p_0 can be normalized to 0 or $-\frac{1}{2}$.

Normal case: $p_0 = -1/2$

According to the Maximum Principle the condition $\frac{\partial H}{\partial u} = 0$ leads to $u_i = H_i$. Plugging such u_i into H leads to the true Hamiltonian in the normal case

$$H_n(z) = \frac{1}{2}\sum_{i=1}^{m} H_i^2$$

A normal extremal is a solution and its projection is called a normal geodesic.

Abnormal case: $p_0 = 0$

In this case the Maximum Principle leads to the conditions: $H_i = 0,\ i = 1,...,m$, thus defining implicitly the abnormal curves related to the structure of the distribution. Solutions are abnormal extremals and their projections are abnormal geodesics.

Next we introduce the basic definitions related to the analysis of the geodesics equations, and generalizing the Riemannian concepts.

Definition 31 *Parametrizing the normal geodesics solutions of* $\vec{H}_n(z)$ *and fixing* $x \in M$*, the exponential map is:* $\exp_x : (p,t) \to \Pi(\exp t\vec{H}_n(z))$ *where* $z(0) = (x,p)$ *and* Π *is the projection* $(x,p) \to x$*.*

Definition 32 *Fix x, the points of SR-distance less than r of x formed the ball of radius r and the sphere* $S(x,r)$ *is formed by points at distance r of x.*

Evaluation of the SR-ball

The computation of SR-ball, even with small radius is a very complicated task. One of the most important result in SR-geometry is an approximation result about ball of small radius, in relation with the structure of the distribution.

Definition 33 *Let* $x \in M$ *and let* f *a germ of a smooth function at x. The multiplicity of* f *at x is the number* $\mu(f)$ *defined by:*

- $\mu(f) = \min\{n;$ *there exist* $X_1,...,X_n \in D(x)$ *such that:* $(L_{X_1}o....oL_{X_n}f)(x) \neq 0\}$*,*
- *if* $f(x) \neq 0$*,* $\mu(f) = 0$ *and* $\mu(0) = +\infty$*.*

Definition 34 *Let* f *be a germ of a smooth function at x,* f *is called privileged at x if* $\mu(f) = \min\{k | df_x(D^k(x)) \neq 0\}$*. A coordinate system* $\{x_1,...,x_n\} : U \to \mathbb{R}$ *defined on an open subset V of x is called privileged if all the coordinates functions* x_i*,* $1 \leq i \leq n$ *are privileged at x.*

Nilpotent Approximation

Having fixed a privileged coordinates system at $x = (x_1,...,x_n)$, where the weight of x_i is $\mu(x_i)$. Each smooth vector field V at x has a formal expansion $V \sim \sum_{n \geq -1} V_n$, where each $V_n = \sum_{i=1}^{d} P_i(x_1,...,x_n)\frac{\partial}{\partial x_i}$ is homogeneous for the weights associated with the coordinate system, and the weight of $\frac{\partial}{\partial x_i}$ is $-\mu(x_i)$.

Proposition 13 *Let* $\{F_1,...,F_m\}$ *be the orthonormous subframe of the distribution D and set* $\widehat{F}_i = F_i^{-1}$*,* $i = 1,...,m$ *in the formal expansion. Then the family* $\widehat{F}_i$ *is a first order approximation of* $\{F_1,...,F_m\}$ *at x as they generate a nilpotent Lie algebra with similar growth vector. Moreover for small x it gives the following estimate of the SR-norm* $|x| = d(0,x) \asymp |x_1|^{1/w_1} + ...|x_n|^{1/w_n}$*.*

See [7], [44] and [38] for the details of the construction of privileged coordinates. Note also that [53] contain also the relation of the integrability issues, important in the practical implementation.

Conjugate and cut loci in SR-geometry

The standard concepts of conjugate and cut point from Riemannian geometry can be generalized in optimal control and thus in SR-geometry.
Notations : consider the SR-problem

$$\dot{x} = \sum_{i=1}^{m} u_i F_i(x), \quad \min_{u(.)} \int_0^T \left(\sum_{i=1}^{m} u_i^2 \right)^{1/2} \mathrm{d}t.$$

Definition 35 *Let $x(t)$ be a reference (normal or abnormal) geodesic on $[0,T]$. The time t_c is called the cut time if the reference geodesic is no more optimal for $t > t_c$ and $x(t_c)$ is called the cut point. Taking all geodesics starting from $x_0 = x(0)$, they will form the cut locus $C_{cut}(x_0)$. The time t_{1c} is called the first conjugate time if the reference geodesic is no more optimal for $t > t_{1c}$ for the C^1-topology on the set of curves, the point $x(t_{1c})$ is called the first conjugate point and taking all geodesics, they will form the (first) conjugate locus $C(x_0)$.*

An important step is to relate the computation of the geometric conjugate locus (using test on Jacobi fields) to the computation of the conjugate locus associated to optimality. It can be done under suitable assumptions in both normal and abnormal case [14] but for simplicity we shall restrict to the normal case.

Conjugate locus computation

Using Maupertius, the SR-problem is equivalent to the (parametrized) energy minimization problem

$$\min_{u(.)} \int_0^T \left(\sum_{i=1}^{m} u_i^2 \right) \mathrm{d}t$$

where T is fixed and one can take $T = 1$.

Let $H_i(z) = \langle p, F_i(x) \rangle$ and let $H_n = \frac{1}{2} \sum_{i=1}^{m} H_i^2$ be the Hamiltonian in the normal case. Take a reference normal geodesic $x(t), t \in [0,1]$ and let $z(t) = (p(t), x(t))$ be a symplectic lift solution of $\overrightarrow{H}_n$. Moreover assume that $x(t)$ is strict, that is is not a projection of an abnormal curve. Then one has

Proposition 14 *The first conjugate time t_{1c} along $x(t)$ corresponds to the first geometric conjugate point and can be computed numerically using the test of section 2.4.*

Integrable case

If the geodesic flow is Liouville integrable then Jacobi equation is integrable and conjugate point can be computed using the parametrization of the geodesic curve. It comes from the following standard lemma from differential geometry.

Lemma 2.1. *Let $J(t) = (\delta x(t), \delta p(t))$ be a Jacobi curve along $z(t) = (x(t), p(t))$, $t \in [0,1]$ and vertical at time $t = 0$, i.e. $\delta x(0) = 0$. Let $\alpha(\varepsilon)$ be any curve in $T^*_{x_0}M$ defined by $p(0) + \varepsilon \delta p(0) + o(\varepsilon)$. Then*

$$J(t) = \frac{\mathrm{d}}{\mathrm{d}\varepsilon}_{|\varepsilon=0} \exp t H_n(x(0), \alpha(\varepsilon)).$$

Nilpotent models in relation with the swimming problem

The models in dimension 3 are related to the classification of stable 2-dimensional distribution, see [66] and will be used for the copepod swimmer. See also [24] for the analysis of the Heisenberg case. For the Purcell swimmer (in dimension 5) we use [60].

Contact case A point $x_0 \in \mathbb{R}^3$ is a *contact point* of the distribution $D = \mathrm{span}\{F_1, F_2\}$ if $[F_1, F_2](x_0) \notin D(x_0)$ and the growth vector is $(2,3)$.
A normal form at $x_0 \sim 0$ is given by

$$x = (x_1, x_2, x_3), \quad D = \ker \alpha, \quad \alpha = x_2 \mathrm{d}x_1 + \mathrm{d}x_3.$$

Observe that

- $\mathrm{d}\alpha = \mathrm{d}x_2 \wedge \mathrm{d}x_1$: Darboux form,
- $\frac{\partial}{\partial x_3}$: Lie bracket $[F_1, F_2]$ and characteristic direction of $\mathrm{d}\alpha$.

This form is equivalent to the so-called *Dido representation*

$$D = \ker \alpha', \quad \alpha' = \mathrm{d}x_3 + (x_1 \mathrm{d}x_2 - x_2 \mathrm{d}x_1)$$

with

$$D = \{F_1, F_2\}, \quad F_1 = \frac{\partial}{\partial x_1} + x_2 \frac{\partial}{\partial x_3},$$
$$F_3 = \frac{\partial}{\partial x_2} - x_1 \frac{\partial}{\partial x_3}, \quad F_3 = [F_1, F_2] = \frac{\partial}{\partial x_3}$$

and the corresponding so-called *Heisenberg SR-case*

$$\dot{x} = \sum_{i=1}^{2} u_i F_i, \quad \min \to \int_0^T (u_1^2 + u_2^2) \mathrm{d}t$$

and it corresponds to minimize the euclidean length of the projection of $t \to x(t)$ on the (x, y)-plane.

Starting from 0, we observe that

$$x_3 = \int_0^T (\dot{x_1}x_2 - \dot{x_2}x_1)\mathrm{d}t$$

is proportional to the area swept by the curve $t \to (x_1(t), x_2(t))$. The SR-problem is dual to the Dido problem: among the closed curves in the plane with fixed length find those for which the enclosed area is minimal. Solutions are well known and are circles.

They can be easily obtained using simple computations. The geodesic equations in the (x,H), $H = (H_1, H_2, H_3)$ are

$$\begin{aligned} \dot{x_1} = H_1, \quad \dot{x_2} = H_2, \quad \dot{x_3} = H_1x_2 - H_2x_1, \\ \dot{H_1} = 2H_2H_3, \quad \dot{H_2} = -2H_1H_3, \quad \dot{H_3} = 0. \end{aligned}$$

Setting: $H_3 = \lambda/2$, we get the equation of a linear pendulum: $\ddot{H_1} + \lambda^2 H_1 = 0$. The integration is direct observing

$$\ddot{x_3} - \frac{\lambda}{2}\frac{\mathrm{d}}{\mathrm{d}t}(x_1^2 + x_2^2) = 0$$

and we get the well known parametrization when $\lambda \neq 0$, which can be assumed positive

$$\begin{aligned} x_1(t) &= \frac{A}{\lambda}\left(\sin(\lambda t + \varphi) - \sin(\varphi)\right) \\ x_2(t) &= \frac{A}{\lambda}\left(\cos(\lambda t + \varphi) - \cos(\varphi)\right) \\ x_3(t) &= \frac{A^2}{\lambda}t - \frac{A^2}{\lambda^2}\sin(\lambda t) \end{aligned}$$

with $A = \sqrt{H_1^2 + H_2^2}$ and φ is the angle of the vector $(\dot{x_1}, -\dot{x_2})$.
If $\lambda = 0$, we have straight-lines.

Conjugate points

The computations of first conjugate points is straightforward using this parameterization.

Only geodesics whose projections are circles have first conjugate point given by $t_c = 2\pi/\lambda$ and corresponds to the first intersection of the geodesic with the axis Ox_3.

Geometrically it is due to the symmetry of revolution along this axis, a one-parameter family of geodesics starting from 0 intersects at such point. This point is also a cut point and a geodesic is optimal up to this point (included).

Note that the Heisenberg case will lead to a geometric interest of the SR-model in the swimming problem: the circles projections correspond to the concept of *stroke*.

But while this model can provide some insights on optimal swimming, it is too primitive because:

1. The geodesic flow is integrable due to the symmetries and every (x_1, x_2) motion is periodic,
2. The model is quasi-homogeneous and x_1, x_2 are not weight 1 and x_2 of weight 2 and invariant in the Heisenberg group.

Martinet case A point x_0 is a *Martinet point* if at x_0, $[F_1, F_2] \in \text{span}\{F_1, F_2\}$ and at least one Lie bracket $[[F_1, F_2], F_1]$ or $[[F_1, F_2], F_2]$ does not belong to D . Hence the growth vector is $(2,2,3)$. Then there exist local coordinates near x_0 identified to 0 such that

$$D = \ker \omega, \quad \omega = \mathrm{d}x_3 - \frac{x_2^2}{2}\mathrm{d}x_1$$

where

$$F_1 = \frac{\partial}{\partial x_1} + \frac{x_2^2}{2}\frac{\partial}{\partial x_3}, \quad F_2 = \frac{\partial}{\partial x_3}, \quad F_3 = [F_1, F_2] = x_2\frac{\partial}{\partial x_3}$$

The surface $\Sigma : \det(F_1, F_2, [F_1, F_2])$ is identified to $x_2 = 0$ and is called the *Martinet surface*. It is foliated by abnormal curves, integral curves of $\frac{\partial}{\partial x_1}$. In particular through 0 it corresponds to the curve $t \to (t, 0, 0)$.

Those two cases are nilpotent Lie algebras associate two nilpotent approximations of the SR-metric in the copepod swimmer and are respectively the Heisenberg case and the Martinet flat case. Also it can be easily checked that this second case leads to integrable geodesic flow using elliptic functions.

Cartan flat case The *Cartan flat case* corresponds to the nilpotent distribution in dimension 5, with growth vector $(2,3,5)$, all Lie brackets of length more than 4 being zero. A normal form is

$$F_1(x) = \frac{\partial}{\partial x_1},$$
$$F_2(x) = \frac{\partial}{\partial x_2} + x_1\frac{\partial}{\partial x_3} + x_3\frac{\partial}{\partial x_4} + x_1^2\frac{\partial}{\partial x_5}$$

2.5.2 Model

Stokes flow

A Newtonian fluid's motion satisfies the Navier-Stokes equation,

$$\rho\frac{\partial \boldsymbol{v}}{\partial t} + \rho\boldsymbol{v}\cdot\nabla\boldsymbol{v} = -\nabla p + \mu\nabla^2\boldsymbol{v}. \tag{2.12}$$

Let U, L, P, ω be the characteristic velocity, length, pressure and frequency, then (2.12) can be written using non-dimensional parameters as

$$\frac{L\omega}{U}\frac{\partial}{\partial \omega t}\left(\frac{\boldsymbol{v}}{U}\right)+\left(\frac{\boldsymbol{v}}{U}\right)\cdot\nabla\left(\frac{\boldsymbol{v}}{U}\right)=-\frac{P}{\rho U^2}\nabla\left(\frac{p}{P}\right)+\frac{\mu}{\rho LU}\nabla^2\left(\frac{\boldsymbol{v}}{U}\right). \quad (2.13)$$

The Reynolds number is defined as $Re=\rho LU/\mu$. Then the motion when $Re \ll 1$ is called creeping motion, for which the term $(\boldsymbol{v}/U)\cdot\nabla(\boldsymbol{v}/U)$ on the left-hand side is negligible with respect to the right-hand side, i.e. the inertial term $\rho\boldsymbol{v}\cdot\nabla\boldsymbol{v}$ is negligible with respect to the viscous term $\mu\nabla^2\boldsymbol{v}$ in (2.12). Furthermore,when ω is small so that the first term

$$\frac{L\omega}{U}\frac{\partial \boldsymbol{v}/U}{\partial \omega t}.$$

is negligible, it is called the Stokes flow or quasi-static creeping motion [36, 48]. (2.12) is simplified to the Stokes equation

$$-\nabla p+\mu\nabla^2\boldsymbol{v}=0. \quad (2.14)$$

The Stokes equation is a linear equation of velocity, so the linear combination of velocity fields (together with the pressure field) which satisfy (2.14) also satisfies (2.14).

Since swimming microorganisms have very small length scales, the Reynolds number is very small, so it is assumed that it moves in a Stokes flow. For the self-propelled organism, there are no external forces other than the hydrodynamical force from the surrounding fluid and its movement is produced by their surface deformation. For example, the spermatozoa is propelled by the oscillation of its tail [35] and E. coli moves by moving its helical flagella [48]. By the deformation, the forward thrust is created.

For the reversible deformation, which means that in a stroke the deformation is the same when the time is reversed, e.g. a scallop, the body cannot be propelled anywhere owe to the reciprocal theorem [59]. In contrast, Purcell proposed a model, the purcell swimmer, which is composed of three thin legs connected by two joints and the two legs at both side rotate to make the movement of the whole body [59]. A small head with several legs around it and propelled by the rotation of the legs is also considered [64].

To study a body moving in Stokes flow, the drag by the fluid is determined by the flow field around it. The drag on a moving ball can be calculated by first solving the velocity and pressure fields by the stream function [36]. But for a body with complicated surface, it is difficult to calculate the velocity field. The propulsion of the swimmer by thin legs are approximated by the slender body theory to determine the relation between the force and the velocity of the legs.

The drag of a ball in the flow

For a body in the fluid, if we don't consider body forces like gravity, the force is from the surface stress, which is expressed by the stress tensor

$$\boldsymbol{T}=-p\boldsymbol{I}+\nu(\nabla\boldsymbol{v}+(\nabla\boldsymbol{v})^T). \quad (2.15)$$

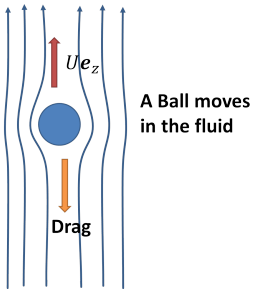

Fig. 2.1

We assume incompressible flow,

$$\nabla \cdot \boldsymbol{v} = 0. \tag{2.16}$$

The first term in (2.15) is the pressure while the second and third terms are the viscous stress and ν is the viscosity. We find from (2.15) that the stress depends on the variation of the velocity in space. Consider a ball moving in the fluid, the drag from the surrounding fluid is the integration

$$\begin{aligned} F &= \int \boldsymbol{T} \cdot \boldsymbol{n} ds \\ &= \int (-p\boldsymbol{I} + \nu(\nabla \boldsymbol{v} + (\nabla \boldsymbol{v})^T)) \cdot \boldsymbol{n} ds. \end{aligned} \tag{2.17}$$

We use the spherical coordinate (r, θ, ϕ), which are defined by the Cartesian coordinates as

$$x = r\sin\theta\cos\phi,\ y = r\sin\theta\sin\phi,\ z = r\cos\theta. \tag{2.18}$$

The unit vectors $(\boldsymbol{e}_r, \boldsymbol{e}_\theta, \boldsymbol{e}_\phi)$ have the relation

$$\begin{aligned} &\boldsymbol{e}_\phi = \boldsymbol{e}_r \times \boldsymbol{e}_\theta,\ \frac{\partial \boldsymbol{e}_r}{\partial \theta} = \boldsymbol{e}_\theta,\ \frac{\partial \boldsymbol{e}_\theta}{\partial \theta} = -\boldsymbol{e}_r, \\ &\frac{\partial \boldsymbol{e}_r}{\partial \phi} = \sin\theta \boldsymbol{e}_\phi,\ \frac{\partial \boldsymbol{e}_\theta}{\partial \phi} = \cos\theta \boldsymbol{e}_\phi,\ \frac{\partial \boldsymbol{e}_\phi}{\partial \phi} = -\sin\theta \boldsymbol{e}_\phi - \cos\theta \boldsymbol{e}_\phi. \end{aligned} \tag{2.19}$$

The gradient operator is

$$\nabla = \boldsymbol{e}_r \frac{\partial}{\partial r} + \boldsymbol{e}_\theta \frac{1}{r}\frac{\partial}{\partial \theta} + \boldsymbol{e}_\phi \frac{1}{r\sin\theta}\frac{\partial}{\partial \phi}. \tag{2.20}$$

A quantity we will use later is

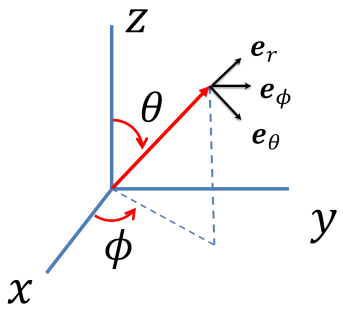

Fig. 2.2

$$\nabla \times (f\boldsymbol{e}_\phi) = \frac{1}{r^2 \sin\theta}\frac{\partial^2 (rf)}{\partial\phi\partial r}\boldsymbol{e}_r + \frac{1}{r^2\sin^2\theta}\frac{\partial^2(\sin\theta f)}{\partial\phi\partial\theta}\boldsymbol{e}_\theta - \frac{1}{r^2}\frac{\partial}{\partial\theta}\left(\frac{1}{\sin\theta}\frac{\partial(\sin\theta f)}{\partial\theta}\boldsymbol{e}_\phi\right). \tag{2.21}$$

Consider a ball moving with constant velocity $\boldsymbol{U} = U\boldsymbol{e}_z$. The fluid velocity induced around the ball is symmetric to the z axis and has only two components: $\boldsymbol{v} = v_r(r,\theta)\boldsymbol{e}_r + v_\theta(r,\theta)\boldsymbol{e}_\theta$.

The velocity can be expressed by a stream function as

$$\boldsymbol{v} = \frac{1}{r\sin\theta}\boldsymbol{e}_\phi \times \nabla\psi = -\nabla\times(\boldsymbol{e}_\phi\frac{\psi}{r\sin\theta}). \tag{2.22}$$

Thus

$$v_r = -\frac{1}{r^2\sin\theta}\frac{\partial\psi}{\partial\theta},\ v_\theta = \frac{1}{r\sin\theta}\frac{\partial\psi}{\partial r}. \tag{2.23}$$

which satisfies the incompressibility assumption $\nabla\cdot\boldsymbol{v} = 0$.

The vorticity $\boldsymbol{\omega}$ is calculated by using (2.21) and that ψ is independent of ϕ,

$$\begin{aligned}
\boldsymbol{\omega} :&= \nabla\times\boldsymbol{v}\\
&= -\nabla\times(\nabla\times(\boldsymbol{e}_\phi\frac{\psi}{r\sin\theta}))\\
&= \frac{1}{r^2\sin\theta}\left(\frac{\partial}{\partial r}\left(r^2\frac{\partial}{\partial r}\left(\frac{\psi}{r\sin\theta}\right)\right) + \frac{\partial}{\partial\theta}\left(\frac{1}{r\sin\theta}\frac{\partial\psi}{\partial\theta}\right)\right)\boldsymbol{e}_\phi\\
&= \frac{1}{r\sin\theta}\left(\frac{1}{\sin\theta}\frac{\partial^2\psi}{\partial r^2} + \frac{1}{r^2}\frac{\partial}{\partial\theta}\left(\frac{1}{\sin\theta}\frac{\partial\psi}{\partial\theta}\right)\right)\boldsymbol{e}_\phi\\
&= \frac{1}{r\sin\theta}(E^2\psi)\boldsymbol{e}_\phi.
\end{aligned} \tag{2.24}$$

where E^2 is an operator defined as

$$E^2 = \frac{1}{\sin\theta}\frac{\partial^2}{\partial r^2} + \frac{1}{r^2}\frac{\partial}{\partial}\left(\frac{1}{\sin\theta}\frac{\partial\psi}{\partial\theta}\right). \tag{2.25}$$

By the incompressibility $\nabla\cdot\boldsymbol{v} = 0$ and the identity $\nabla\times(\nabla\times\boldsymbol{v}) = \nabla(\nabla\cdot\boldsymbol{v}) - \nabla^2\boldsymbol{v}$, the Stokes equation (2.14) can be written as

$$\nabla p = -\mu\nabla\times(\nabla\times\boldsymbol{v}). \tag{2.26}$$

By applying $(\nabla\times)$ to (2.26), we obtain

$$\nabla\times(\nabla\times\boldsymbol{\omega}) = 0. \tag{2.27}$$

Making use of (2.21) again to $\boldsymbol{\omega}$ in (2.27) leads to

$$\frac{1}{r\sin\theta}(E^4\psi)\boldsymbol{e}_\phi = 0. \tag{2.28}$$

So to solve the velocity field $\boldsymbol{v}$ we only need to solve ψ from

$$E^4\psi = 0. \tag{2.29}$$

Assume $\psi = \sin^2\theta F(r)$ [36], then

$$E^2\psi = \sin^2\theta(G'' - \frac{2}{r^2}G),\ E^4\psi = \sin^2\theta(g'' - \frac{2}{r^2}g),\ g = G'' - \frac{2}{r^2}G. \tag{2.30}$$

$E^4\psi = 0$ results in

$$g'' - \frac{2}{r^2}g = 0. \tag{2.31}$$

Then g is solved as $g(r) = C_1r^2 + C_2/r$ and furthermore $G(r) = C_1r^4/10 - C_2r/2 + C_3r^2 + C_4/r$ and the velocity becomes

$$v_r = -2\cos\theta(\frac{C_1r^2}{10} - \frac{C_2}{2r} + C_3 + \frac{C_4}{r^3}),\ v_\theta = \sin\theta(\frac{2C_1r^2}{5} - \frac{C_2}{2r} + 2C_3 - \frac{C_4}{r^3}) \tag{2.32}$$

To determine the constants in (2.32), we use the boundary condition that infinitely far away, the velocity is 0, and at the surface $(r = R_0)$ of the ball, the flow satisfies the non-slip condition, i.e. the flow has the same velocity as the ball.

$$\begin{aligned} &v_r(\theta,\infty) = 0, v_\theta(\theta,\infty) = 0,\\ &v_r(\theta,R_0) = U\cos\theta,\ v_\theta(\theta,R_0) = -U\sin\theta. \end{aligned} \tag{2.33}$$

so (2.33) and (2.32) determines $C_1 = C_3 = 0$, $C_2 = 3R_0U/2$ and $C_4 = R_0^3U/4$ and

$$v_r = U\cos\theta\left(\frac{3R_0}{2r} - \frac{R_0^3}{2r^3}\right),\ v_\theta = -U\sin\theta\left(\frac{3R_0}{4r} + \frac{R_0^3}{4r^3}\right). \tag{2.34}$$

The pressure p is solved by using (2.26), i.e.

$$\begin{aligned}
\nabla p &= -\mu\nabla\times\boldsymbol{\omega} \\
&= -\mu\nabla\times\frac{1}{r\sin\theta}(E^2\psi)\boldsymbol{e}_\phi \\
&= -\mu\left(\boldsymbol{e}_r\frac{\partial}{\partial r}+\boldsymbol{e}_\theta\frac{1}{r}\frac{\partial}{\partial\theta}+\boldsymbol{e}_\phi\frac{1}{r\sin\theta}\frac{\partial}{\partial\phi}\right)\times\frac{E^2\psi}{r\sin\theta}\boldsymbol{e}_\phi \\
&= -\mu\boldsymbol{e}_\theta\frac{\partial}{\partial r}\left(\frac{E^2\psi}{r\sin\theta}\right)-\boldsymbol{e}_r\frac{1}{r}\frac{\partial}{\partial\theta}\left(\frac{E^2\psi}{r\sin\theta}\right)+\frac{E^2\psi}{r^2\sin^2\theta}(\sin\theta\boldsymbol{e}_\theta-\cos\theta\boldsymbol{e}_r) \\
&= \frac{3\mu UR_0}{2r^3}(\cos\theta\boldsymbol{e}_r+\sin\theta\boldsymbol{e}_\theta),
\end{aligned}\tag{2.35}$$

where we used (2.19) and (2.20). Finally, p in (2.35) can be integrated to be

$$p = p_\infty+\frac{3\mu UR_0\cos\theta}{2r^2},\tag{2.36}$$

where p_∞ is the pressure at $r=\infty$.

After the velocity and pressure are obtained, we can calculate the drag $\boldsymbol{F}$ in (2.17). By the symmetry about the z axis, the force should only have component in the z direction, i. e. $\boldsymbol{F}=F\boldsymbol{e}_z$

$$\begin{aligned}
F(r) &= \int\boldsymbol{e}_z\cdot\boldsymbol{T}\cdot\boldsymbol{e}_r 2\pi r^2\sin\theta d\theta \\
&= \int\boldsymbol{e}_z\cdot(-p\boldsymbol{I}+\nu(\nabla\boldsymbol{v}+(\nabla\boldsymbol{v})^T))\cdot\boldsymbol{e}_r 2\pi r^2\sin\theta d\theta.
\end{aligned}\tag{2.37}$$

In order to integrate, we need the tensor

$$\begin{aligned}
\nabla\boldsymbol{v} &= \left(\boldsymbol{e}_r\frac{\partial}{\partial r}+\boldsymbol{e}_\theta\frac{1}{r}\frac{\partial}{\partial\theta}+\boldsymbol{e}_\phi\frac{1}{r\sin\theta}\frac{\partial}{\partial\phi}\right)(v_r\boldsymbol{e}_r+v_\theta\boldsymbol{e}_\theta) \\
&= \boldsymbol{e}_r\boldsymbol{e}_r\left(\frac{\partial v_r}{\partial r}\right)+\boldsymbol{e}_\theta\boldsymbol{e}_\theta\left(\frac{1}{r}\frac{\partial v_\theta}{\partial\theta}+\frac{v_r}{r}\right)+\boldsymbol{e}_r\boldsymbol{e}_\theta\left(\frac{\partial v_\theta}{\partial r}\right)+\boldsymbol{e}_\theta\boldsymbol{e}_r\left(\frac{1}{r}\frac{\partial v_r}{\partial\theta}-\frac{v_\theta}{r}\right)
\end{aligned}\tag{2.38}$$

Then

$$\begin{aligned}
\boldsymbol{e}_z\cdot\boldsymbol{T}\cdot\boldsymbol{e}_r &= (\boldsymbol{e}_r\cos\theta-\boldsymbol{e}_\theta\sin\theta)\cdot(-\boldsymbol{e}_r\boldsymbol{e}_r p-\boldsymbol{e}_\theta\boldsymbol{e}_\theta p-\boldsymbol{e}_\phi\boldsymbol{e}_\phi p+\mu(\nabla v+(\nabla v)^T))\cdot\boldsymbol{e}_r \\
&= -p\cos\theta+(\boldsymbol{e}_r\cos\theta-\boldsymbol{e}_\theta\sin\theta)\cdot(\mu(\nabla v+(\nabla v)^T))\cdot\boldsymbol{e}_r \\
&= -p\cos\theta+\mu\cos\theta\left(2\frac{\partial v_r}{\partial r}\right)-\mu\sin\theta\left(\frac{1}{r}\frac{\partial v_r}{\partial\theta}+\frac{\partial v_\theta}{\partial r}-\frac{v_\theta}{r}\right) \\
&= -p_\infty\cos\theta-\frac{9}{2r^2}\mu UR_0\cos^2\theta+\frac{3}{r^4}\mu UR_0^3\cos^2\theta-\frac{3}{2r^4}\mu UR_0^3\sin^2\theta
\end{aligned}\tag{2.39}$$

At the surface of the ball,

$$\boldsymbol{e}_z \cdot \boldsymbol{T} \cdot \boldsymbol{e}_r(r = R_0) = -p_\infty \cos\theta - \frac{3\mu U}{2R_0}. \tag{2.40}$$

As a consequence, by substituting (2.40) into (2.37) the drag from the fluid on the ball is

$$\begin{aligned} F(R_0) &= \int \boldsymbol{e}_z \cdot \boldsymbol{T} \cdot \boldsymbol{e}_r 2\pi R_0^2 \sin\theta d\theta \\ &= \int_0^\pi -p_\infty \cos\theta - \frac{3}{2}\mu U 2\pi R_0^2 \sin\theta d\theta \\ &= -3\pi\mu U R_0 \int_0^\pi \sin\theta d\theta \\ &= -6\pi\mu U R_0. \end{aligned} \tag{2.41}$$

Stokeslet

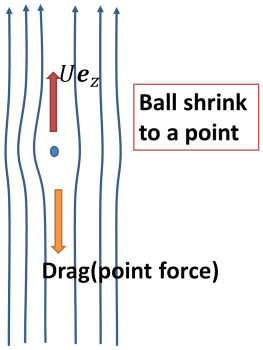

Fig. 2.3

In the last section we saw that when a ball is moving in the fluid, then the hydrodynamical force, the drag, acts on it. By the action and reaction law, at the same time, the ball also exerts force on the fluid, $\boldsymbol{F}_1 = -\boldsymbol{F}$, in the opposite direction of the drag. When the ball is shrunk to a point, this force is regarded as a point force, and the flow is called a Stokelet. For a Stokeslet, the Stokes equation with an external point force at $\boldsymbol{x}'$ is

$$-\nabla p + \mu\nabla^2 \boldsymbol{v} = -\delta(\boldsymbol{x} - \boldsymbol{x}')\boldsymbol{F}_1. \tag{2.42}$$

And the incompressibility of flow is also assumed, $\nabla \cdot \boldsymbol{v} = 0$. We will use the Fourier transformation

$$F(g(\boldsymbol{x}))(\boldsymbol{k}) = \widehat{g} = \int_{R^3} g(\boldsymbol{x}) e^{-i\boldsymbol{k}\cdot\boldsymbol{x}} d\boldsymbol{x}. \tag{2.43}$$

By Fourier transformation, ((2.42)) and the $(\nabla \cdot \boldsymbol{v} = 0)$ becomes

$$-i\boldsymbol{k}\widehat{p} - \mu \boldsymbol{k}^2 \widehat{\boldsymbol{v}} = -\boldsymbol{F}_1 e^{-i\boldsymbol{k}\cdot\boldsymbol{x}'},\ i\boldsymbol{k}\cdot\widehat{\boldsymbol{v}} = 0. \tag{2.44}$$

where for the last term, we used

$$\int_{R^3} \delta(\boldsymbol{x}-\boldsymbol{x}') e^{-i\boldsymbol{k}\cdot\boldsymbol{x}} d\boldsymbol{x} = e^{-i\boldsymbol{k}\cdot\boldsymbol{x}'}, \tag{2.45}$$

by the definition of $\delta-$function.

By the inner product of $\boldsymbol{k}$ with the first one in (2.44) and using the second one, it can be solved

$$\widehat{p} = \frac{\boldsymbol{F}_1 \cdot \boldsymbol{k}}{i\boldsymbol{k}\cdot\boldsymbol{k}} e^{-i\boldsymbol{k}\cdot\boldsymbol{x}'}. \tag{2.46}$$

Notice

$$\begin{aligned} \nabla^2\left(\frac{1}{4\pi|\boldsymbol{x}|}\right) &= -\delta(\boldsymbol{x}) = -\frac{1}{(2\pi)^3}\int_{R^3} e^{i\boldsymbol{k}\cdot\boldsymbol{x}} d\boldsymbol{k}, \\ \nabla^4\left(\frac{|\boldsymbol{x}|}{8\pi}\right) &= -\delta(\boldsymbol{x}) = -\frac{1}{(2\pi)^3}\int_{R^3} e^{i\boldsymbol{k}\cdot\boldsymbol{x} d\boldsymbol{k}}. \end{aligned} \tag{2.47}$$

Making the inverse Fourier transform to (2.46),

$$\begin{aligned} p &= \frac{1}{(2\pi)^3}\int_{R^3} \frac{\boldsymbol{F}_1\cdot\boldsymbol{k}}{i\boldsymbol{k}\cdot\boldsymbol{k}} e^{i\boldsymbol{k}\cdot(\boldsymbol{x}-\boldsymbol{x}')} d\boldsymbol{k} \\ &= -\boldsymbol{F}_1 \cdot \nabla\left(\frac{1}{4\pi|\boldsymbol{x}-\boldsymbol{x}'|}\right) \\ &= \frac{\boldsymbol{F}_1\cdot(\boldsymbol{x}-\boldsymbol{x}')}{4\pi|\boldsymbol{x}-\boldsymbol{x}'|^3}. \end{aligned} \tag{2.48}$$

Substitute (2.46) into the first equation in (2.44), we get

$$\widehat{\boldsymbol{v}} = \left(\frac{\boldsymbol{F}_1}{\mu\boldsymbol{k}^2} - \frac{\boldsymbol{k}\boldsymbol{F}_1\cdot\boldsymbol{k}}{\mu\boldsymbol{k}^4}\right) e^{-i\boldsymbol{k}\cdot\boldsymbol{x}'}. \tag{2.49}$$

Similarly, by making the inverse Fourier transform to (2.49), the velocity is solved as

$$\begin{aligned}\boldsymbol{v}(\boldsymbol{x}) &= \frac{1}{(2\pi)^3}\int_{R^3}\left(\frac{\boldsymbol{F}_1}{\mu\boldsymbol{k}^2}-\frac{\boldsymbol{k}\boldsymbol{F}_1\cdot\boldsymbol{k}}{\mu\boldsymbol{k}^4}\right)e^{i\boldsymbol{k}\cdot(\boldsymbol{x}-\boldsymbol{x}')}d\boldsymbol{k}\\ &= \frac{\boldsymbol{F}_1}{4\pi\mu\,|\boldsymbol{x}-\boldsymbol{x}'|}-\frac{\boldsymbol{F}_1}{\mu}\cdot\nabla\nabla\left(\frac{|\boldsymbol{x}-\boldsymbol{x}'|}{8\pi}\right)\\ &= \boldsymbol{F}_1\cdot\left(\frac{\boldsymbol{I}}{8\pi\mu\,|\boldsymbol{x}-\boldsymbol{x}'|}+\frac{(\boldsymbol{x}-\boldsymbol{x}')(\boldsymbol{x}-\boldsymbol{x}')}{8\pi\mu\,|\boldsymbol{x}-\boldsymbol{x}'|^3}\right).\end{aligned} \tag{2.50}$$

where $\boldsymbol{I}$ is the unit matrix.

Recall for a ball, (2.34) and (2.41) are used to rewrite velocity by force as

$$v_r = -\frac{F}{6\pi\mu}\cos\theta\left(\frac{3}{2r}-\frac{R_0^2}{2r^3}\right),\ v_\theta = \frac{F}{6\pi\mu}\sin\theta\left(\frac{3}{4r}+\frac{R_0^2}{4r^3}\right). \tag{2.51}$$

By setting $|\boldsymbol{x}-\boldsymbol{x}'|=r$, $\boldsymbol{x}-\boldsymbol{x}'=r\boldsymbol{e}_r$ and $\boldsymbol{F}_1=-F\boldsymbol{e}_z$ in (2.50) and setting , it can be verified that expression (2.50) is the same as (2.51) when $R_0\to 0$. This explains and also checks that the Stokeslet is taken by the approximation of an infinitely small ball.

Slender body approximation

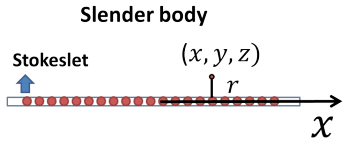

Fig. 2.4

A long and thin body can be viewed approximately as a distribution of Stokeslet [5], i.e. a line force composed of point force. By the linearity of the Stokes equation, the resultant velocity field is a linear combination of the velocity fields created by all of the point forces. Without loss of generality, let the body set on the x axis, and $\boldsymbol{x}=(x,y,z)$, $r=\sqrt{y^2+z^2}$ as shown in the figure. By using (2.50), the velocity around a slender-body becomes [5]

$$\boldsymbol{v}(\boldsymbol{x}) = \frac{1}{8\pi\mu}\int_{-l/2}^{l/2}\left(\frac{\boldsymbol{F}_1(x')}{\sqrt{(x'-x)^2+r^2}}+\boldsymbol{F}_1(x')\cdot\frac{(\boldsymbol{x}-\boldsymbol{x}')(\boldsymbol{x}-\boldsymbol{x}')}{\sqrt{(x-x')^2+r^2}^3}\right)dx'. \tag{2.52}$$

where in the second term on the right-hand side

$$\begin{aligned}\boldsymbol{F_1(x')}\cdot(\boldsymbol{x}-\boldsymbol{x'})(\boldsymbol{x}-\boldsymbol{x'}) &= F_{1x}(x-x')((x-x')\boldsymbol{e}_x+y\boldsymbol{e}_y+z\boldsymbol{e}_z)\\ &\quad +F_{1y}y((x-x')\boldsymbol{e}_x+y\boldsymbol{e}_y+z\boldsymbol{e}_z)\\ &\quad +F_{1z}z((x-x')\boldsymbol{e}_x+y\boldsymbol{e}_y+z\boldsymbol{e}_z). \qquad (2.53)\end{aligned}$$

In order to calculate the integral (2.52) we consider separately the terms and use the slender-body approximation that $r/l \ll 1$ [5]

$$\begin{aligned}I_1 &= \int_{-l/2}^{l/2}\left(\frac{\boldsymbol{F}_1(x')}{\sqrt{(x'-x)^2+r^2}}\right)dx'\\ &= \int_{-l/2}^{l/2}\left(\frac{\boldsymbol{F}_1(x)}{\sqrt{(x'-x)^2+r^2}}\right)dx' + \int_{-l/2}^{l/2}\left(\frac{\boldsymbol{F}_1(x')-\boldsymbol{F}_1(x)}{\sqrt{(x-x')^2+r^2}}\right)dx'\\ &= \boldsymbol{F}_1(x)\ln(x'-x+\sqrt{(x'-x)^2+r^2})\Big|_{-l/2}^{l/2} + \int_{-l/2}^{l/2}\left(\frac{\boldsymbol{F}(\boldsymbol{x'})_1-\boldsymbol{F}_1(x)}{\sqrt{(x-x')^2+r^2}}\right)dx'\\ &= \boldsymbol{F}_1(x)\ln\frac{l/2-x+\sqrt{(l/2-x)^2+r^2}}{-l/2-x+\sqrt{(l/2+x)^2+r^2}} + \int_{-l/2}^{l/2}\left(\frac{\boldsymbol{F}_1(x')-\boldsymbol{F}_1(x)}{\sqrt{(x-x')^2+r^2}}\right)dx'\\ &= \boldsymbol{F}_1(x)2\ln 2+\boldsymbol{F}_1\ln\left(\frac{l^2}{4r^2}\left(1-\frac{4x^2}{l^2}\right)\right) + \int_{-l/2}^{l/2}\left(\frac{\boldsymbol{F}_1(x')-\boldsymbol{F}_1(x)}{\sqrt{(x-x')^2+r^2}}\right)dx'\\ &= \boldsymbol{F}_1(x)2\ln\left(\frac{l}{r}\right)+o(1), \qquad (2.54)\end{aligned}$$

where at the last line we used the assumption that $\left(\frac{\boldsymbol{F}_1(x')-\boldsymbol{F}_1(x)}{x-x'}\right)$ is bounded.

$$\begin{aligned}I_2 &= \int_{-l/2}^{l/2}\left(\frac{\boldsymbol{F}_1(x')r(x'-x)}{((x'-x)^2+r^2)^{3/2}}\right)dx'\\ &= \int_{-l/2}^{l/2}\left(\frac{\boldsymbol{F}_1(x)r(x'-x)}{((x'-x)^2+r^2)^{3/2}}\right)dx' + \int_{-l/2}^{l/2}\left(\frac{(\boldsymbol{F}_1(x')-\boldsymbol{F}_1(x))r(x'-x)}{((x'-x)^2+r^2)^{3/2}}\right)dx'\\ &= -\frac{1}{\sqrt{(x'-x)^2+r^2}}\Big|_{-l/2}^{l/2}+o(r)\\ &= o(r). \qquad (2.55)\end{aligned}$$

$$
\begin{aligned}
I_3 &= \int_{-l/2}^{l/2} \left(\frac{\boldsymbol{F}_1(x')(x'-x)^2}{((x'-x)^2+r^2)^{3/2}} \right) dx' \\
&= \int_{-l/2}^{l/2} \left(\frac{\boldsymbol{F}_1(x)(x'-x)^2}{((x'-x)^2+r^2)^{3/2}} \right) dx' + \int_{-l/2}^{l/2} \left(\frac{(\boldsymbol{F}_1(x')-\boldsymbol{F}_1(x))(x'-x)^2}{((x'-x)^2+r^2)^{3/2}} \right) dx' \\
&= \left(\frac{x-x'}{\sqrt{(x'-x)^2+r^2}} + \ln(x'-x+\sqrt{(x'-x)^2+r^2}) \right) |_{-l/2}^{l/2} \\
&\quad + \int_{-l/2}^{l/2} \left(\frac{(\boldsymbol{F}_1(x')-\boldsymbol{F}_1(x))(x'-x)^2}{((x'-x)^2+r^2)^{3/2}} \right) dx' \\
&= -2 + I_1 + o(1).
\end{aligned} \tag{2.56}
$$

$$
\begin{aligned}
I_4 &= \int_{-l/2}^{l/2} \left(\frac{\boldsymbol{F}_1(x')r^2}{((x'-x)^2+r^2)^{3/2}} \right) dx' \\
&= \int_{-l/2}^{l/2} \left(\frac{\boldsymbol{F}_1(x)r^2}{((x'-x)^2+r^2)^{3/2}} \right) dx' + \int_{-l/2}^{l/2} \left(\frac{(\boldsymbol{F}_1(x')-\boldsymbol{F}_1(x))}{((x'-x)^2+r^2)^{3/2}} \right) dx' \\
&= \left(\frac{x'-x}{\sqrt{(x'-x)^2+r^2}} \right) |_{-l/2}^{l/2} + \int_{-l/2}^{l/2} \left(\frac{(\boldsymbol{F}_1(x')-\boldsymbol{F}_1(x))r^2}{((x'-x)^2+r^2)^{3/2}} \right) dx' \\
&= -2 + o(r^2).
\end{aligned} \tag{2.57}
$$

In (2.52), we take only the leading order $\varepsilon^{-1} := \ln(\frac{l}{r})$, and notice that in (2.53), only the term $F_{1x}(x-x')(x-x')\boldsymbol{e}_x$ can contribute to the leading order, so approximately we have

$$
\boldsymbol{v}(\boldsymbol{x}) \approx \frac{\boldsymbol{F}_1}{8\pi\mu} \cdot \left(2\ln\left(\frac{l}{r}\right) \boldsymbol{I} + 2\ln\left(\frac{l}{r}\right) \boldsymbol{e}_x \right). \tag{2.58}
$$

i. e.

$$
\begin{aligned}
v_x(\boldsymbol{x}) &\approx \frac{\varepsilon^{-1}}{2\pi\mu} \cdot (F_{1x}), \\
v_y(\boldsymbol{x}) &\approx \frac{\varepsilon^{-1}}{4\pi\mu} \cdot (F_{1y}), \\
v_z(\boldsymbol{x}) &\approx \frac{\varepsilon^{-1}}{4\pi\mu} \cdot (F_{1z}).
\end{aligned}
$$

It is convenient to express the relation of force and velocity in (2.59) as

$$
\begin{aligned}
F_{1x} &\approx 2\pi\mu v_x \varepsilon \\
F_{1y} &\approx 4\pi\mu v_y \varepsilon \\
F_{1}z &\approx 4\pi\mu v_z \varepsilon.
\end{aligned} \tag{2.59}
$$

which concludes that the drag coefficient [48] parallel to the body is half of that in the perpendicular direction.

Model 1

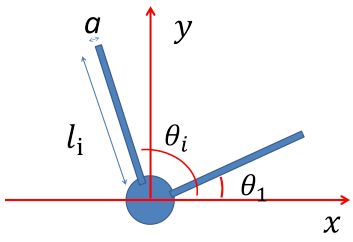

Fig. 2.5

A model is considered in [64], that a ball with N slender legs of length l and radius a, $a \ll l$, moves along the x axis by the rotation of the legs. The position of ball center is $x_0(t)$. θ_i is the angle between the ith leg and $\boldsymbol{e}_x$ direction, which varies with time. Let s denote the distance of a point away from the surface of the ball and R_0 be the radius of the ball. By the slender-body approximation, the formula of the velocity of the swimmer proposed in [64] is calculated in the same way. A point on ith arm has coordinates

$$\boldsymbol{x}(t) = \boldsymbol{x}_0(t) + (R_0 + s)\boldsymbol{\tau}_i, \ \boldsymbol{\tau}_i = \cos\theta_i \boldsymbol{e}_x + \sin\theta_i \boldsymbol{e}_y. \tag{2.60}$$

Taking time derivative of (2.60), we obtain

$$\boldsymbol{v} = \boldsymbol{x}(t) = \dot{\boldsymbol{x}}_0(t) + (R_0 + s)\dot{\boldsymbol{\tau}}_i, \ \dot{\boldsymbol{\tau}}_i = -\sin\theta_i \dot{\theta}_i \boldsymbol{e}_x + \cos\theta_i \dot{\theta}_i \boldsymbol{e}_y. \tag{2.61}$$

Then (2.59) can be written as,

$$\boldsymbol{v} = -\frac{1}{4\pi\mu} \ln\left(\frac{l}{a}\right)(I + \boldsymbol{\tau}_i\boldsymbol{\tau}_i)\cdot F_i = -\frac{\varepsilon^{-1}}{4\pi\mu}(I + \boldsymbol{\tau}_i\boldsymbol{\tau}_i)\cdot F_i. \tag{2.62}$$

On the other hand, we know that the drag acting on the ball is $F_{ball} = -6\pi\mu R_0 \dot{x_0}\boldsymbol{e}_x$.

For a self-propelled swimmer, there is no external non-hydrodynamical force acting on it, and the movement is quasi-static, so we have the total force acting on it by the surrounding fluid is 0, i.e

$$\boldsymbol{F}_{ball} + \sum_{i=1}^{N} \int_0^l \boldsymbol{F}_i ds = 0. \tag{2.63}$$

By combination of (2.61) and (2.62) consider $\boldsymbol{e}_x$ and $\boldsymbol{e}_y$ direction separately,

$$\begin{aligned} \dot{x_0} - \sin\theta_i\dot{\theta}_i(R_0+s) &= -\frac{\varepsilon^{-1}}{4\pi\mu}(F_{ix}+\cos^2\theta_i F_{ix}+\sin\theta_i\cos\theta_i F_{iy}), \\ (R_0+s)\cos\theta_i\dot{\theta}_i &= -\frac{\varepsilon^{-1}}{4\pi\mu}(F_{iy}+\sin^2\theta_i F_{iy}+\sin\theta_i\cos\theta_i F_{ix}). \end{aligned} \tag{2.64}$$

F_{ix} can be solved by (2.64) to be

$$F_{ix} = -4\pi\mu\varepsilon\frac{(\dot{x_0}-\sin\theta_i\dot{\theta}_i(R_0+s))(1+\sin^2\theta_i)-(R_0+s)\sin\theta_i\cos^2\theta_i\dot{\theta}_i}{1+\sin^2\theta_i+\cos^2\theta_i} \tag{2.65}$$

$$\int_0^l F_{ix}ds = -4\pi\mu l\varepsilon\frac{\dot{x_0}(1+\sin^2\theta_i)-2(R_0+l/2)\dot{\theta}_i\sin\theta_i}{1+\sin^2\theta_i+\cos^2\theta_i}. \tag{2.66}$$

Equation (2.63) finally gives the desired relation

$$\dot{x_0} = \frac{\sum_{i=1}^N 2l(R_0+l/2)\dot{\theta}_i\sin\theta_i}{3R_0\varepsilon^{-1}+\sum_{i=1}^N(1+\sin^2\theta_i)}. \tag{2.67}$$

Where the ball shrinks to a point, i. e. $R_0 \to 0$, (2.67) becomes

$$\dot{x_0} = \frac{\sum_{i=1}^N l^2\dot{\theta}_i\sin\theta_i}{\sum_{i=1}^N(1+\sin^2\theta_i)}. \tag{2.68}$$

Purcell swimmer

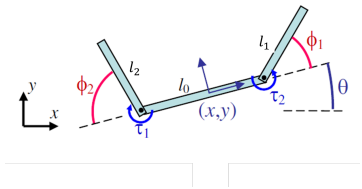

Fig. 2.6

Consider the first link with the length l_1, the hydrodynamical force acting on it can be composed of two parts $\boldsymbol{F}(s)+\widehat{\boldsymbol{F}}(s)$, where $\boldsymbol{F}(s)$ is the force induced by the uniform velocity $(v_x, v_y, 0)$, and $\widehat{\boldsymbol{F}}(s)$ is induced by the rotation around the center of the link. By the symmetry around the center, the integration of force $\widehat{\boldsymbol{F}}(s)$ over the whole link is 0. For the first link, using (2.59),

$$\boldsymbol{\tau}_1 \cdot \boldsymbol{F} = 2\pi\mu\varepsilon \boldsymbol{v} \cdot \boldsymbol{\tau}_1 . \boldsymbol{n}_1 \cdot \boldsymbol{F} = 2\pi\mu\varepsilon \boldsymbol{v} \cdot \boldsymbol{n}_1, \tag{2.69}$$

where the tangential and normal unit vector is

$$\begin{aligned} \boldsymbol{\tau}_1 &= (\cos\phi_1\cos\theta - \sin\phi_1\sin\theta, \cos\phi_1\sin\theta + \sin\phi_1\cos\theta, 0) = (\cos\alpha_1, \sin\alpha_1, 0), \\ \boldsymbol{n}_1 &= (\cos\phi_1\sin\theta + \sin\phi_1\cos\theta, -\cos\phi_1\cos\theta + \sin\phi_1\sin\theta, 0) = (\sin\alpha_1, -\cos\alpha_1, 0), \\ \alpha_1 &= \phi_1 + \theta. \end{aligned} \tag{2.70}$$

the equations (2.69) and (2.70) gives

$$\begin{aligned} F_x\cos\alpha_1 + F_y\sin\alpha_1 &= 2\pi\mu\varepsilon(v_x\cos\alpha_1 + v_y\sin\alpha_1), \\ F_x\sin\alpha_1 - F_y\cos\alpha_1 &= 4\pi\mu\varepsilon(v_x\sin\alpha_1 - v_y\cos\alpha_1). \end{aligned} \tag{2.71}$$

Consequently, we obtain

$$\begin{aligned} F_x &= 2\pi\mu\varepsilon(v_x(1+\sin^2\alpha_1) - v_y\sin\alpha_1\cos\alpha_1), \\ F_y &= 2\pi\mu\varepsilon(v_x\sin\alpha_1\cos\alpha_1 + v_y(1+\sin^2\alpha_1)). \end{aligned} \tag{2.72}$$

The torque about the center of the leg is

$$\tau = \int_0^l \widehat{\boldsymbol{F}} \cdot \boldsymbol{n}(s - \frac{l}{2})ds. \tag{2.73}$$

$$\widehat{\boldsymbol{v}}(s) = \omega_1(s - \frac{l}{2})\boldsymbol{n}_1, \widehat{F}(s) = 2\pi\mu\varepsilon\omega_1(s - \frac{l}{2})\boldsymbol{n}_1. \tag{2.74}$$

Substitute the $\widehat{F}$ into (2.74),

$$\begin{aligned} \tau &= \int_0^l 4\pi\mu\varepsilon\omega(s - \frac{l}{2})^2 ds \\ &= 4\pi\mu\varepsilon\frac{\omega}{12}. \end{aligned} \tag{2.75}$$

After similar calculations on the other two links, we have

$$\begin{pmatrix} F_{ix} \\ F_{iy} \\ \tau_i \end{pmatrix} = 2\pi\mu\varepsilon \begin{pmatrix} 1+\sin^2\alpha_i & -\sin\alpha_i\cos\alpha_i & 0 \\ -\sin\alpha_i\cos\alpha_i & 1+\cos^2\alpha_i & 0 \\ 0 & 0 & \frac{l_i^2}{6} \end{pmatrix} \begin{pmatrix} v_{ix} \\ v_{iy} \\ \omega_i \end{pmatrix}. \tag{2.76}$$

where $\alpha_i = \phi_i + \theta$ and for l_0, $\phi_0 = 0$. The equation (2.76) is same as (18) in [56].

Purcell swimmer

The 3-link Purcell swimmer is modeled by the position of the center of the second stick $\boldsymbol{x} = (x,y)$, the angle θ representing the orientation and the shape of the swimmer is described by the two relative angles α_1 and α_2. We also denote by L and L_2 the length of the two extremal arms and central link. The system is written:

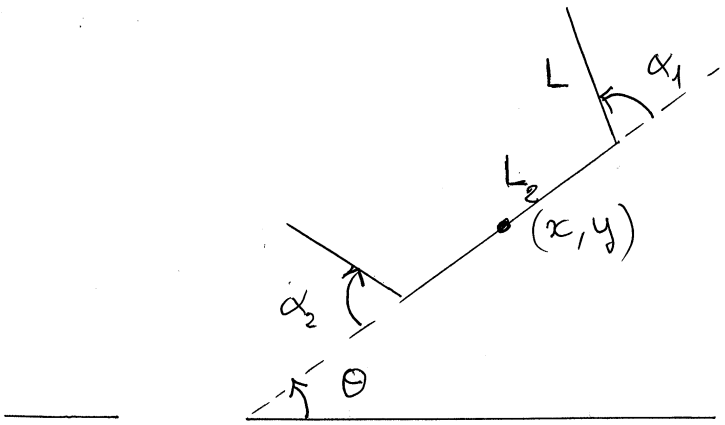

Fig. 2.7 Purcell Swimmer

$$A(z)\begin{pmatrix}\dot{x}\\ \dot{\theta}\end{pmatrix} - B(z)\begin{pmatrix}\dot{\alpha}_1\\ \dot{\alpha}_2\end{pmatrix} = 0$$

where $z = (\alpha_1, \alpha_2, x, y, \theta)$ and inverting A one gets the following structure equations

$$\begin{pmatrix}\dot{x}\\ \dot{y}\\ \dot{\theta}\end{pmatrix} = D(\theta)G(\alpha_1,\alpha_2), \quad \dot{\alpha}_1 = u_1, \quad \dot{\alpha}_2 = u_2$$

where $D(\theta)$ is the rotation matrix

$$D(\theta) = \begin{pmatrix}\cos(\theta) & -\sin(\theta) & 0\\ \sin(\theta) & \cos(\theta) & 0\\ 0 & 0 & 1\end{pmatrix}.$$

and $G(\alpha_1,\alpha_2)$ the 3×2 matrix

$$G = \frac{g_{ij}}{\Delta G}$$

where g_{11}, g_{21}, g_{31} and ΔG are polynomial functions of the shape variables α_1, α_2 and the remaining coefficients defining G are defined by symmetry setting

$$g_{12} = -\Gamma(g_{11}), \quad g_{22} = \Gamma(g_{21}), \quad g_{32} = -\Gamma(g_{31})$$

where Γ amounts to interchange the two angles α_1, α_2.

Hence we have with the relation

$$\begin{pmatrix} \dot{x} \\ \dot{y} \\ \dot{\theta} \end{pmatrix} = \frac{1}{\Delta G} \begin{pmatrix} \cos(\theta) & -\sin(\theta) & 0 \\ \sin(\theta) & \cos(\theta) & 0 \\ 0 & 0 & 1 \end{pmatrix} . \begin{pmatrix} g_{11} & g_{12} \\ g_{21} & g_{22} \\ g_{31} & g_{32} \end{pmatrix} \begin{pmatrix} \dot{\alpha_1} \\ \dot{\alpha_2} \end{pmatrix}$$

$$\begin{aligned} \dot{x} &= \frac{1}{\Delta G}(\cos(\theta)(\dot{\alpha_1} g_{11} + \dot{\alpha_2} g_{12}) - \sin(\theta)(\dot{\alpha_1} g_{21} + \dot{\alpha_2} g_{22})) \\ \dot{y} &= \frac{1}{\Delta G}(\sin(\theta)(\dot{\alpha_1} g_{11} + \dot{\alpha_2} g_{12}) + \cos(\theta)(\dot{\alpha_1} g_{21} + \dot{\alpha_2} g_{22})) \\ \dot{\theta} &= \frac{1}{\Delta G}(\dot{\alpha_1} g_{31} + \dot{\alpha_2} g_{32}) \\ \dot{\alpha_1} &= u_1 \\ \dot{\alpha_2} &= u_2 \end{aligned} \tag{2.77}$$

where the functions g_{11}, g_{12}, g_{31} and Δ are described in [57].

The cost function is defined by the expanded mechanical power defined by the matrix $H : \dot{\alpha} = H(\alpha)\tau = u$ where τ is the physical control torque and is given by $\tau u = uH^{-1}u$ and the symmetric matrix $H^{-1}(\alpha)$ is described in [57].

Copepod swimmer

It is a simplified model proposed by [64] of a symmetric swimming where only line displacement is authorized. It consists in two pairs of symmetric links of equal lengths with respective angles θ_1, θ_2 with respect to the displacement directions Ox while the body is an infinitesimal sphere, see Fig. 2.8 The swimming velocity at x_0

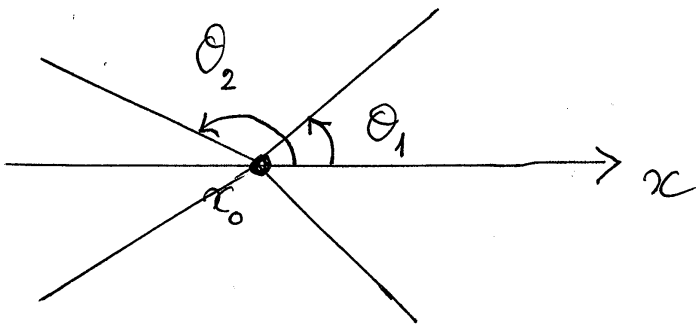

Fig. 2.8 (Symmetric) copepod swimmer

is given by

$$\dot{x_0} = \frac{\dot{\theta}_1 \sin(\theta_1) + \dot{\theta}_2 \sin(\theta_2)}{2 + \sin^2(\theta_1) + \sin^2(\theta_2)}$$

and

$$\dot{\theta}_1 = u_1, \qquad \dot{\theta}_2 = u_2.$$

The mechanical energy is the quadratic form $\dot{q}M\dot{q}^t$ where $q = (x_0, \theta_1, \theta_2)$ is the state variable and M is the symmetric matrix

$$M = \begin{pmatrix} 2 - 1/2(\cos^2(\theta_1) + \cos^2(\theta_2)) & -1/2\sin(\theta_1) & -1/2\sin(\theta_2) \\ -1/2\sin(\theta_1) & 1/3 & 0 \\ -1/2\sin(\theta_2) & 0 & 1/3 \end{pmatrix}$$

and the corresponding Riemannian metric defined the associated SR-metric thanks to the relation between $\dot{x_0}$ and $\dot{\theta}_1, \dot{\theta}_2$.

2.5.3 Some geometric remarks

In order to analyze the swimming problem one must introduce the concept of stroke.

Definition 36 *A stroke is a periodic motion of the shape variables associated with a periodic control producing a net displacement of the displacement variable after one period. Observe that due to SR-structure one can fix the period of the stroke to* 2π.

A first geometric analysis is to consider bang-bang controls and the associated strokes. For a single link one gets the famous *scallop theorem*

Theorem 2.2. *A scallop cannot swim.*

Proof. The relation between the displacement and angular velocity is given by the relation

$$\dot{x} = \frac{\sin(\alpha)}{2 - \cos^2(\alpha)}\dot{\alpha}, \qquad \dot{\alpha} = u$$

where α is the angle of the symmetric link with respect to the axis.

Let γ be the angle with respect to the vertical and a stroke is given by

$$\begin{aligned} u = 1 : &\qquad \alpha : \pi/2 - \gamma \to \pi/2 \\ u = -1 : &\qquad \alpha : \pi/2 \to \pi/2 - \gamma \end{aligned}$$

and the control $u = 1$ produces a displacement: $x_0 \to x_1$ while the control $u = -1$ reverses the motion: $x_1 \to x_0$.

The net displacement of the stroke is zero and clearly is related to the reversibility of the SR-model.

A similar computation can be obtained for the Purcell swimmer using a square stroke as in the original paper ([59]).

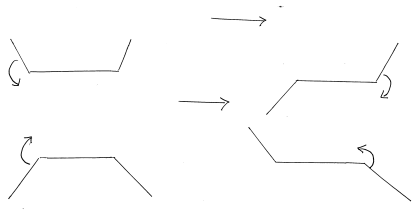

Fig. 2.9 Purcell stroke

Writing the dynamics (2.77) as

$$\dot{\boldsymbol{x}} = \sum_{i=1}^{2} u_i F_i(x),$$

the displacement associated with the sequence stroke is given by

$$\beta(t) = (\exp tF_2 \ \exp -tF_1 \ \exp -tF_2 \ \exp tF_1)\,(x(0))$$

and using Baker-Campbell-Hausdorff formula one has

$$\beta(t) = \exp(t^2[F_1,F_2] + o(t^2))(x(0))$$

which gives for small stroke t a displacement of

$$\beta(t) \sim x(0) + t^2[F_1,F_2](x(0)).$$

Compare with [6].

Hence for a small square stroke the displacement can be evaluated using (2.77).

In the case of the copepod swimmer, due to the constraints $\theta_i \in [0,\pi]$, $\theta_1 \leq \theta_2$ on the shape variable, a geometric stroke corresponds to a triangle vs a rectangle in the shape variable and is defined by
that $\theta_2 : 0 \to \pi;\ \theta_1 : 0 \to \pi$ and $\theta_1 = \theta_2 : \pi \to 0$.

See in the specific analysis of the copepod swimmer the interpretation of this stroke.

2.5.4 Purcel swimmer

We present some preliminary results concerning the Purcell swimmer. The first result concerns the computation of the nilpotent model.

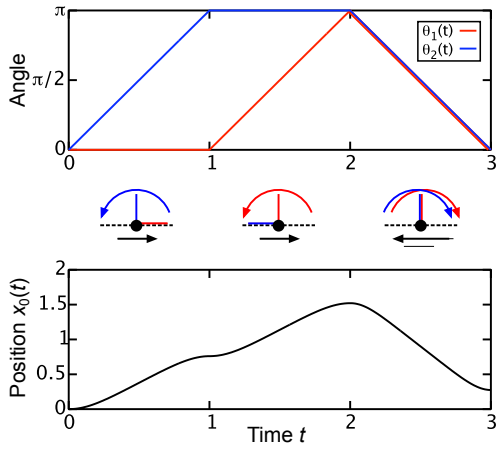

Fig. 2.10 Copepod triangle stroke

Notations

Let us define the variables x_i $i = 1, \cdots, 5$ as $x_1 = \alpha_1$, $x_2 = \alpha_2$, $(x_3, x_4) = \mathbf{x}$, $x_5 = \theta$.
In the rest of the computations, we set $L = 1$, $L_2 = 2$, $\xi = 1$, $\eta = 2$.
Hence, the 2-jets of F_1 and F_2 at zero are expressed by

$$\begin{aligned} F_1(x) = \frac{\partial}{\partial x_1} &+ \left(-\frac{1}{6}x_5 - \frac{4}{27}x_1 - \frac{2}{27}x_2\right)\frac{\partial}{\partial x_3} \\ &+ \left(\frac{1}{6} - \frac{1}{12}{x_5}^2 - \frac{2}{27}x_5x_2 - \frac{4}{27}x_5x_1 - \frac{1}{27}{x_1}^2 - \frac{1}{27}x_1x_2 - \frac{1}{36}{x_2}^2\right)\frac{\partial}{\partial x_4} \\ &+ \left(-\frac{7}{27} + \frac{2}{81}{x_1}^2 - \frac{2}{81}x_1x_2 - \frac{5}{162}{x_2}^2\right)\frac{\partial}{\partial x_5} + O(|x|^3) \end{aligned}$$

$$\begin{aligned} F_2(x) = \frac{\partial}{\partial x_2} &+ \left(\frac{1}{6}x_5 + \frac{4}{27}x_2 + \frac{2}{27}x_1\right)\frac{\partial}{\partial x_3} \\ &+ \left(-\frac{1}{6} + \frac{1}{12}{x_5}^2 + \frac{4}{27}x_5x_2 + \frac{2}{27}x_5x_1 + \frac{1}{36}{x_1}^2 + \frac{1}{27}x_1x_2 + \frac{1}{27}{x_2}^2\right)\frac{\partial}{\partial x_4} \\ &+ \left(-\frac{7}{27} - \frac{5}{162}{x_1}^2 - \frac{2}{81}x_1x_2 + \frac{2}{81}{x_2}^2\right)\frac{\partial}{\partial x_5} + O(|x|^3) \end{aligned}$$

Proposition 15 *There exists a local change of coordinates φ such that the images of F_1, F_2 are in the Cartan flat normal form*

- $(\varphi * F_1) = \frac{\partial}{\partial x_1} + O(|x|^3)$,
- $(\varphi * F_2) = \frac{\partial}{\partial x_2} + x_1 \frac{\partial}{\partial x_3} + \frac{\partial}{\partial x_4} + x_1^2 \frac{\partial}{\partial x_5} + O(|x|^3)$.

where the weights of the variables are: $x_1, x_2 : 1$, $x_3 : 2$, $x_4, x_5 : 3$, thus providing the nilpotent approximation of the metric at 0.

We refer the reader for these constructs for instance to [7].

We introduce the weights 1 for x_1, x_2, 2 for x_3 and 3 for x_4, x_5. If x_i is of order p, $\frac{\partial}{\partial x_i}$ is of order $-p$ to define the nilpotent normal form of order -1.
We write $\varphi = \varphi_N \, o \, ... \, o \, \varphi_1 : \mathbb{R}^5 \to \mathbb{R}^5$. At each step i, for $i = 1, ..., N$ of the computations we shall use $N = 13$ steps :

. $x = (x_1, x_2, x_3, x_4, x_5)$ are the old local coordinates and $y = (y_1, y_2, y_3, y_4, y_5)$ the new ones resulting from the change of variables φ_i,

. $x_j = \varphi_i^{(j)}(y_j) : \mathbb{R} \to \mathbb{R}$ denoting the j$^{\text{th}}$ component of φ_i for some $j \in \{1, ..., 5\}$. The other components $\varphi_i^{(k)}$, $k \neq j$ are the identity transformations.

The successive change of variables are given by

1. $x_5 = \varphi_1^{(5)}(y_5) = y_5 - \frac{7}{27} y_1$,
2. $x_3 = \varphi_2^{(3)}(y_3) = y_3 - \frac{1}{6} y_5 y_1 - \frac{17}{324} y_1^2 - \frac{2}{27} y_2 y_1$,
3. $x_4 = \varphi_3^{(4)}(y_4) = y_4 + \frac{1}{6} y_1 - \frac{37}{3 \times 8748} y_1^3$,
4. $x_5 = \varphi_4^{(5)}(y_5) = y_5 + \frac{2}{24} y_1^3 - \frac{2}{162}$,
5. $x_5 = \varphi_5^{(5)}(y_5) = y_5 - \frac{7}{27} y_2$,
6. $x_3 = \varphi_6^{(3)}(y_3) = \frac{5}{81} y_3 + \frac{17}{324} y_2^2 + \frac{1}{6} y_5 y_2$,
7. $x_4 = \varphi_7^{(4)}(y_4) = y_4 - y_3 y_2$,
8. $x_4 = \varphi_8^{(4)}(y_4) = y_4 + \frac{37}{3 \times 8748} y_2^3$,
9. $x_4 = \varphi_9^{(4)}(y_4) = y_4 - 54 \times \frac{83}{8748} y_5$,
10. $x_4 = \varphi_{10}^{(4)}(y_4) = y_4 + \frac{2270}{2187} y_2 y_3 + \frac{5}{81} y_5 y_3 + \frac{83}{3 \times 6561} y_2^3$,
11. $x_4 = \varphi_{11}^{(4)}(y_4) = -\frac{83}{2187} y_4$,
12. $x_5 = \varphi_{12}^{(5)}(y_5) = y_5 + \frac{1}{27} y_3 y_2 + \frac{2}{3 \times 81} y_2^3$,
13. $x_5 = \varphi_{13}^{(5)}(y_5) = -\frac{1}{54} y_5 - \frac{1}{27} y_4$.

Neglecting terms of order greater than 3, we denote by $\widehat{F_1}, \widehat{F_2}$ the resulting vector fields.

Remark 2.2. The construction of the diffeomorphism relates the normalized coordinates to the physical coordinates. A similar transformation details the effect on a frame.

Integration of extremal trajectories

2.5.5 Integration of extremal trajectories

For two vector fields F and G, we use the following Lie bracket convention

$$[F,G](x) = \frac{\partial F}{\partial x}(x)G(x) - \frac{\partial G}{\partial x}(x)F(x)$$

Computing we have

$$\widehat{F}_1(x) = \frac{\partial}{\partial x_1}, \qquad \widehat{F}_2(x) = \frac{\partial}{\partial x_2} + x_1\frac{\partial}{\partial x_3} + x_3\frac{\partial}{\partial x_4} + x_1^2\frac{\partial}{\partial x_5},$$
$$[\widehat{F}_1,\widehat{F}_2](x) = -\frac{\partial}{\partial x_3} - 2x_1\frac{\partial}{\partial x_5}, \quad [[\widehat{F}_1,\widehat{F}_2],\widehat{F}_1](x) = -2\frac{\partial}{\partial x_5},$$
$$[[\widehat{F}_1,\widehat{F}_2],\widehat{F}_2](x) = \frac{\partial}{\partial x_4}.$$

All brackets of length greater than 3 are zero.
We introduce

$$H_1 = \langle p,\widehat{F}_1(x)\rangle = p_1, \qquad H_2 = \langle p,\widehat{F}_2(x)\rangle = p_2 + p_3x_1 + p_4x_3 + p_5x_1^2,$$
$$H_3 = \langle p,[\widehat{F}_1,\widehat{F}_2](x)\rangle = -p_3 - 2x_1p_5, \quad H_4 = \langle p,[[\widehat{F}_1,\widehat{F}_2],\widehat{F}_1](x)\rangle = -2p_5,$$
$$H_5 = \langle p,[[\widehat{F}_1,\widehat{F}_2],\widehat{F}_2](x)\rangle = p_4.$$

We recall the following relation for the Poisson brackets of two lifting Hamiltonians H_F and H_G of vector fields F and G.
If

$$H_F = \langle p,F(x)\rangle, \quad H_G = \langle p,G(x)\rangle,$$

are the Hamiltonian lifts of vector fields of F and G, then we have

$$\{H_F,H_G\} = \langle p,[F,G](x)\rangle.$$

We consider the SR-Cartan flat case [60], [26]

$$\dot{x} = \sum_{i=1}^{2} u_iF_i, \quad \min_u \int_0^T (u_1^2+u_2^2)dt.$$

Normal case.

The pseudo Hamiltonian is

$$\overrightarrow{H} = \sum_i u_i H_i - \frac{1}{2}(u_1^2 + u_2^2).$$

The Pontryagin maximum principle [58] gives $u_i = H_i$.
Hence, the true Hamiltonian is

$$H_n = \frac{1}{2}(H_1^2 + H_2^2). \tag{2.78}$$

Computing we have

$$\dot{H}_1 = dH_1(H_n) = \{H_1, H_2\}H_2 = \langle p, [\widehat{F}_1, \widehat{F}_2](x)\rangle H_2 = H_2 H_3,$$

$$\begin{aligned} &\dot{H}_2 = -H_3 H_1, && \dot{H}_3 = H_1 H_4 + H_2 H_5, \\ &\dot{H}_4 = 0 \quad \text{hence} \quad H_4 = c_4, && \dot{H}_5 = 0 \quad \text{hence} \quad H_5 = c_5. \end{aligned}$$

Fixing the level energy, $H_1^2 + H_2^2 = 1$ we set $H_1 = \cos(\theta)$ and $H_2 = \sin(\theta)$.

$$\dot{H}_1 = -\sin(\theta)\dot{\theta} = H_2 H_3 = \sin(\theta) H_3.$$

Hence $\dot{\theta} = -H_3$ and

$$\ddot{\theta} = -(H_1 c_4 + H_2 c_5) = -c_4 \cos(\theta) - c_5 \sin(\theta) = -A \sin(\theta + \phi)$$

where A is a constant.
By identification, we get $A\sin(\phi) = c_4$ and $A\cos(\phi) = c_5$.
Let $\psi = \theta + \phi$, we get

$$\frac{1}{2}\dot{\psi}^2 - A\cos(\psi) = B, \tag{2.79}$$

where B is a constant.
We have the two following cases :

Oscillating case

$$\dot{\psi}^2 = 4A\left(\frac{1}{2} + \frac{B}{2A} - \sin^2(\psi/2)\right).$$

We introduce $\omega^2 = A$ and $k^2 = \frac{1}{2} + \frac{B}{2A}$ with $0 < k < 1$, and we obtain [49]

$$\sin(\psi/2) = k\,\mathrm{sn}(s,k), \quad \cos(\psi/2) = \mathrm{dn}(s,k)$$

where $s = \omega t + \varphi_0$.
H_1 and H_2 are elliptic functions of the first kind. Therefore the system becomes

$$\begin{aligned} &\dot{x}_1 = H_1, && \dot{x}_2 = H_2, && \dot{x}_3 = H_2 x_1, \\ &\dot{x}_4 = H_2 x_3, && \dot{x}_5 = H_2 x_1^2. \end{aligned} \tag{2.80}$$

Parameterizing (2.80) with respect to s we have

$$\frac{\mathrm{d}x_1}{\mathrm{d}s} = \frac{1}{\omega}\cos(\theta\left((s-\varphi_0)/\omega\right)) = \frac{1}{\omega}\left[2k\sin\left(\phi\right)\mathrm{sn}\left(s\right)\mathrm{dn}\left(s\right) + \left(2\,\mathrm{dn}^2\left(s\right)-1\right)\cos\left(\phi\right)\right]. \tag{2.81}$$

$$\frac{\mathrm{d}x_2}{\mathrm{d}s} = \frac{1}{\omega}\sin(\theta\left((s-\varphi_0)/\omega\right)) = \frac{1}{\omega}\left[2k\cos\left(\phi\right)\mathrm{sn}\left(s\right)\mathrm{dn}\left(s\right) + \left(1-2\,\mathrm{dn}^2\left(s\right)\right)\sin\left(\phi\right)\right]. \tag{2.82}$$

$$\begin{aligned}\frac{\mathrm{d}x_3}{\mathrm{d}s} &= \frac{1}{\omega}\sin(\theta((s-\varphi_0)/\omega))x_1((s-\varphi_0)/\omega)\\ &= \frac{1}{\omega^2}\Big[-4k^2\sin\left(\phi\right)\cos\left(\phi\right)\mathrm{cn}\left(s\right)\mathrm{sn}\left(s\right)\mathrm{dn}\left(s\right)+2E\left(s\right)\Big)\sin\left(\phi\right)\cos\left(\phi\right)\\ &+2x_1(\varphi_0)k\cos\left(\phi\right)\mathrm{sn}\left(s\right)\mathrm{dn}\left(s\right)+\left(-2\,\mathrm{dn}^2\left(s\right)+1\right)x_1(\varphi_0)\sin\left(\phi\right)\\ &+\Big(-2s\,\mathrm{sn}\left(s\right)\mathrm{dn}\left(s\right)-4\,\mathrm{cn}\left(s\right)\mathrm{dn}^2\left(s\right)+4\,\mathrm{sn}\left(s\right)\mathrm{dn}\left(s\right)E\left(s\right)\\ &+2\,\mathrm{cn}\left(s\right)\Big)k\cos^2(\phi)+\left(2s\,\mathrm{dn}^2\left(s\right)-4\,\mathrm{dn}^2\left(s\right)E\left(s\right)-s\right.\\ &+\left.\left(4\,\mathrm{cn}\left(s\right)\mathrm{dn}^2\left(s\right)-2\,\mathrm{cn}\left(s\right)\right)k\Big].\end{aligned} \tag{2.83}$$

$$
\begin{aligned}
\frac{\mathrm{d}x_4}{\mathrm{d}s} &= \frac{1}{\omega}\sin(\theta((s-\varphi_0)/\omega))x_3((s-\varphi_0)/\omega)\\
&= \frac{1}{\omega^3}\Big[4k^4\cos^3(\phi)\,\mathrm{sn}^4(s) - 8k^4\cos(\phi)\,\mathrm{sn}^4(s)\\
&\quad -4k^2x_1(\varphi_0)\cos^2(\phi)\,\mathrm{cn}(s)\,\mathrm{sn}(s)\,\mathrm{dn}(s) + 2x_3(\varphi_0)k\cos(\phi)\,\mathrm{sn}(s)\,\mathrm{dn}(s)\\
&\quad +4k^3\sin(\phi)\,\mathrm{sn}(s)\,\mathrm{dn}(s) + \big(-s^2\,\mathrm{sn}(s)\,\mathrm{dn}(s) - 4s\,\mathrm{cn}(s)\,\mathrm{dn}^2(s)\\
&\quad +4s\,\mathrm{sn}(s)\,\mathrm{dn}(s)E(s) + 8\,\mathrm{cn}(s)\,\mathrm{dn}^2(s)E(s) - 4\,\mathrm{sn}(s)\,\mathrm{dn}(s)E(s)^2\\
&\quad +2s\,\mathrm{cn}(s) - 4\,\mathrm{cn}(s)E(s) - 2\,\mathrm{sn}(s)\,\mathrm{dn}(s)\big)k\sin(\phi)\\
&\quad +\big(4s\,\mathrm{cn}(s)\,\mathrm{sn}(s)\,\mathrm{dn}(s) - 8\,\mathrm{cn}(s)\,\mathrm{sn}(s)\,\mathrm{dn}(s)E(s)\\
&\quad +4\,\mathrm{dn}^2(s) - 2\big)k^2\cos^3(\phi) + \big(-2x_3(\varphi_0)\,\mathrm{dn}^2(s) + x_3(\varphi_0)\big)\sin(\phi)\\
&\quad +\big(s^2\,\mathrm{sn}(s)\,\mathrm{dn}(s) + 4s\,\mathrm{cn}(s)\,\mathrm{dn}^2(s) - 4s\,\mathrm{sn}(s)\,\mathrm{dn}(s)E(s)\\
&\quad -8\,\mathrm{cn}(s)\,\mathrm{dn}^2(s)E(s) + 4\,\mathrm{sn}(s)\,\mathrm{dn}(s)E(s)^2 - 2s\,\mathrm{cn}(s)\\
&\quad +4\,\mathrm{cn}(s)E(s)\big)k\sin^3(\phi) + \big(2s\,\mathrm{dn}^2(s) - 4\,\mathrm{dn}^2(s)E(s) - s\\
&\quad +2E(s)\big)x_1(\varphi_0)\cos^2(\phi) + \big(-s^2\,\mathrm{dn}^2(s) + 4s\,\mathrm{dn}^2(s)E(s)\\
&\quad -4\,\mathrm{dn}^2(s)E(s)^2 + 1/2s^2 - 2sE(s) + 2\,\mathrm{dn}^2(s) + 2E(s)^2 - 2\big)\cos^3(\phi)\\
&\quad +\big(s^2\,\mathrm{dn}^2(s) - 4s\,\mathrm{dn}^2(s)E(s) + 4\,\mathrm{dn}^2(s)E(s)^2\\
&\quad -1/2s^2 + 2sE(s) - 6\,\mathrm{dn}^2(s) - 2E(s)^2 + 6\big)\cos(\phi)\\
&\quad +\big(2s\,\mathrm{sn}(s)\,\mathrm{dn}(s) + 4\,\mathrm{cn}(s)\,\mathrm{dn}^2(s) - 4\,\mathrm{sn}(s)\,\mathrm{dn}(s)E(s)\\
&\quad -2\,\mathrm{cn}(s)\big)\cos(\phi)k x_1(\varphi_0)\sin(\phi) + \big(-4\,\mathrm{dn}^2(s) + 2\big)k^2\cos(\phi)\\
&\quad +\big(4\,\mathrm{sn}^3(s)\,\mathrm{dn}(s) - 4\,\mathrm{sn}(s)\,\mathrm{dn}(s)\big)k^3\sin^3(\phi)\\
&\quad +\big(-2s\,\mathrm{dn}^2(s) + 4\,\mathrm{dn}^2(s)E(s) + s - 2E(s)\big)x_1(\varphi_0)\Big].
\end{aligned}
$$

$$
\begin{aligned}
\frac{\mathrm{d}x_5}{\mathrm{d}s} &= \frac{1}{\omega}\sin(\theta((s-\varphi_0)/\omega))x_1((s-\varphi_0)/\omega)^2 \\
&= \frac{1}{\omega^3}\Big[-8k^4\sin^3(\phi)\,\mathrm{sn}^4(s) - 8k^2x_1(\varphi_0)\,\sin(\phi)\cos(\phi)\,\mathrm{cn}(s)\,\mathrm{sn}(s)\,\mathrm{dn}(s) \\
&+ 2x_1(\varphi_0)^2k\cos(\phi)\,\mathrm{sn}(s)\,\mathrm{dn}(s) + \big(-8s\,\mathrm{cn}(s)\,\mathrm{sn}(s)\,\mathrm{dn}(s) \\
&+ 16\,\mathrm{cn}(s)\,\mathrm{sn}(s)\,\mathrm{dn}(s)E(s) - 8\,\mathrm{dn}^2(s) + 4\big)k^2\sin^3(\phi) \\
&+ \big(4s\,\mathrm{dn}^2(s) - 8\,\mathrm{dn}^2(s)E(s) - 2s + 4E(s)\big)\,x_1(\varphi_0)\,\sin(\phi)\cos(\phi) \\
&+ \big(-2s^2\,\mathrm{dn}^2(s) + 8s\,\mathrm{dn}^2(s)E(s) - 8\,\mathrm{dn}^2(s)E(s)^2 \\
&+ s^2 - 4sE(s) + 4E(s)^2\big)\sin(\phi) + \big(-2\,\mathrm{dn}^2(s) + 1\big)\,x_1(\varphi_0)^2\sin(\phi) \\
&+ (8s\,\mathrm{cn}(s)\,\mathrm{sn}(s)\,\mathrm{dn}(s) - 16\,\mathrm{cn}(s)\,\mathrm{sn}(s)\,\mathrm{dn}(s)E(s))\,k^2\sin(\phi) \\
&+ \big(2s^2\,\mathrm{sn}(s)\,\mathrm{dn}(s) + 8s\,\mathrm{cn}(s)\,\mathrm{dn}^2(s) - 8s\,\mathrm{sn}(s)\,\mathrm{dn}(s)E(s) \\
&- 16\,\mathrm{cn}(s)\,\mathrm{dn}^2(s)E(s) + 8\,\mathrm{sn}(s)\,\mathrm{dn}(s)E(s)^2 - 4s\,\mathrm{cn}(s) \\
&+ 8\,\mathrm{cn}(s)E(s)\big)k\cos^3(\phi) + \big(8\,\mathrm{sn}^3(s)\,\mathrm{dn}(s) - 8\,\mathrm{sn}(s)\,\mathrm{dn}(s)\big)k^3\cos^3(\phi) \\
&+ \big(-4s\,\mathrm{sn}(s)\,\mathrm{dn}(s) - 8\,\mathrm{cn}(s)\,\mathrm{dn}^2(s) + 8\,\mathrm{sn}(s)\,\mathrm{dn}(s)E(s) \\
&+ 4\,\mathrm{cn}(s)\big)x_1(\varphi_0)\,k\cos^2(\phi) + \big(-8s\,\mathrm{cn}(s)\,\mathrm{dn}^2(s) - 8\,\mathrm{cn}(s)E(s) \\
&+ 4s\,\mathrm{cn}(s) - 8\,\mathrm{cn}(s)E(s)\big)k\cos(\phi) + \big(-8\,\mathrm{sn}^3(s)\,\mathrm{dn}(s) \\
&+ 8\,\mathrm{sn}(s)\,\mathrm{dn}(s)\big)k^3\cos(\phi) + \big(2s^2\,\mathrm{dn}^2(s) - 8s\,\mathrm{dn}^2(s)E(s) \\
&+ 8\,\mathrm{dn}^2(s)E(s)^2 - s^2 + 4sE(s) - 4\,\mathrm{dn}^2(s) - 4E(s)^2 + 4\big)\sin^3(\phi) \\
&+ \big(8\,\mathrm{cn}(s)\,\mathrm{dn}^2(s) - 4\,\mathrm{cn}(s)\big)x_1(\varphi_0)\,k\Big].
\end{aligned}
$$

Proposition 2.1. *The solution $x(s)$ of the system* (2.80) *can be expressed as a polynomial function of $(s, \mathrm{sn}(s), \mathrm{cn}(s), \mathrm{dn}(s), E(s))$.*

Proof. Integrating equations (2.81) to (2.5.5) thanks to formulae (2.84) gives the result.

Remark 2.3. [49]

- sn, cn are $4K$-periodics,
- dn is $2K$-periodic,
- $E(s) = \frac{E}{K}s + Z(s)$ where E, K are complete integrals and Z is the $2K$-periodic zeta function.

The next step is to compute the x variables using quadratures in the oscillating case. Since $x(0) = 0$, solutions depend upon 4 independent parameters $H_i(0)$ for $i = 1, ..., 5$ coupled with the relation $H_1(t=0)^2 + H_2(t=0)^2 = 1$.
To integrate the equations (2.81)-(2.5.5) explicitly, we use the following primitive functions (see [49])

$$
\begin{aligned}
&\int \mathrm{dn}^2(s)ds = E(s), \quad \int \mathrm{cn}(s)\,\mathrm{dn}(s)ds = \mathrm{sn}(s), \quad \int \mathrm{cn}(s)\,\mathrm{sn}(s)\,\mathrm{dn}(s)ds = -\frac{1}{2}\,\mathrm{cn}(s)^2,\\
&\int \mathrm{cn}(s)ds = \frac{1}{k}\arctan\left(k\frac{\mathrm{sn}(s)}{\mathrm{dn}(s)}\right), \quad \int s\,\mathrm{sn}(s)\,\mathrm{dn}(s)ds = \frac{1}{k}\arctan\left(k\frac{\mathrm{sn}(s)}{\mathrm{dn}(s)}\right) - s\,\mathrm{cn}(s),\\
&\int E(s)\,\mathrm{sn}(s)\,\mathrm{dn}(s)ds = -E(s)\,\mathrm{cn}(s) + \frac{1}{2k}\arctan\left(k\frac{\mathrm{sn}(s)}{\mathrm{dn}(s)}\right) + \frac{1}{2}\,\mathrm{dn}(s)\,\mathrm{sn}(s),\\
&\int \mathrm{cn}(s)\,\mathrm{dn}^2(s)ds = \frac{1}{2k}\arctan\left(k\frac{\mathrm{sn}(s)}{\mathrm{dn}(s)}\right) + \frac{1}{2}\,\mathrm{dn}(s)\,\mathrm{sn}(s),\\
&\int E(s)\,\mathrm{dn}^2(s)ds = \frac{1}{2}E(s)^2, normal-form \quad \int \mathrm{cn}^2(s)ds = \frac{E(s)+(k^2-1)s}{k^2},\\
&\int \mathrm{sn}^4(s)ds = \frac{1}{3k^4}\left(k^2\,\mathrm{sn}(s)\,\mathrm{dn}(s)\,\mathrm{cn}(s) + (2+k^2)s - 2(k^2+1)E(s)\right),\\
&\int E(s)\,\mathrm{dn}(s)\,\mathrm{sn}(s)\,\mathrm{cn}(s)ds = \frac{1}{6k^2}\left((1-2k^2)E(s) + (k^2-1)s\right.\\
&\qquad \left. + k^2\,\mathrm{dn}(s)\,\mathrm{sn}(s)\,\mathrm{cn}(s) + 3k^2\,\mathrm{sn}^2(s)E(s)\right),\\
&\int E(s)^2\,\mathrm{dn}(s)\,\mathrm{sn}(s)ds = -\mathrm{cn}(s)E(s)^2 + 2\int E(s)\,\mathrm{dn}(s)^2\,\mathrm{cn}(s)ds\\
&\qquad = -\mathrm{cn}(s)E(s)^2 + E(s)\,\mathrm{dn}(s)\,\mathrm{sn}(s) - 1/3\,\mathrm{cn}(s)(-3+2k^2+k^2\,\mathrm{sn}^2(s)) + \int E(s)\,\mathrm{cn}(s)ds,\\
&\int \mathrm{sn}^3(s)\,\mathrm{dn}(s)ds = -1/3\,\mathrm{cn}(s)(2+\mathrm{sn}^2(s)), \quad \int s^2\,\mathrm{dn}(s)\,\mathrm{sn}(s)ds = -s^2\,\mathrm{cn}(s) + 2\int s\,\mathrm{cn}(s)ds,\\
&\int s\,\mathrm{dn}^2(s)\,\mathrm{cn}(s)ds = 1/2(\mathrm{dn}(s)\,\mathrm{sn}(s) + \mathrm{cn}(s) + \int s\,\mathrm{cn}(s)ds),\\
&\int s\,\mathrm{sn}(s)\,\mathrm{cn}(s)\,\mathrm{dn}(s)ds = \frac{1}{2}\left(\frac{E(s)+(k^2-1)s}{k^2} - s\,\mathrm{cn}^2(s)\right),\\
&\int sE(s)\,\mathrm{sn}(s)\,\mathrm{dn}(s)ds = s(-E(s)\,\mathrm{cn}(s) + 1/2\,\mathrm{dn}(s)\,\mathrm{sn}(s)) + 1/2\,\mathrm{cn}(s) + 1/2\int s\,\mathrm{cn}(s) + \int E(s)\,\mathrm{cn}(s).
\end{aligned}
\tag{2.84}
$$

The final expressions of the solution $(x_i(s))_{i=1,\dots,5}$ of (2.80). (we supply a MAPLE code to check the correctness of the expressions)

- $x_1(s) = \dfrac{1}{\omega}\left[x_1(\varphi_0) - 2k\,\sin(\phi)\,\mathrm{cn}(s) + (-s+2E(s))\cos(\phi)\right].$
- $x_2(s) = \dfrac{1}{\omega}\left[x_2(\varphi_0) - 2k\,\cos(\phi)\,\mathrm{cn}(s) + (s-2E(s))\sin(\phi)\right].$
- $x_3(s) = \dfrac{1}{\omega^2}\Big[x_3(\varphi_0) - \sin(2\phi)(\mathrm{sn}(s))^2k^2 + k^2\sin(2\phi) - 1/4\,\sin(2\phi)s^2$
  $+ \cos(2\phi)\,\mathrm{cn}(s)ks - 2kx_1(\varphi_0)\,\cos(\phi)\,\mathrm{cn}(s) - 2\,\mathrm{E}(s)\,\mathrm{cn}(s)k + s\,\mathrm{cn}(s)k$
  $- \sin(2\phi)(\mathrm{E}(s))^2 - 2x_1(\varphi_0)\,\sin(\phi)\,\mathrm{E}(s) + \sin(2\phi)s\,\mathrm{E}(s)$
  $+ 2\,\mathrm{dn}(s)k\,\mathrm{sn}(s) + x_1(\varphi_0)\,\sin(\phi)s - 2\cos(2\phi)\,\mathrm{cn}(s)\,\mathrm{E}(s)k\Big].$

- $$x_4(s) = \frac{1}{\omega^3}\Big[x_4(\varphi_0) - 2\cos^3(\phi)sk^2 + 2k^2x_1(\varphi_0)\cos^2(\phi) + 4\cos^3(\phi)\mathrm{E}(s)k^2$$
$$+ x_3(\varphi_0)\sin(\phi)s - 2x_3(\varphi_0)\sin(\phi)\mathrm{E}(s) - \cos^3(\phi)s^2\mathrm{E}(s)$$
$$+ 2\cos^3(\phi)s(\mathrm{E}(s)^2 + \cos(\phi)s^2\mathrm{E}(s) - 1/6\cos(\phi)s^3 - 4/3\cos^3(\phi)\mathrm{E}(s)^3$$
$$- 1/2x_1(\varphi_0)\cos^2(\phi)s^2 - 2x_1(\varphi_0)\cos^2(\phi)\mathrm{E}(s)^2 - 2\cos(\phi)s\mathrm{E}(s)^2$$
$$- 2x_1(\varphi_0)s\mathrm{E}(s) + k\sin(\phi)\mathrm{cn}(s)s^2\cos^2(\phi) + 2\cos^3(\phi)sk^2\mathrm{sn}(s)^2$$
$$- 2/3\cos(\phi)\mathrm{E}(s) + 4/3k^3\mathrm{cn}(s)\mathrm{sn}(s)^2\sin(\phi)\cos^2(\phi) + 2k\sin(\phi)\mathrm{cn}(s)$$
$$+ 2/3\cos(\phi)s - 8/3\cos(\phi)k^2\mathrm{dn}(s)\mathrm{sn}(s)\mathrm{cn}(s) - 8/3k^3\sin(\phi)\mathrm{cn}(s)$$
$$+ 4/3\,\mathrm{E}(s)k^2\cos(\phi) - 2/3sk^2\cos(\phi) - 4\cos^3(\phi)k^2\mathrm{sn}(s)^2\mathrm{E}(s)$$
$$+ 2x_1(\varphi_0)\cos^2(\phi)s\mathrm{E}(s) - 2x_3(\varphi_0)k\cos(\phi)\mathrm{cn}(s) + 1/2x_1(\varphi_0)s^2$$
$$- 4/3k^3\sin(\phi)\mathrm{cn}(s)\cos^2(\phi) - 2k\sin(\phi)\mathrm{cn}(s)x_1(\varphi_0)\cos(\phi)s$$
$$+ 4k\sin(\phi)\mathrm{cn}(s)x_1(\varphi_0)\cos(\phi)\mathrm{E}(s) + 1/6\cos^3(\phi)s^3 + 4/3\cos(\phi)(\mathrm{E}(s)^3$$
$$- 4/3k^3\mathrm{cn}(s)\mathrm{sn}(s)^2\sin(\phi) - 2k^2x_1(\varphi_0)\cos^2(\phi)\mathrm{sn}(s)^2 + 2x_1(\varphi_0)\,\mathrm{E}(s)^2$$
$$- 4k\sin(\phi)\mathrm{cn}(s)s\mathrm{E}(s)\cos^2(\phi) + 4k\sin(\phi)\mathrm{cn}(s)\mathrm{E}(s)^2\cos^2(\phi)\Big].$$
- $$x_5(s) = \frac{1}{\omega^3}\Big[x_5(\varphi_0) + -4k^2x_1(\varphi_0)\sin(\phi)\cos(\phi)\mathrm{sn}(s)^2 - 4/3s\sin(\phi)$$
$$+ 4\cos^2(\phi)\sin(\phi)sk^2\mathrm{sn}(s)^2 - 8\cos^2(\phi)\sin(\phi)k^2\mathrm{sn}(s)^2\mathrm{E}(s)$$
$$+ 4x_1(\varphi_0)\cos^2(\phi)sk\,\mathrm{cn}(s) - 8x_1(\varphi_0)\cos^2(\phi)\mathrm{E}(s)k\,\mathrm{cn}(s)$$
$$+ 8k\cos(\phi)\mathrm{E}(s)\mathrm{sn}(s)\mathrm{dn}(s) - 4k\cos(\phi)s\,\mathrm{sn}(s)\,\mathrm{dn}(s)$$
$$+ 8k\cos^3(\phi)\mathrm{cn}(s)s\mathrm{E}(s) + 4x_1(\varphi_0)\sin(\phi)\cos(\phi)s\mathrm{E}(s)$$
$$+ 4k^2x_1(\varphi_0)\sin(\phi)\cos(\phi) + 8\cos^2(\phi)\sin(\phi)\mathrm{E}(s)k^2 - 8/3\sin(\phi)\mathrm{E}(s)k^2$$
$$- 4\cos^2(\phi)\sin(\phi)sk^2 - 2k\cos^3(\phi)\mathrm{cn}(s)s^2 - 8k\cos^3(\phi)\mathrm{cn}(s)\mathrm{E}(s)^2$$
$$+ 4\sin(\phi)\cos^2(\phi)s\mathrm{E}(s)^2 - 2\sin(\phi)\cos^2(\phi)s^2\mathrm{E}(s) - x_1(\varphi_0)\cos(\phi)\sin(\phi)s^2$$
$$- 2x_1(\varphi_0)^2k\cos(\phi)\mathrm{cn}(s) - 4x_1(\varphi_0)\sin(\phi)\cos(\phi)(\mathrm{E}(s)^2 + 4k\cos(\phi)\mathrm{cn}(s)$$
$$- 8k^3\cos(\phi)\mathrm{cn}(s) - 2x_1(\varphi_0)^2\sin(\phi)\mathrm{E}(s) + 1/3\sin(\phi)\cos^2(\phi)s^3$$
$$- 8/3\sin(\phi)\cos^2(\phi)\mathrm{E}(s)^3 + x_1(\varphi_0)^2\sin(\phi)s - 8/3k^3\cos^3(\phi)\mathrm{cn}(s)\,\mathrm{sn}(s)^2$$
$$+ 4/3\,\mathrm{E}(s)\sin(\phi) + 4/3\sin(\phi)sk^2 - 8/3k^2\mathrm{dn}(s)\mathrm{sn}(s)\mathrm{cn}(s)\sin(\phi)$$
$$+ 4x_1(\varphi_0)k\,\mathrm{sn}(s)\,\mathrm{dn}(s) + 8/3k^3\cos^3(\phi)\mathrm{cn}(s)\Big].$$

Rotating case

We can perform the same computations as in the oscillating case. This is not necessary in the Purcell case since the shape variables are bounded.

Abnormal case.

According to [14], we consider the minimal time problem for the single-input affine system

$$\dot{x}(t) = \widehat{F}_1(x(t)) + s(t)\widehat{F}_2(x(t))$$

where s is a scalar control.
Denoting $x(.)$ a reference minimum time trajectory, it follows from the Pontryagin maximum principle that along the extremal lift of $x(.)$, there must hold $H_2(x(.),p(.)) = 0$ and derivating with respect to t, $\{H_1,H_2\}(x(.),p(.)) = 0$ must hold too. Thanks to a further derivation, the extremals associated with the controls

$$u_a(x,p) = \frac{\{H_1,\{H_2,H_1\}\}(x,p)}{\{H_2,\{H_1,H_2\}\}(x,p)} = \frac{2p_5}{p_4}$$

satisfy the constraints $H_2 = \{H_1,H_2\} = 0$ along $(x(.),p(.))$ and are solutions of

$$\dot{x} = \frac{\partial H_a}{\partial p}, \quad \dot{p} = -\frac{\partial H_a}{\partial x}$$

where H_a is the true Hamiltonian

$$H_a(x,p) = H_1(x,p) + u_a H_2(x,p) = p_1 + 2\,\frac{p_5\,\left(p_2 + p_3 x_1 + p_4 x_3 + p_5 {x_1}^2\right)}{p_4}.$$

We consider the abnormal extremals that is the constraint $H_1(x(.),p(.)) = 0$ must hold. The extremal system subject to the constraints $H_1 = H_2 = \{H_1,H_2\} = 0$ is integrable and solutions can be written as

$$x_1(t) = t + x_1(0), \qquad x_2(t) = 2\,\frac{p_5(0)\,t}{p_4(0)} + x_2(0),$$

$$x_3(t) = \frac{p_5(0)\,t^2}{p_4(0)} + 2\,\frac{p_5(0)\,x_1(0)\,t}{p_4(0)} + x_3(0),$$

$$x_4(t) = 2/3\,\frac{p_5(0)^2 t^3}{p_4(0)^2} - 2\,\frac{p_5(0)\,\Big(p_5(0)\,x_1(0)^2 + p_3(0)\,x_1(0) + p_2(0)\Big)\,t}{p_4(0)^2} - \frac{p_5(0)\,p_3(0)\,t^2}{p_4(0)^2} + x_4(0),$$

$$x_5(t) = 2/3\,\frac{p_5(0)\,t^3}{p_4(0)} + \frac{(4\,p_5(0)\,x_1(0) + p_3(0))\,t^2}{p_4(0)} + 2\,\frac{\Big(2\,p_5(0)\,x_1(0)^2 + p_3(0)\,x_1(0) + x_3(0)\,p_4(0) + p_2(0)\Big)\,t}{p_4(0)} + x_5(0),$$

$$p_1(t) = \left(-2\,\frac{p_5(0)\,p_3(0)}{p_4(0)} - 4\,\frac{p_5(0)^2 x_1(0)}{p_4(0)}\right) t + p_1(0),$$

$$p_2(t) = p_2(0), \qquad p_3(t) = -2\,p_5(0)\,t + p_3(0), \qquad p_4(t) = p_4(0), \qquad p_5(t) = p_5(0)$$

with $(x_1(0), x_2(0), x_3(0), x_4(0), x_5(0), p_1(0), p_2(0), p_3(0), p_4(0), p_5(0))$ are constants satisfying

$$p_1(0) = 0,\ p_2(0) = p_5(0)x_1(0)^2 - p_4(0)x_3(0),\ p_3(0) = -2p_5(0)x_1(0).$$

2.6 Numerical results

This section presents the numerical simulations performed on the Purcell swimmer problem. Simulations are performed using both direct and indirect methods, using the solvers BOCOP and HAMPATH. We use the multipliers from the solutions of the direct method to initialize the costate variables in the indirect approach. We show the optimal trajectories obtained for the nilpotent approximation and the true mechanical system.

BOCOP.

BOCOP (`www.bocop.org`, [11]) implements a so-called direct transcription method. Namely, a time discretization is used to rewrite the optimal control problem as a finite dimensional optimization problem (i.e nonlinear programming), solved by an interior point method (IPOPT). We recall below the optimal control problem, formulated with the state $q = (\alpha_1, \alpha_2, x, y, \theta)$ and control $u = (\dot{\alpha}_1, \dot{\alpha}_2)$

$$\begin{cases} \text{Min } \int_0^T E(u(t))dt \\ \dot{q}(t) = F_1(q(t))\,u_1(t) + F_2(q(t))\,u_2(t) \\ \alpha_{1|2}(t) \in [-a,a] \\ x(0) = y(0) = 0,\ x(T) = x_f \\ y(T) = y_f,\ \theta(T) = \theta(0),\ \alpha_{1|2}(T) = \alpha_{1|2}(0) \end{cases} \tag{2.85}$$

HAMPATH.

The HAMPATH software (`http://cots.perso.enseeiht.fr/hampath/`, [29]) is based upon indirect methods to solve optimal control problems using simple shooting methods and testing the local optimality of the solutions.
More precisely two purposes are achieved with HAMPATH:

- *Shooting equations:* to compute periodic trajectories of the Purcell swimmer, we consider the true Hamiltonian H given by the Pontryagin maximum principle and the transversality conditions associated with. The normal and regular minimizing curves are the projection of extremals solutions of the boundary two values problem

$$\begin{cases} \dot{q} = \frac{\partial H}{\partial p}, \qquad \dot{p} = -\frac{\partial H}{\partial q}, \\ x(0) = x_0, \quad x(T) = x_f, \quad y(0) = 0, \quad y(T) = y_f \\ \alpha_{1|2}(T) = \alpha_{1|2}(0), \quad \theta(T) = \theta(0), \\ p_{\alpha_{1|2}}(T) = p_{\alpha_{1|2}}(0), \quad p_\theta(T) = p_\theta(0). \end{cases} \tag{2.86}$$

  where $q = (x, y, \alpha_1, \alpha_2, \theta)$, $p = (p_x, p_y, p_{\alpha_1}, p_{\alpha_2}, p_\theta)$ and $T > 0$ is fixed.
  Due to the sensitivity of the initialization of the shooting algorithm, the latter is initialized with direct methods namely the BOCOP toolbox.
- *Local optimality:* to show that the normal stroke is optimal we perform a rank test on the subspaces spanned by solutions of the variational equation with suitable initial conditions [14].

2.6.1 Nilpotent approximation

Notations: state $x = (x_1, x_2, x_3, x_4, x_5)$, costate $p = (p_1, p_2, p_3, p_4, p_5)$, $\widehat{F}_1, \widehat{F}_2$ the normal form given by (15), and H_1, H_2 are the respective Hamiltonian lifts.

Normal case

In the normal case, we consider the extremal system given by the true Hamiltonian given by (2.78). We compute the optimal trajectories with HAMPATH, and show the state and adjoint variables as functions of time on Fig.2.11. We also illustrate

the conjugate points computed according to the algorithm in [21], as well as the smallest singular value for the rank test.

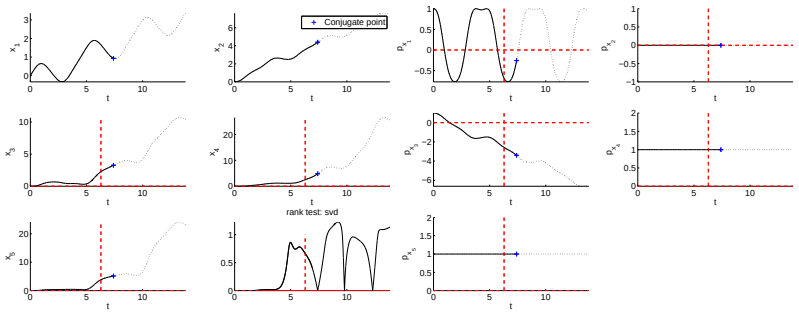

Fig. 2.11 Nilpotent approximation (normal case): state, adjoint variables and first conjugate point (blue cross), with the smallest singular value of the rank test.

Property on the first conjugate point. Let us consider the fixed energy level $H_1(t=0)^2 + H_2(t=0)^2 = 1$ along the extremals and the initial state $x(0) = 0$. We take a large number of random initial adjoint vectors $p(0)$ and numerically integrate the extremal system. For each normal extremal, we compute the first conjugate time t_{1c}, the pulsation $\omega = (p_4(0)^2 + 4\,p_5(0)^2)^{1/4}$, and the complete elliptic integral $K(k)$, where k is the amplitude

$$k = \frac{1}{2}\sqrt{\frac{2\sqrt{p_4(0)^2 + 4\,p_5(0)^2} + p_3(0)^2 - 2\,p_1(0)\,p_4(0) - 4\,p_5(0)\,p_2(0) - 4\,p_5(0)\,p_4(0)\,x_3(0)}{\sqrt{p_4(0)^2 + 4\,p_5(0)^2}}}.$$

Let $\gamma(.)$ be a normal extremal starting at $t = 0$ from the origin and defined on $[0, +\infty[$. As illustrated on Fig.2.12, there exists a first conjugate point along γ corresponding to a conjugate time t_{1c} satisfying the inequality:

$$0.3\omega t_{1c} - 0.4 < K(k) < 0.5\omega t_{1c} - 0.8.$$

Remark 2.4. In section 2.5.5 $u = \omega t + \varphi_0$ is the normalized parametrization of the solutions.

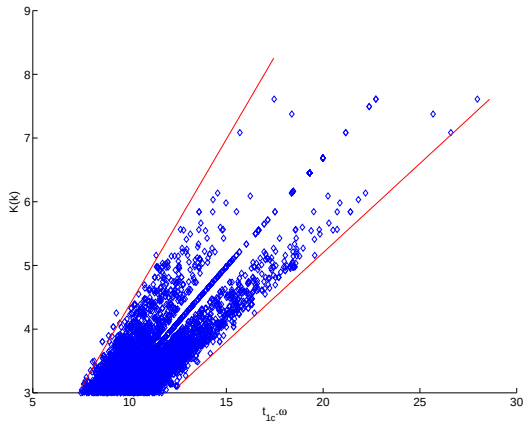

Fig. 2.12 Normal extremals with constant energy $H_1^2 + H_2^2 = 1$. The first conjugate point on the elliptic integral $K(k, \omega t_c)$ satisfies $0.3\omega t_{1c} - 0.4 < K(k) < 0.5\omega t_{1c} - 0.8$. Illustration for random initial costate $p(0)$.

Abnormal case

Fig.2.13 illustrates the time evolution of the state variables. We check the second order optimality conditions thanks to the algorithm given in [14]. The determinant test and smallest singular value for the rank condition both indicate that there is no conjugate time for abnormal extremals (Fig.2.14).

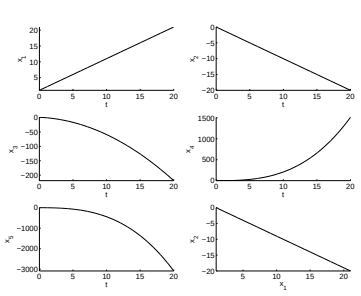

Fig. 2.13 Abnormal case: state variables for $x(0) = (1,0,1,0,0)$, $p(0) = (0,0,-2,1,1)$.

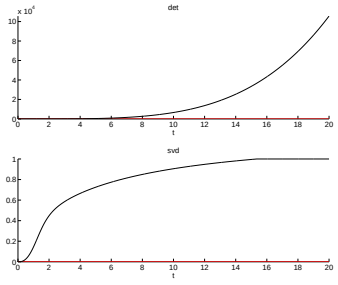

Fig. 2.14 Abnormal case: the second order sufficient condition indicates there is no conjugate point.

2.6.2 True mechanical system

We now consider the optimal control problem (2.85) consisting in minimizing either the mechanical energy (2.5.2) or the criterion $|u|^2$.

Direct method. In the first set of simulations performed by BOCOP, we set $T = 10$, $x_f = 0.5$, and the bounds $a = 3$ large enough so that the solution is actually unconstrained. The state and control variables for the optimal trajectory are shown on Fig.2.15, 2.16 and 2.17, and we observe that the trajectory is actually a sequence of identical strokes. Fig.2.18 shows the phase portrait for the shape angles α_1, α_2, which is an ellipse. The constant energy level satisfied by the optimal trajectory means the phase portrait of the controls is a circle for the $|u|^2$ criterion, but not for the energy criterion. The adjoint variables (or more accurately in this case, the multipliers associated to the discretized dynamics) are shown on Fig.2.19-2.20.

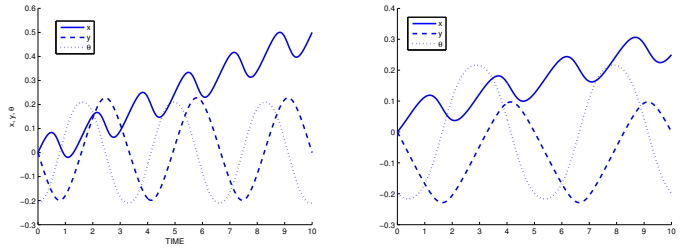

Fig. 2.15 Optimal trajectory for $|u|^2$ and energy criterion - state variables x, y, θ

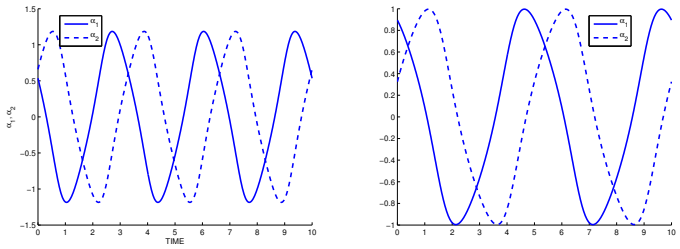

Fig. 2.16 Optimal trajectory for $|u|^2$ and energy criterion - state variables α_1, α_2

Indirect method. Now we use the multipliers from the BOCOP solutions to initialize the shooting algorithm of HAMPATH. Fig.2.21-2.22 and Fig.2.23-2.24 represent respectively an non intersecting curve and an eight shape curve with the same boundary values. Fig.2.25-2.26 shows another eight shape curve obtained for different boundary values. In this three cases, we check the second order optimality

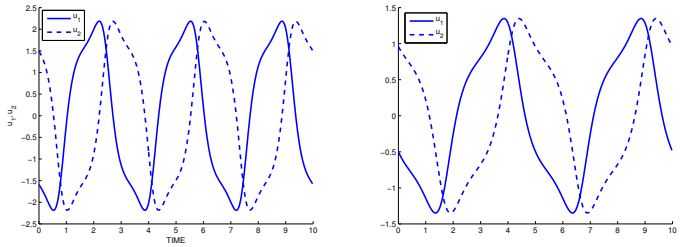

Fig. 2.17 Optimal trajectory for $|u|^2$ and energy criterion - control variables

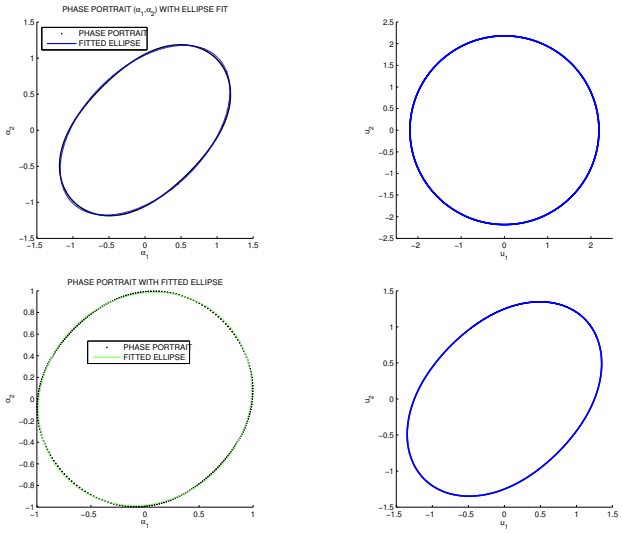

Fig. 2.18 Optimal trajectory for $|u|^2$ and energy criterion - Phase portrait (ellipse) and controls

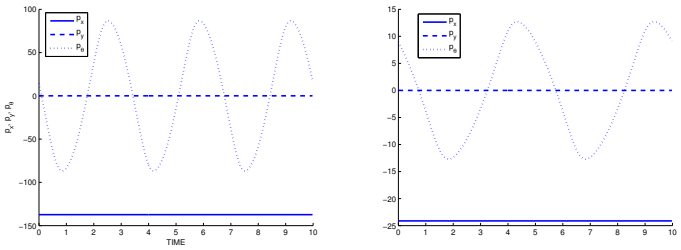

Fig. 2.19 Optimal trajectory for $|u|^2$ and energy criterion - adjoint variables

conditions according to [21] and observe that there is no conjugate point on $[0,T]$ where $T = 2\pi$.

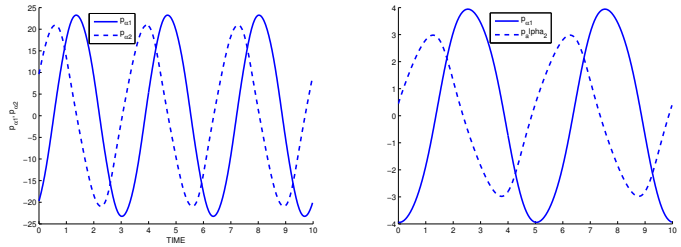

Fig. 2.20 Optimal trajectoryfor $|u|^2$ and energy criterion - adjoint variables $p_{\alpha_1}, p_{\alpha_2}$

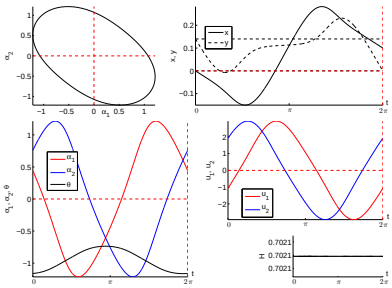

Fig. 2.21 Non self-intersecting solution for the $|u|^2$ criterion ($x_0 = 0$, $y_0 = 0.14$, $x_f = 0.1$, $y_f = 0$).

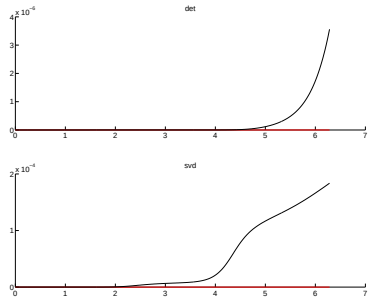

Fig. 2.22 Second order conditions: no conjugate time $t_{1c} \in [0, 2\pi]$.

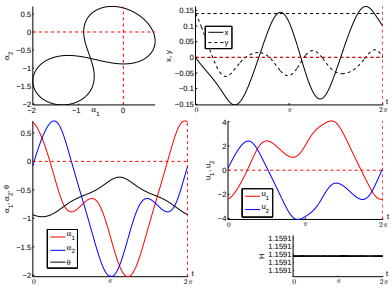

Fig. 2.23 Solution `8-SONE` for the $|u|^2$ criterion ($x_0 = 0$, $y_0 = 0.14$, $x_f = 0.1$, $y_f = 0$).

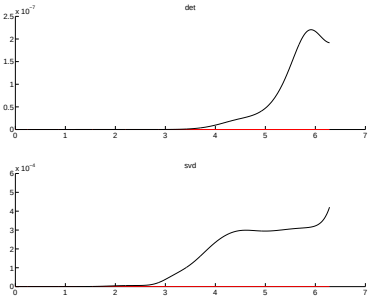

Fig. 2.24 Second order conditions: no conjugate time $t_{1c} \in [0, 2\pi]$.

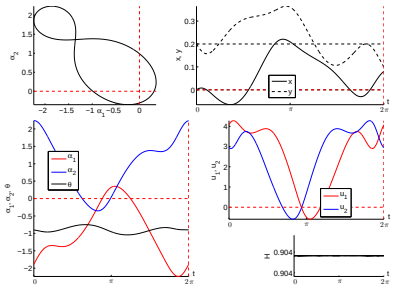

Fig. 2.25 Solution `8-NOSE` for the $|u|^2$ criterion ($x_0 = 0$, $y_0 = 0.2$, $x_f = 0.08$, $y_f = 0.1$).

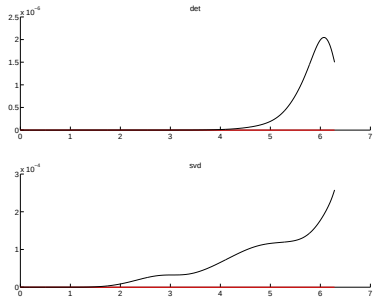

Fig. 2.26 Second order conditions: no conjugate time $t_{1c} \in [0, 2\pi]$.

2.6.3 Copepod swimmer

Geometric analysis of a copepod swimmer

In [64], two types of geometric motions are described.

First case: (Fig. 2.27) The two legs are assumed to oscillate sinusoidally according to

$$\theta_1 = \Phi_1 + a\cos(t), \quad \theta_2 = \Phi_2 + a\cos(t + k_2)$$

with $a = \pi/4$, $\Phi_1 = \pi/4$, $\Phi_2 = 3\pi/4$ and $k_2 = \pi/2$. This produces a displacement $x_0(2\pi) = 0.2$.

Second case: (Fig. 2.29) The two legs are paddling in sequence followed by a recovery stroke performed in unison. In this case the controls $u_1 = \dot{\theta}_1$, $u_2 = \dot{\theta}_2$ produce bang arcs to steer the angles between from the boundary 0 of the domain to the boundary π, while the unison sequence corresponds to a displacement from π to 0 with the constraint $\theta_1 = \theta_2$.

Our first objective is to relate these properties to geometric optimal control.

Abnormal curves in the copepod swimmer

Let $q = (x_0, \theta_1, \theta_2)$, then the system takes the form

$$\dot{q}(t) = \sum_{i=1}^{2} u_i(t) F_i(q(t))$$

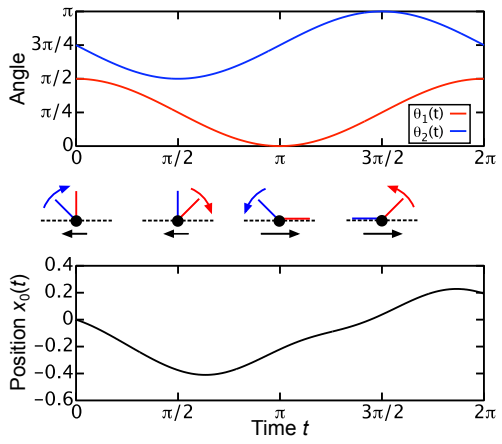

Fig. 2.27 Two legs oscillating sinusoidally according to $\theta_1 = \pi/4 + a\cos t$ and $\theta_2 = 3\pi/4 + a\cos(t+\pi/2)$, where $a = \pi/4$ is the amplitude. The second leg (blue) oscillates about $\Phi_2 = 3\pi/4$, while the first leg (red) oscillates about $\Phi_1 = \pi/4$ with a phase lag of $\pi/2$. The swimmer position x_0 translates about a fifth of the leg length after one cycle.

where the control vector fields are given by

$$F_i = \frac{\sin(\theta_i)}{\Delta}\frac{\partial}{\partial x_0} + \frac{\partial}{\partial \theta_i}$$

Lie brackets in the copepod case

$$F_3 = [F_1, F_2] = F(\theta_1, \theta_2)\frac{\partial}{\partial x_0}$$

with

$$\begin{aligned} F(\theta_1,\theta_2) &= \frac{2\sin(\theta_1)\sin(\theta_2)(\cos(\theta_1)-\cos(\theta_2))}{\Delta^2}, \\ [[F_1,F_2],F_1] &= \frac{\partial F}{\partial \theta_1}(\theta_1,\theta_2)\frac{\partial}{\partial x_0}, \\ [[F_1,F_2],F_2] &= \frac{\partial F}{\partial \theta_2}(\theta_1,\theta_2)\frac{\partial}{\partial x_0}. \end{aligned}$$

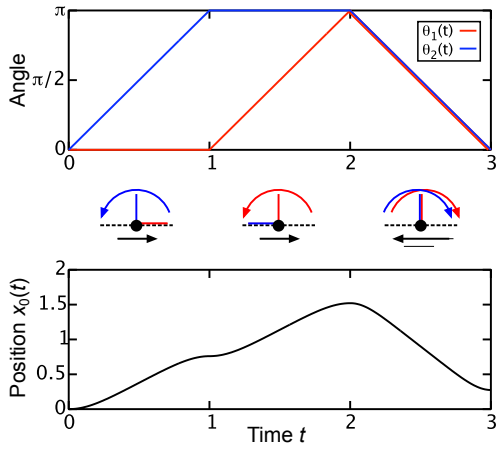

Fig. 2.28 Two legs paddling in sequence. The legs perform power strokes in sequence and then a recovery stroke in unison, each stroke sweeping an angle π.

Lemma 2.2. *The singular set* $\Sigma : \{q;\ \det(F_1(q), F_2(q), [F_1,F_2](q)) = 0\}$*, where the vector fields* $F_1, F_2, [F_1,F_2]$ *are collinear, is given by* $2\sin(\theta_1)\sin(\theta_2)(\cos(\theta_1) - \cos(\theta_2)) = 0$ *that is*

- $\theta_i = 0$ *or* π $i = 1,2$,
- $\theta_1 = \theta_2$

and formed the boundary of the physical domain: $\theta_i \in [0,\pi], \theta_1 \leq \theta_2$*, with respective controls* $u_1 = 0,\ u_2 = 0$ *or* $u_1 = u_2$ *forming a stroke of a triangle shape.*

Remark 2.5. Each point of the boundary is a Martinet point except at the non smooth points (vertices).

Hence we get the interpretation of the triangle shape stroke in terms of abnormal curves.

To rely smooth policies to optimal control we must introduce the cost function related to the mechanical energy. Recall that according to [57] the mechanical energy of the copepod swimmer is given by

$$\int_0^T \dot{q}^t M \dot{q} dt$$

where $q = (x_0, \theta_1, \theta_2)$, M is the symmetric matrix

$$M = \begin{pmatrix} 2 - 1/2(\cos^2(\theta_1) + \cos^2(\theta_2)) & -1/2\sin(\theta_1) & -1/2\sin(\theta_2) \\ -1/2\sin(\theta_1) & 1/3 & 0 \\ -1/2\sin(\theta_2) & 0 & 1/3 \end{pmatrix}. \tag{2.87}$$

Taking into account the velocities constraints, the integrand can be written as

$$a(q)u_1^2 + 2b(q)u_1u_2 + c(q)u_2^2$$

where

$$\begin{aligned} a &= \frac{1}{3} - \frac{\sin^2\theta_1}{2(2+\sin^2\theta_1+\sin^2\theta_2)}, \\ b &= -\frac{\sin\theta_1\sin\theta_2}{2(2+\sin^2\theta_1+\sin^2\theta_2)}, \\ c &= \frac{1}{3} - \frac{\sin^2\theta_2}{2(2+\sin^2\theta_1+\sin^2\theta_2)}. \end{aligned}$$

The pseudo-Hamiltonian in the normal case is

$$H(q,p) = u_1H_1(q,p) + u_2H_2(q,p) - \frac{1}{2}\Big(a(q)u_1^2 + 2b(q)u_1u_2 + c(q)u_2^2\Big).$$

The normal controls are computed solving the equations

$$\frac{\partial H}{\partial u_1} = 0, \qquad \frac{\partial H}{\partial u_2} = 0.$$

Computing one gets

$$\begin{aligned} u_1 &= -\frac{3(4H_1 + 2H_1\sin^2\theta_1 + 3H_2\sin\theta_1\sin\theta_2 - H_1\sin^2\theta_2)}{\sin^2\theta_1 + \sin^2\theta_2 - 4}, \\ u_2 &= -\frac{9H_1\sin\theta_1\sin\theta_2 + 6H_2(2+\sin^2\theta_2) - 3H_2\sin^2\theta_1}{\sin^2\theta_1 + \sin^2\theta_2 - 4}. \end{aligned}$$

and plugging such u into the pseudo-Hamiltonian gives the true Hamiltonian which is denoted H_n.

Note also that H_n can be computed constructing an orthonormal basis of the metric using a feedback transformation $u = \beta(q)v$ to transform the problem into

$$\dot{q} = (F\beta)(v), \quad \min \to \int_0^T (v_1^2 + v_2^2)dt$$

where F is the matrix (F_1, F_2). Writing $F\beta = (F_1', F_2')$, F_1', F_2' will form an orthonormal frame. The computation is straightforward and the normal Hamiltonian H_n takes the form $H_n = \frac{1}{2}(H_1'^2 + H_2'^2)$ where H_i' is the Hamiltonian lift of F_i'.

Geometric classification of smooth strokes

The expected strokes are related to the classification of smooth curves in the plane up to a diffeomorphism relaxing in our discussion the state constraints on the shape variable. This problem was studied by Whitney (1937) and Arnold (1994) , see [8]. In this classification we have in particular

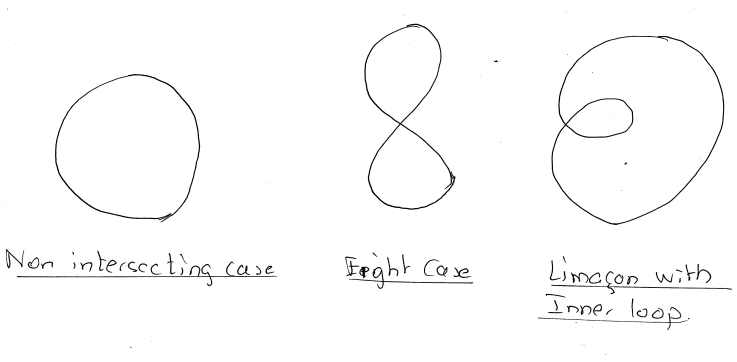

Fig. 2.29 Some examples of plane curves

Each such curve having a physical interpretation.

Numerical computations

In this final section we present the numerical computation of the stroke using the weak Maximum Principle. An important point is the transversality condition associated with the periodicity requirement $\theta_i(0) = \theta_i(2\pi),\ i = 1,2$ and the corresponding conditions are

$$p_{\theta_i}(0) = p_{\theta_i}(2\pi),\ i = 1,2.$$

The solutions are computed via a shooting method using the Hampath code and we perform the usual test to evaluate the conjugate point on a given stroke. Finally we evaluate numerically the value function which reduces to $2\pi H_n$ the given reference geodesic, since H_n is constant.

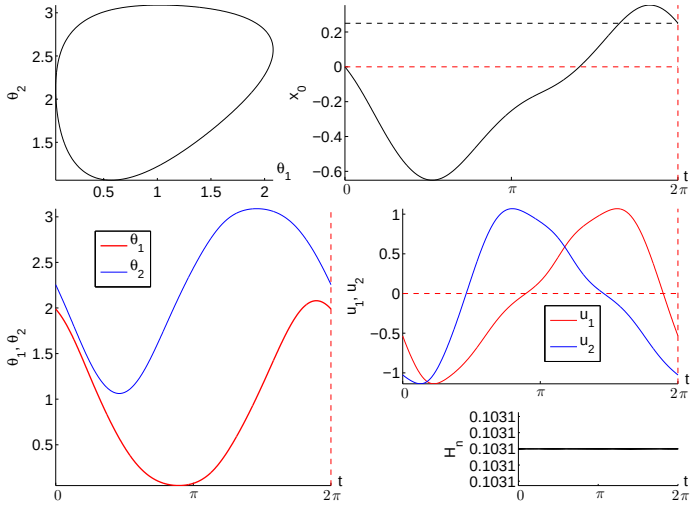

Fig. 2.30 Optimal stroke for the mechanical cost: non intersecting case. We fixed the displacement to $x_0(2\pi) = 0.25$.

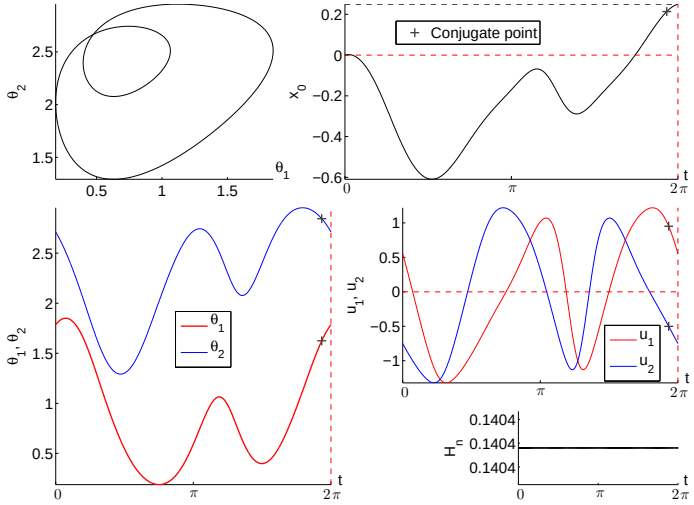

Fig. 2.31 Optimal stroke for the mechanical cost: limaçon with inner loop case. We fixed the displacement to $x_0(2\pi) = 0.25$.

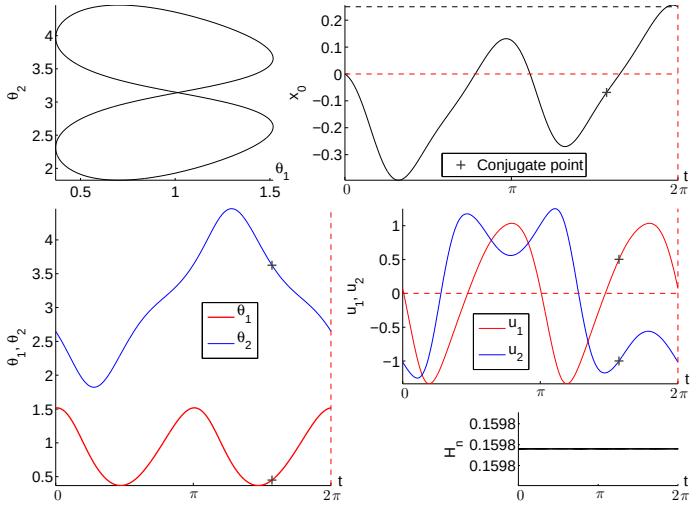

Fig. 2.32 Optimal stroke for the mechanical cost: eight case. We fixed the displacement to $x_0(2\pi) = 0.25$.

Chapter 3
Maximum Principle and Application to Nuclear Magnetic Resonance and Magnetic Resonance Imaging

3.1 Maximum Principle

In this section we state the Pontryagin maximum principle and we outline the proof. We adopt the presentation from Lee and Markus [50] where the result is presented into two theorems. The complete proof is complicated but rather standard, see the original book from the authors [58].

Theorem 6 *We consider a system of* $\mathbb{R}^n : \dot{x}(t) = f(x(t), u(t))$*, where* $f : \mathbb{R}^{n+m} \to \mathbb{R}^n$ *is a* C^1*-mapping. The family* $\mathscr{U}$ *of admissible controls is the set of bounded measurable mappings* $u(\cdot)$*, defined on* $[0,T]$ *with values in a control domain* $\Omega \subset \mathbb{R}^m$ *such that the response* $x(\cdot, x_0, u)$ *is defined on* $[0,T]$*. Let* $\bar{u}(\cdot) \in \mathscr{U}$ *be a control and let* $\bar{x}(\cdot)$ *be the associated trajectory such that* $\bar{x}(T)$ *belongs to the boundary of the accessibility set* $A(x_0, T)$*. Then there exists* $\bar{p}(\cdot) \in \mathbb{R}^n \setminus \{0\}$*, an absolutely continuous function defined on* $[0,T]$ *solution almost everywhere of the adjoint system:*

$$\dot{p}(t) = -p(t)\frac{\partial f}{\partial x}(\bar{x}(t), \bar{u}(t)) \tag{3.1}$$

such that for almost every $t \in [0,T]$ *we have*

$$H(\bar{x}(t), \bar{p}(t), \bar{u}(t)) = M(\bar{x}(t), \bar{p}(t)) \tag{3.2}$$

where

$$H(x, p, u) = \langle p, f(x, u) \rangle$$

and

$$M(x, p) = \max_{u \in \Omega} H(x, p, u)$$

Moreover $t \mapsto M(\bar{x}(t), \bar{p}(t))$ *is constant on* $[0,T]$.

Proof. The accessibility set is not in general convex and it must be approximated along the reference trajectory $\bar{x}(\cdot)$ by a convex cone. The approximation is obtained

by using *needle type variations* of the control $\bar{u}(\cdot)$ which are closed for the L^1-topology. (We do not use L^∞ perturbations and the Fréchet derivative of the end-point mapping computed in this Banach space.)

Needle type approximation

We say that $0 \leq t_1 \leq T$ is a *regular time* for the reference trajectory if

$$\frac{d}{dt}_{|t=t_1} \int_0^t f(\bar{x}(\tau), \bar{u}(\tau)) d\tau = f(\bar{x}(t_1), \bar{u}(t_1))$$

and from measure theory we have that almost every point of $[0,T]$ is regular.

At a regular time t_1, we define the following L^1-perturbation $\bar{u}_\varepsilon(\cdot)$ of the reference control: we fix $l, \varepsilon \geq 0$ small enough and we set

$$\bar{u}_\varepsilon(t) = \begin{cases} u_1 \in \Omega \text{ constant on } [t_1 - l\varepsilon, t_1] \\ \bar{u}(t) \text{ otherwise on } [0,T] \end{cases}$$

We denote by $\bar{x}_\varepsilon(\cdot)$ the associated trajectory starting at $\bar{x}_\varepsilon(0) = x_0$. We denote by $\varepsilon \mapsto \alpha_t(\varepsilon)$ the curve defined by $\alpha_t(\varepsilon) = \bar{x}_\varepsilon(t)$ for $t \geq t_1$. We have

$$\bar{x}_\varepsilon(t_1) = \bar{x}(t_1 - l\varepsilon) + \int_{t_1 - l\varepsilon}^{t_1} f(\bar{x}_\varepsilon(t), \bar{u}_\varepsilon(t)) dt$$

where $\bar{u}_\varepsilon = u_1$ on $[t_1 - l\varepsilon, t_1]$, Moreover

$$\bar{x}(t_1) = \bar{x}(t_1 - l\varepsilon) + \int_{t_1 - l\varepsilon}^{t_1} f(\bar{x}(t), \bar{u}(t)) dt$$

and since t_1 is a regular time for $\bar{x}(\cdot)$ we have

$$\bar{x}_\varepsilon(t_1) - \bar{x}(t_1) = l\varepsilon(f(\bar{x}(t_1), u_1) - f(\bar{x}(t_1), \bar{u}(t_1))) + o(\varepsilon).$$

In particular if we consider the curve $\varepsilon \mapsto \alpha_{t_1}(\varepsilon)$, it is a curve with origin $\bar{x}(t_1)$ and whose tangent vector is given by

$$v = l(f(\bar{x}(t_1), u_1) - f(\bar{x}(t_1), \bar{u}(t_1))). \tag{3.3}$$

For $t \geq t_1$, consider the local diffeomorphism: $\phi_t(y) = x(t, t_1, y, \bar{u})$ where $x(\cdot, t_1, y, \bar{u})$ is the solution corresponding to $\bar{u}(\cdot)$ and starting at $t = t_1$ from y. By construction we have $\alpha_t(\varepsilon) = \phi_t(\alpha_t(\varepsilon))$ for ε small enough and moreover for $t \geq t_1$, $v_t = \frac{d}{d\varepsilon}_{|\varepsilon=0} \alpha_t(\varepsilon)$ is the image of v by the Jacobian $\frac{\partial \phi_t}{\partial x}$. In other words v_t is the solution at time t of the variated equation

$$\frac{dV}{dt} = \frac{\partial f}{\partial x}(\bar{x}(t), \bar{u}(t)) V \tag{3.4}$$

with condition $v_t = v$ for $t = t_1$. We can extend v_t on the whole interval $[0,T]$. The construction can be done for an arbitrary choice of t_1, l and u_1. Let $\Pi = \{t_1, l, u_1\}$ be fixed, we denote by $v_\Pi(t)$ the corresponding vector v_t.

Additivity property

Let t_1, t_2 be two regular points of $\bar{u}(\cdot)$ with $t_1 < t_2$ and l_1, l_2 small enough. We define the following perturbation

$$\bar{u}_\varepsilon(t) = \begin{cases} u_1 \text{ on } [t_1 - l_1\varepsilon, t_1] \\ u_2 \text{ on } [t_2 - l_2\varepsilon, t_2] \\ \bar{u}(t); \text{ otherwise on } [0,T] \end{cases}$$

where u_1, u_2 are constant values of Ω and let $\bar{x}_\varepsilon(\cdot)$ be the corresponding trajectory. Using the composition of the two elementary perturbations $\Pi_1 = \{t_1, l_1, u_1\}$ and $\Pi_2 = \{t_2, l_2, u_2\}$ we define a new perturbation $\Pi : \{t_1, t_2, l_1, l_2, u_1, u_2\}$. If we denote by $v_{\Pi_1}(t), v_{\Pi_2}(t)$ and $v_\Pi(t)$ the respective tangent vectors, a computation similar to the previous one gives us:

$$v_\Pi(t) = v_{\Pi_1}(t) + v_{\Pi_2}(t), \qquad \text{for } t \geq t_2.$$

We can deduce the following lemma.

Lemma 2 *Let $\Pi = \{t_1, \cdots, t_s, \lambda_1 l_1, \cdots, \lambda_s l_s, u_1, \cdots, u_s\}$ be a perturbation at regular times $t_i, t_1 < \cdots < t_s, l_i \geq 0, \lambda_i \geq 0, \sum_{i=1}^s \lambda_i = 1$ and corresponding to elementary perturbations $\Pi_i = \{t_i, l_i, u_i\}$ with tangent vectors $v_{\Pi_i}(t)$. Let $\bar{x}_\varepsilon(\cdot)$ be the associated response with perturbation Π. Then we have*

$$\bar{x}_\varepsilon(t) = \bar{x}(t) + \sum_{i=1}^{s} \varepsilon\lambda_i v_{\Pi_i}(t) + o(\varepsilon) \tag{3.5}$$

where $\frac{o(\varepsilon)}{\varepsilon} \to 0$, uniformly for $0 \leq t \leq T$ and $0 \leq \lambda_i \leq 1$.

Definition 37 *Let $\bar{u}(\cdot)$ be an admissible control and $\bar{x}(\cdot)$ its associated trajectory defined for $0 \leq t \leq T$. The first Pontryagin's cone $K(t), 0 < t \leq T$ is the smallest convex cone at $\bar{x}(t)$ containing all elementary perturbation vectors for all regular times t_i.*

Definition 38 *Let $v_1, \cdots, v_n$ be linearly independent vectors of $K(t)$, each v_i being formed as convex combinations of elementary perturbation vectors at distinct times. An elementary simplex cone C is the convex hull of the vectors v_i.*

Lemma 3 *Let v be a vector interior to $K(t)$. Then there exists an elementary simplex cone C containing v in its interior.*

Proof. In the construction of the interior of $K(t)$, we use the convex combination of elementary perturbation vectors at regular times not necessarily distinct. Clearly

by continuity we can replace such a combination by a cone C in the interior with n distinct times.

Approximation lemma

An important technical lemma is the following topological result whose proof uses the Brouwer fixed point theorem.

Lemma 4 *Let v be a nonzero vector interior to $K(t)$, then there exists $\lambda > 0$ and a conic neighborhood N of λv such that N is contained in the accessibility set $A(x_0, T)$.*

Proof. See [50].

The meaning of the lemma is the following. Since v is interior to $K(T)$, there exists an elementary simplex cone C such that v is interior to C. Hence for each $w \in C$ there exists $\bar{u}_\varepsilon(\cdot)$ a perturbation of $\bar{u}(\cdot)$ such that its corresponding trajectory satisfies

$$\bar{x}_\varepsilon(T) = \bar{x}(T) + \varepsilon w + o(w).$$

In particular there exists a control $\bar{u}_\varepsilon(\cdot)$ such that we have

$$\bar{x}_\varepsilon(T) = \bar{x}(T) + \varepsilon v + o(w).$$

By construction, $\bar{x}_\varepsilon(T) \in K(T)$. In other words $K(T)$ is a closed convex approximation of $A(x_0, T)$.

Separation step

To finish the proof, we use the geometric Hahn-Banach theorem. Indeed if $\bar{x}(T) \in \partial A(x_0, T)$ there exists a sequence $x_n \notin A(x_0, T)$ such that $x_n \to \bar{x}(T)$ when $n \to +\infty$ and the unit vectors $\frac{x_n - x(T)}{|x_n - x(T)|}$ have a limit ω when $n \to \infty$. The vector ω is not interior to $K(T)$ otherwise from Lemma 4 there would exist $\lambda > 0$ and a conic neighborhood of $\lambda\omega$ in $A(x_0, T)$ and this contradicts the fact that $x_n \notin A(x_0, T)$ for any n. Let π be any hyperplane at $\bar{x}(T)$ separating $K(T)$ from ω and let $\bar{p}$ be the exterior unit normal to π at $\bar{x}(T)$. Let us define $\bar{p}(\cdot)$ as the solution of the adjoint equation

$$\dot{p}(t) = -p(t)\frac{\partial f}{\partial x}(\bar{x}(t), \bar{u}(t))$$

satisfying $p(T) = \bar{p}$. By construction we have

$$\bar{p}(T)v(T) \leq 0$$

for each elementary perturbation vector $v(T) \in K(T)$ and since for $t \in [0, T]$ the following equations hold:

$$\dot{\bar{p}}(t) = -\bar{p}(t)\frac{\partial f}{\partial x}(\bar{x},\bar{u}), \qquad \dot{v}(t) = \frac{\partial f}{\partial x}(\bar{x},\bar{u})v$$

we have

$$\frac{d}{dt}\bar{p}(t)v(t) = 0.$$

Hence $\bar{p}(t)v(t) = \bar{p}(T)v(T) \leq 0, \forall t$. Assume that the maximization condition (3.2) is not satisfied on some subset S of $0 \leq t \leq T$ with positive measure. Let $t_1 \in S$ be a regular time, then there exists $u_1 \in \Omega$ such that

$$\bar{p}(t_1)f(\bar{x}(t_1),\bar{u}(t_1)) < \bar{p}(t_1)f(\bar{x}(t_1),u_1).$$

Let us consider the elementary perturbation $\Pi_1 = \{t_1, l, u_1\}$ and its tangent vector

$$v_{\Pi_1}(t_1) = l\left[f(\bar{x}(t_1),u_1) - f(\bar{x}(t_1),\bar{u}(t_1))\right].$$

Then using the above inequality we have that

$$\bar{p}(t_1)v_{\Pi_1}(t_1) > 0$$

which contradicts $\bar{p}(t_1)v_{\Pi_1}(t_1) \leq 0$, for all t. Therefore the inequality

$$H(\bar{x}(t),\bar{p}(t),\bar{u}(t)) = M(\bar{x}(t),\bar{p}(t))$$

is satisfied almost everywhere on $0 \leq t \leq T$. Using a standard reasoning we can prove that $t \mapsto M(\bar{x}(t),\bar{p}(t))$ is absolutely continuous and has zero derivative almost everywhere on $0 \leq t \leq T$, see [50].

Theorem 7 *Let us consider a general control system: $\dot{x}(t) = f(x(t),u(t))$ where f is a continuously differentiable function and let M_0, M_1 be two C^1 submanifolds of $\mathbb{R}^n$. We assume the set $\mathscr{U}$ of admissible controls to be the set of bounded measurable mappings $u : [0,T(u)] \to \Omega \in \mathbb{R}^m$, where Ω is a given subset of $\mathbb{R}^m$. Consider the following minimization problem: $\min_{u\in\mathscr{U}} C(u)$, $C(u) = \int_0^T f^0(x(t),u(t))dt$ where $f^0 \in C^1, x(0) \in M_0, x(T) \in M_1$ and T is not fixed. We introduce the augmented system:*

$$\dot{x}^0(t) = f^0(x(t),u(t)), \qquad x^0(0) = 0 \tag{3.6}$$

$$\dot{x}(t) = f(x(t),u(t)), \tag{3.7}$$

$\widehat{x}(t) = (x^0(t),x(t)) \in \mathbb{R}^{n+1}, \widehat{f} = (f^0,f)$. If $(x^*(\cdot),u^*(\cdot)$ is optimal on $[0,T^*]$, then there exists $\widehat{p}^*(\cdot) = (p^0,p(\cdot)) : [0,T^*] \to \mathbb{R}^{n+1} \setminus \{0\}$ absolutely continuous, such that $(\widehat{x}^*(\cdot),\widehat{p}^*(\cdot),u^*(\cdot))$ satisfies the following equations almost everywhere on $0 \leq t \leq T*$:

$$\dot{\widehat{x}}(t) = \frac{\partial \widehat{H}}{\partial \widehat{p}}(x(t),\widehat{p}(t),u(t)), \quad \dot{\widehat{p}}(t) = -\frac{\partial \widehat{H}}{\partial \widehat{x}}(x(t),\widehat{p}(t),u(t)) \tag{3.8}$$

$$\widehat{H}(x(t),\widehat{p}(t),u(t)) = \widehat{M}(x(t),\widehat{p}(t)) \tag{3.9}$$

where

$$\widehat{H}(x(t),\widehat{p}(t),u(t)) = \langle \widehat{p}, \widehat{f}(x,u)\rangle, \widehat{M}(\widehat{x},\widehat{p}) = \max_{u\in\Omega} \widehat{H}(\widehat{x},\widehat{p},u).$$

Moreover, we have

$$\widehat{M}(x(t),\widehat{p}(t)) = 0, \forall t,\ p^0 \leq 0 \tag{3.10}$$

and the boundary conditions (transversality conditions):

$$x^*(0) \in M_0,\ x^*(T^*) \in M_1, \tag{3.11}$$

$$p^*(0) \perp T_{x^*(0)}M_0,\ p^*(T^*) \perp T_{x^*(T)}M_1. \tag{3.12}$$

Proof. (For the complete proof, see [50] or [58].) Since $(x^*(\cdot),u^*(\cdot))$ is optimal on $[0,T^*]$, the augmented trajectory $t \mapsto \widehat{x}^*(t)$ is such that $\widehat{x}^*(T)$ belongs to the boundary of the accessibility set $\widehat{A}(x^*(0),T^*)$. Hence by applying Theorem 6 to the augmented system, one gets the conditions (3.8), (3.9) and $\widehat{M}$ constant. To show that $\widehat{M} \equiv 0$, we construct an approximated cone $K'(T)$ containing $K(T)$ but also the two vectors $\pm\widehat{f}(x^*(T),u^*(T))$ using time variations (the transfer time is not fixed). To prove the transversality conditions, we use a standard separation lemma as in the proof of Theorem 6.

Definition 39 *A triplet $(x(\cdot),p(\cdot),u(\cdot))$ solution of the maximum principle is called an extremal.*

3.2 Special cases

Minimal Time

Consider the time minimum case: $f^0 = 1$. In this case, an optimal control u^* on $[0,t^*]$ is such that the corresponding trajectory $x^*(.)$ is such that for each $t > 0$, $x^*(t)$ belongs to the boundary of the accessibility set $A(x^*(0),t)$. The pseudo-Hamiltonian of the augmented system is written:

$$\widehat{H}(\widehat{x},\widehat{p},u) = H(x,p,u) + p_0$$

with $H(x,p,u)$ is the reduced pseudo-Hamiltonian and since $p_0 \leq 0$, conditions 3.9, 3.10 become

$$H(x^*(t),p^*(t),u^*(t)) = M(x^*(t),p^*(t)) \quad a.e.$$

with $M(x,p) = \underset{u\in\Omega}{\text{Max}}\, H(x,p,u)$ and $M(x^*(t),p^*(t)) \geq 0$ is constant everywhere.

Mayer Problem

A *Mayer problem* is an optimal control problem for a system $\frac{\mathrm{d}x}{\mathrm{d}t} = f(x,u),\ u \in \Omega,\ x(0) = x_0$, where the cost to be minimized is of the form:

$$\underset{u\in\Omega}{\mathrm{Min}}\, c(x(t_f))$$

where $c : \mathbb{R}^n \longrightarrow \mathbb{R}$ is smooth the transfer time t_f is fixed and the final boundary conditions are of the form: $g(x(t_f))$, with $g : \mathbb{R}^n \to \mathbb{R}^k$ is smooth.
In this case the maximum principle and the geometric interpretation of this principle lead to the following:

- Each optimal control u^* on $[0,t_f]$ with response $x^*(.)$ is such that $x^*(t_f)$ belongs to the boundary of the accessibility set $A(x_0,t_f)$ and at the final point the adjoint vector $p^*(t_f)$ is orthogonal to the manifold defined by the boundary conditions and the cost function:

$$M\ :\ \{\ x;\ g(x) = 0,\ c(x) = m\ \}$$

  where m is the minimum.

Introducing the pseudo-Hamiltonian

$$H(x,p,u) = \langle p, f(x,u)\rangle$$

the necessary optimality conditions are:

$$\frac{\mathrm{d}x^*}{\mathrm{d}t} = \frac{\partial H}{\partial p}(x^*,p^*,u^*),\ \frac{\mathrm{d}p^*}{\mathrm{d}t} = -\frac{\partial H}{\partial x}(x^*,p^*,u^*), \tag{3.13}$$

$$H(x^*,p^*,u^*) = \max_{u\in\Omega} H(x^*,p^*,u) \tag{3.14}$$

and the following boundary conditions

$$f(x^*(t_f)) = 0, \tag{3.15}$$

$$p^*(t_f) = p_0.\frac{\partial c}{\partial x}(x^*(t_f)) + \delta.\frac{\partial g}{\partial x}(x^*(t_f)), \tag{3.16}$$

$$p_0 \leq 0 \text{ (transversality conditions).}$$

Exercise 3.1. Write the necessary optimality conditions for a *Bolza problem* where the cost problem is of the form:

$$C(u) = g(x(t_f)) + \int_0^{t_f} f^0(x(t),u(t))\mathrm{d}t$$

3.3 Application to NMR and MRI

Optimal control was very recently applied very successively to a general research project initiated by S. Glaser: the control of spins systems with applications to Nuclear Magnetic Resonance (NMR) and Magnetic Resonance Imaging (MRI). Such success is partially explained by an accurate representation of the control problem by the *Bloch equations* introduced in 1946 and F. Bloch and E.M. Purcell were awarded the 1952 Nobel Prizes for Physics for "their development of new ways and method for NMR", Purcell providing a nice link between our two working examples.
Next, we make a mathematical introduction of Bloch equations and the concept of *resonance*, in order to model the class of associate problems objects of our research program.

3.3.1 Model

The Bloch equations are a set of macroscopic equations which accurately describe the experimental model in NMR and MRI [51] based on the concept of the dynamics of a spin-1/2 particle. At this level it is represented by a *magnetization vector* $M = (M_x, M_y, M_z)$ in the *laboratory reference frame* which evolves according to

$$\frac{\mathrm{d}M}{\mathrm{d}\tau} = \gamma M \wedge B + R(M) \tag{3.17}$$

where γ is the *gyromagnetic ratio*, $B = (B_x, B_y, B_z)$ is the applied magnetic field which decomposes into a *strong polarizing field* $B_z = B_0$ in the z-direction, while B_x, B_y are the components of a *Rf-magnetic field* in the transverse direction and corresponds to the control field and $R(M)$ is the dissipation of the form:

$$\left(-\frac{M_x}{T_2}, -\frac{M_y}{T_2}, -\frac{(M_z - M_0)}{T_1}\right)$$

where T_1, T_2 are the *longitudinal and transverse relaxation parameters* characteristic of the chemical species, e.g. water, fat, blood.

The parameter M_0 is normalized to 1 up to a rescaling of M. We denote $\omega_0 = -\gamma B_0$ the *resonant frequency* and let introduce the control components: $u(\tau) = -\gamma B_y$ and $v(\tau) = -\gamma B_x$. The Bloch equations in the stationary frame can be written in the matrix form:

$$\frac{\mathrm{d}}{\mathrm{d}\tau}\begin{bmatrix} M_x \\ M_y \\ M_z \end{bmatrix} = \begin{bmatrix} 0 & -\omega_0 & u(\tau) \\ \omega_0 & 0 & -v(\tau) \\ -u(\tau) & v(\tau) & 0 \end{bmatrix}\begin{bmatrix} M_x \\ M_y \\ M_z \end{bmatrix} - \begin{bmatrix} \frac{M_x}{T_2} \\ \frac{M_y}{T_2} \\ \frac{M_z - 1}{T_1} \end{bmatrix} \tag{3.18}$$

The Bloch equations can be represented in a *rotating frame of reference*: $S(\tau) = \exp(\tau\omega\Omega_z)$, $M = S(\tau)q$, $q = (x,y,z)$,

$$\Omega_z = \begin{bmatrix} 0 & -1 & 0 \\ 1 & 0 & 0 \\ 0 & 0 & 0 \end{bmatrix}$$

and introducing the control representation:

$$\begin{aligned} u_1 &= u\cos\omega\tau - v\sin\omega\tau \\ u_2 &= u\sin\omega\tau + v\cos\omega\tau, \end{aligned}$$

one gets the Bloch equations in the moving frame:

$$\frac{\mathrm{d}}{\mathrm{d}\tau}\begin{bmatrix} x \\ y \\ z \end{bmatrix} = \begin{bmatrix} 0 & -\Delta\omega & u_2 \\ \Delta\omega & 0 & -u_1 \\ -u_2 & u_1 & 0 \end{bmatrix}\begin{bmatrix} x \\ y \\ z \end{bmatrix} - \begin{bmatrix} \frac{x}{T_2} \\ \frac{y}{T_2} \\ \frac{z-1}{T_1} \end{bmatrix} \tag{3.19}$$

where $\Delta\omega = \omega_0 - \omega$ is the *resonance offset*.

The control is bounded by m, $m = 2\pi \times 32.3$Hz being the experimental intensity of the experiments. Assuming $\Delta\omega = 0$ (resonance), and using the normalized time $t = \tau m$, denoting $\Gamma = 1/mT_2$, $\gamma = 1/mT_1$ and the physical parameters satisfying the constraint: $2\Gamma \geq \gamma \geq 0$, the system is normalized to:

$$\begin{aligned} \frac{\mathrm{d}x}{\mathrm{d}t} &= -\Gamma x + u_2 z \\ \frac{\mathrm{d}y}{\mathrm{d}t} &= -\Gamma y - u_1 z \\ \frac{\mathrm{d}z}{\mathrm{d}t} &= \gamma(1-z) + u_1 y - u_2 x, \end{aligned} \tag{3.20}$$

where $|u| \leq 1$. Moreover since $2\Gamma \geq \gamma \geq 0$, one has that the *Bloch ball* $|q| \leq 1$ is invariant for the dynamics.

This equation describes the evolution of the magnetization vector in NMR. The choice of $\omega = \omega_0$ corresponding to resonance neutralized the existence of the strong polarizing field B_0, except the side effect of a stable unique equilibrium, corresponding to the North pole $N = (0,0,1)$ of the Bloch equation for the uncontrolled motion.

In MRI, the situation is more complex due to the spatial position of the image and one must control an ensemble of spins corresponding to each pixel. Due to this localization they are some *distortions* corresponding to B_0 *and* B_1 *inhomogeneities*. The variation of B_0 producing a resonance offset and $\Delta\omega$ belongs to some intervals, while B_1-inhomogeneity introduces a scaling factor $a_i \geq 0$ depending on the spatial position of the spin in the image modeling the distortion of the amplitude of the control field and the equation transforms into

$$\begin{aligned}\frac{\mathrm{d}x}{\mathrm{d}t} &= -\Gamma x + a_i u_2 z\\ \frac{\mathrm{d}y}{\mathrm{d}t} &= -\Gamma y - a_i u_1 z\\ \frac{\mathrm{d}z}{\mathrm{d}t} &= \gamma(1-z) + a_i(u_1 y - u_2 x),\end{aligned} \tag{3.21}$$

In the general case one must consider both inhomogeneities producing a detuning and amplitude alteration. Note that such distortions cannot be modelized and have to be *experimentally determined*.

To relate Bloch equation to imaging we associate to the amplitude $|q|$ of the normalized magnetization vector a *grey level where* $|q| = 1$ *corresponds to white while the center of the Bloch ball defined by* $|q| = 0$ *corresponds to black.*

3.3.2 The problems

Having introduced the control systems in relation with Bloch equations taking into account B_0 and B_1 inhomogeneities one can present the fundamental problems studied in NMR and MRI.

Saturation problem

The objective of the saturation problem for a single spin is to bring the magnetization vector q from the North pole $N = (0,0,1)$ of the Bloch ball (which is the equilibrium of the free system) to the center $O = (0,0,0)$ of the Bloch ball, recalling that $|q|$ corresponds to a grey level where the sphere $|q| = 1$ corresponds to white and $|q| = 0$ to black.

A direct generalization being to consider an *ensemble of spin particles* corresponding to the same chemical species and to bring each spin of this ensemble from the North pole to the center, corresponding to the *multisaturation problem*.

The contrast problem

In the contrast problem in NMR called *ideal contrast problem* we consider two pairs of (uncoupled) spin-1/2 systems corresponding to different chemical species, each of them solutions of the Bloch equations (3.21) with respective parameters (γ_1, Γ_1) and (γ_2, Γ_2) controlled by the same magnetic field. Denoting each system by $\frac{\mathrm{d}q_i}{\mathrm{d}t} f(q_i, \Lambda_i, u)$, $\Lambda_i = (\gamma_i, \Gamma_i)$ and $q_i = (x_i, y_i, z_i)$ is the magnetization vector representating each spin particle, $i = 1,2$. This leads to the consideration of the system abbreviated as: $\frac{\mathrm{d}q}{\mathrm{d}t} = f(q,u)$, where $q = (q_1, q_2)$ is the state variable. The constrast problem by saturation is the following optimal control problem: starting from the

equilibrium point $q_0 = ((0,0,1),(0,0,1))$ where both chemical species are white and hence *indistinguishable*, reach in a given transfer time t_f the final state $q_1(t_f)$ corresponding to saturation of the first spin while maximizing $|q_2(t_f)|^2$, the final observed contrast being $|q_2(t_f)|$.

Obvious generalization of the problems in MRI, taking into account B_0 and B_1 inhomogeneities, is to consider in the image an ensemble of N pairs of chemical species, e.g. water or fat, and distributed in the image and the objective is to provide multisaturation of the ensemble of spins of the first species in a small ball centered at $|q_2(t_f)|$ where $|q_2(t_f)$ corresponds to the contrast calculated in NMR.

The objective in MRI is to produce a *robust control* taking into account the B_0 and B_1 inhomogeneities.

In the sequel and in order to present the concepts and the theoretical tools, we shall restrict to the saturation problem of a single spin and the contrast problem by saturation in NMR. It is the preliminary step to the analysis of an ensemble of spins which is in the applications treated numerically using adapted softwares e.g. `Bocop`and `HamPath`representative respectively of direct and indirect methods in numeric optimal control.

3.3.3 The saturation problem in minimum time for a single spin

The saturation problem in minimum time was completely solved in [46] and was an important step to the applications of geometric optimal control to the dynamics of spins particles.

Preliminaries

First of all, since the transfer is from the North pole $N = (0,0,1)$ to the center of the Bloch ball $O = (0,0,0)$ which belongs to the z-axis of revolution of the system corresponding to polarization the system can be restricted to the two-dimensional plane of the Bloch ball and the control $u = (u_1, u_2)$ reduces to the $u_1$component. The system is compactly written as: $\frac{\mathrm{d}q}{\mathrm{d}t} = F(q) + u_1 G(q)$, while the control is bounded by $|u| \leq 1$ and $q = (y,z)$. We have

$$F = -\Gamma y \frac{\partial}{\partial y} + \gamma(1-z)\frac{\partial}{\partial z} \tag{3.22}$$

$$G = -z\frac{\partial}{\partial y} + y\frac{\partial}{\partial z} \tag{3.23}$$

According to the maximum principle an optimal trajectory is a concatenation of bang arcs where $u(t) = \mathrm{sign}\langle p(t), G(q(t))\rangle$ and singular arcs where $\langle p(t), G(q(t))\rangle$. The following Lie brackets are relevant in our analysis. Denoting $\delta = \gamma - \Gamma$, we have

$$[G,F] = (-\gamma+\delta z)\frac{\partial}{\partial y} + \delta y\frac{\partial}{\partial z}$$
$$[[G,F],F] = (\gamma(\gamma-2\Gamma)-\delta^2 z)\frac{\partial}{\partial y} + \delta^2 y\frac{\partial}{\partial z}$$
$$[[G,F],G] = 2\delta y\frac{\partial}{\partial y} + (\gamma-2\delta z)\frac{\partial}{\partial z}$$

Singular trajectories and optimality

The singular trajectories are located on the set S : $\det(\, G,[G,F]\,) = 0$ which is given by $y(-2\delta z+\gamma) = 0$. Hence it is formed by

- the z-axis of revolutions $y = 0$,
- the horizontal line $z = \gamma/(2\delta)$. This line intersects the Bloch ball $|z| < 1$ when $2\Gamma > 3\gamma$ and moreover z is negative. The singular control is given by $D' + u_s D = 0$, where $D = \det(\, G,[[G,F],G]\,)$ and $D' = \det(\, G,[G,F]\,)$.
- for $y = 0$, $D = -z(\gamma-2\delta z)$ and $D' = 0$. The singular control is zero and a singular trajectory is a solution of $\dot{y} = -y$, $\dot{z} = \gamma(1-z)$ where the equilibrium point $(0,1)$ is a stable node if $\gamma \neq 0$.
- for $z = \gamma(2\delta)$, $D = -2\delta y^2$, $D' = y\gamma(2\Gamma-\gamma)$ and $u_s = \gamma(2\Gamma-\gamma)/(2\delta y)$, $2\Gamma-\gamma \geq 0$. Hence along the horizontal direction, the flow: $\dot{y} = -\Gamma y - \gamma^2\frac{2\Gamma-\gamma}{4\delta^2 y}$ and $|u_s| \to \infty$ when $y \to 0$.

An easy computation gives the following proposition.

Proposition 3.1. *Ig $\gamma \neq 0$, the singular control along the singular line is L^1 but not L^2.*

The maximum principle selects the singular line but the high order maximum principle and the so-called generalized Legendre-Clebsch condition [42] has to used to distinguish between small time minimum and maximum solution. It can be easily understood using the two seminal examples:

$$\dot{x} = 1-u^2, \qquad \dot{x} = 1+u^2,$$
$$\dot{y} = u,\ |u| \leq 1, \qquad \dot{y} = u,\ |u| \leq 1$$

where in both case the x-axis is the singular line and is time minimizing in the first case and time maximizing in the second case. The optimality condition takes the following form in our case. Let $D'' = \det(G,F) = \gamma z(z-1)+\Gamma\gamma^2$. The set C : $D'' = 0$ is the *collinear set*. If $\gamma \neq 0$, this set forms an oval joining the North pole to the center of the Bloch ball and the intersection with the singular line is empty. Denoting $D = \det(G,[[G,F],G])$ the singular lines are fast displacement direction if $DD'' > 0$ and slow if $DD'' < 0$. From this condition, one deduces that the z-axis of

revolution is fast if $1 > z > z = \gamma/(2\delta)$ and slow if $z = \gamma/(2\delta) > z > -1$, while the horizontal singular line is fast.

From the analysis we deduce first

Lemma 3.1. *If the condition $2\Gamma > 3\gamma$ is not satisfied the horizontal singular line doesn't intersect the Bloch ball $|q| < 1$ and the optimal solution is the standard inversion sequence used in practices: apply a bang control to steer $(0,1)$ to $(0,-*)$. Followed by $u = 0$ to relax the system to $(0,0)$ along the z-axis.*

If $2\Gamma > 3\gamma$ the existence of the fast displacement horizontal line will determine the optimal policy. First of all observe that since $u_S \to \infty$, when $q \to 0$ along this line, it is saturating the constraint $|u| < 1$ at a point of this line. Hence this line has to be quitted before this point. The exact exit point is determined by the maximum principle because such point has to be a switching point at both extremities for the corresponding bang arc. Such an arc is called a bridge.

From this analysis we deduce the following theorem, see [46] for further details.

Theorem 3.1. *If $2\Gamma > 3\gamma$, in the time minimal saturation problem is of the form: $\delta_+ \delta_s^h \delta_+ \delta_s^v$, concatenating the bang arc to quit the North pole to the horizontal singular line, followed by the bridge and relaxation to 0 along the z-axis of revolution.*

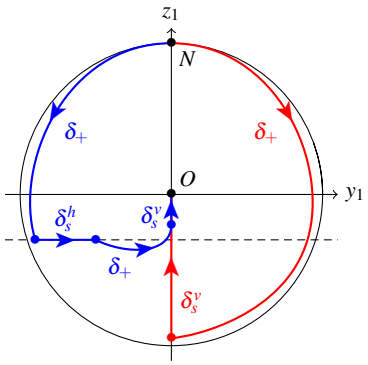

Fig. 3.1 Time minimal solution (left) compared with inversion sequence (right).

This gives a complete solution to the saturation problem using a careful geometric analysis to understand the interaction between the two singular lines. Moreover a similar analysis leads to a complete understanding of the time minimum synthesis to transfer any point of the Bloch ball to the center.

Extension of this type of results to an ensemble of two or more spins is an important issue. The complexity is related to the analysis of singular extremals at two levels. First of all, in general the symmetry of revolution due to z-polarization cannot be invoked to reduced the bi-inputs case to the single single-input case. Secondly, in dimension ≥ 3, the analysis of the singular flow even in the single-input case is

a complicated task. Next, we shall present this complexity in the contrast problem and present some achievements.

3.3.4 The maximum principle in the contrast problem by saturation

The system is written as:

$$\dot{q} = F_0(q) + u_1 F_1(q) + u_2 F_2(q),\ |u| \leq 1$$

where $q = (q_1, q_2) \in \{\ |q_1| \leq 1,\ |q_2| \leq 1\ \}$ and q_1, q_2 represents the normalized magnetization vector of the first and second spin, $q_i = (x_i, y_i, z_i),\ i = 1,2$. Using the notation of the section 3.2 for a Mayer problem, the cost function is $c(q(t_f)) = -|q_2(t_f)|^2$ and the final boundary condition is $F(q(t_f)) = q_1(t_f) = 0$. Splitting the adjoint vector into $p = (p_1, p_2) \in \mathbb{R}^3 \times \mathbb{R}^3$, the transversality condition is:

$$p_2(t_f) = -2p^0 q_2(t_f),\ p^0 \leq 0$$

and if $p^0 \neq 0$ it can be normalized to $p^0 = -1/2$.

We denote $z = (q, p)$, $H_i = \langle p, F_i(q) \rangle,\ i = 0,1,2$, the Hamiltonian lift of the system $\dot{z} = \overrightarrow{H}_0 + \sum_{i=1}^{2} \overrightarrow{H}_i(z)$. If $(H_1, H_2) \neq 0$, the maximization condition of the maximum principle leads to the following parametrization of the controls

$$u_1 = \frac{H_1}{\sqrt{H_1^2 + H^2}}, \qquad u_2 = \frac{H_2}{\sqrt{H_1^2 + H_2^2}}.$$

Define the *switching surface*:

$$\Sigma\ :\ H_1 = H_2 = 0.$$

Plugging such u into the pseudo-Hamiltonian gives the true Hamiltonian: $H_n = H_0 + \sqrt{H_1^2 + H_2^2}$. The corresponding extremal solutions are called zero.

Besides those generic extremals, additional extremals are related to Lie algebraic properties of the system and a careful analysis is the key factor to determine the properties of the optimal solutions.

Lie bracket computations

Due to the bilinear structure of the Bloch equations, Lie brackets can be easily computed, which is crucial in our analysis.

Recall that the Lie bracket of two vectors fields F, G is computed with the convention

$$[F, G](q) = \frac{\partial F}{\partial q}(q) G(q) - \frac{\partial G}{\partial q}(q) F(q)$$

and if H_F, H_G are the Hamiltonian lifts, recall that the Poisson bracket is

$$\{H_F, H_G\}(z) = \mathrm{d}H_F(\overrightarrow{G})(z) = H_{[F,G]}(z).$$

To simplify the computation, each spin system is lifted on the *semi-direct Lie product* $GL(3,\mathbb{R}) \times \mathbb{R}^3$ acting on the q-space using the action $(A,a).q = Aq + a$. The Lie bracket computation rule is $((A,a),B,b) = ([A,B],Ab - Ba)$ where $[A,B] = AB - BA$.

Introducing $F_0 = (A_0, a_0)$, with $A_0 = \mathrm{diag}(-\Gamma_1, -\Gamma_1, -\gamma_1, -\Gamma_2, -\Gamma_2, -\gamma_2)$ and $a_0 = (0,0,\gamma_1,0,0,\gamma_2)$ whereas the control fields (F_1, F_2) are identified to $B_1 = \mathrm{diag}(C_1, C_1)$ and $B_2 = \mathrm{diag}(C_2, C_2)$ where C_1, C_2 are the antisymmetric matrices $C_1 = E_{32} - E_{23}$, $C_2 = (E_{13} - E_{31})$ with $E_{ij} = (\delta_{ij})$ (Kronecker symbol). See [17] for more details.

Next, we present in details the Lie brackets needed in our computations, each entry form by a couple (v_1, v_2) and we use the notation omitting the indices. We set $\delta = \gamma - \Gamma$.

- *Length 1:*

$$\begin{aligned} F_0 &= (-\Gamma x, -\Gamma y, \gamma(1-z)) \\ F_1 &= (0, -z, y) \\ F_2 &= (z, 0, -x) \end{aligned}$$

- *Length 2:*

$$\begin{aligned} [F_0, F_1] &= (0, \gamma - \delta z, -\delta y) \\ [F_0, F_2] &= (-\gamma + \delta z, 0, \delta x) \\ [F_1, F_2] &= (-y, x, 0) \end{aligned}$$

- *Length 3:*

$$\begin{aligned} [[F_1, F_2], F_0] &= 0 \\ [[F_1, F_2], F_1] &= F_2 \\ [[F_1, F_2], F_2] &= -F_1 \\ [[F_0, F_1], F_1] &= (0, -2\delta y, -\gamma + 2\delta z) \\ [[F_0, F_1], F_2] &= (\delta y, \delta x, 0) = [[F_0, F_2], F_1] \\ [[F_0, F_2], F_2] &= (-2\delta x, 0, 2\delta z - \gamma) \\ [[F_0, F_1], F_0] &= (0, -\gamma(\gamma - 2\Gamma) + \delta^2 z, -\delta^2 y) \\ [[F_0, F_2], F_0] &= (\gamma(\gamma - 2\Gamma) - \delta^2 z, 0, \delta^2 x) \end{aligned}$$

3.3.5 Stratification of the surface $\Sigma : H_1 = H_2 = 0$ and partial classification of the extremal flow near Σ

Let $z = (q, p)$ be a curve solution of $\overrightarrow{H}_0 + u_1 \overrightarrow{H}_1 + u_2 \overrightarrow{H}_2$. Differentiating H_1 and H_2 along such a solution, one gets:

$$\begin{aligned} \dot{H}_1 &= \{H_1, H_0\} + u_2 \{H_1, H_2\} \\ \dot{H}_2 &= \{H_2, H_0\} + u_1 \{H_2, H_1\} \end{aligned} \tag{3.24}$$

Hence we have:

Proposition 3.2. *Let $z_0 \subset \Sigma_1 = \Sigma \setminus \{H_1, H_2\} = 0$ and define the control u_s by:*

$$u_s(z) = \frac{(-\{H_0, H_2\}(z), \{H_0, H_1\}(z))}{\{H_1, H_2\}(z)}, \tag{3.25}$$

and plugging such u_s into H defines the true Hamiltonian

$$H_s(z) = H_0(z) + u_{s,1}(z) H_1(z) + u_{s,2}(z) H_2(z)$$

which parameterizes the singular solutions of the bi-input system contained in Σ_1.

This gives the first stratum of the surface Σ. Moreover, the behaviors of the extremals of order zero near a point z_0 of Σ_1 can be easily analyzed using (3.24) and a nilpotent model where all Lie brackets at $z_0 \in \Sigma_1$ of length ≥ 3 are zero. See [13, 25] for similar computations. Denoting:

$$\{H_1, H_0\}(z_0) = a_1, \quad \{H_2, H_0\}(z_0) = a_2, \quad \{H_2, H_1\}(z_0) = b$$

and using polar coordinates $H_1 = r\cos\theta$, $H_2 = r\sin\theta$, then (3.24) becomes:

$$\begin{aligned} \dot{r} &= a_1 \cos\theta + a_2 \sin\theta \\ \dot{\theta} &= \frac{1}{r}(b - a_1 \sin\theta + a_2 \cos\theta). \end{aligned} \tag{3.26}$$

To analyze this equation, we write:

$$a_1 \sin\theta - a_2 \cos\theta = A \sin(\theta + \phi)$$

with $A \tan\phi = -a_2/a_1, A = \sqrt{a_1^2 + a_2^2}$. Hence the equation $\dot{\theta} = 0$ leads to the relation

$$A \sin(\theta + \phi) = b,$$

which has two distinct solutions on $[0, 2\pi[$ denoted θ_0, θ_1 if and only if $A > |b|$, one solution if $A = |b|$ and zero solution if $|A| < |b|$. Moreover $\theta_1 - \theta_0 = \pi$ if and only if $b = 0$. Plugging θ_0, θ_1 in (3.26), one gets two solutions of (3.26). Hence we deduce:

Lemma 3.2. *If* $\sqrt{a_1^2+a_2^2} > |b|$ *and* $b \neq 0$*, we have a broken extremal formed by concatenating two extremals of order zero at each point* z_0 *of* Σ_1.

At such a point z_0 of Σ_1, the singular control (3.25) is such that

$$u_{s,1}^2 + u_{s,2}^2 = \frac{a_1^2+a_2^2}{b^2} > 1$$

and *hence is not admissible*.

Next we analyze more degenerated situations and one needs the following concept.

Goh condition

Higher order necessary optimality conditions along singular extremals in the bi-input case are related to finiteness of the index of the quadratic forms associated with the second order derivative [15] known as *Goh condition* which is the relation:

$$\{H_1, H_2\} = 0. \tag{3.27}$$

Using $H_1 = H_2 = \{H_1, H_2\} = 0$ and (3.24), one gets the additional relations:

$$\{H_1, H_2\} = \{H_0, H_1\} = \{H_0, H_2\} = 0. \tag{3.28}$$

Then differentiating again along a solution leads to the relations:

$$\{\{H_1, H_2\}, H_0\} + u_1\{\{H_1, H_2\}, H_1\} + u_2\{\{H_1, H_2\}, H_2\} = 0 \tag{3.29}$$

$$\begin{cases} \{\{H_0, H_1\}, H_0\} + u_1\{\{H_0, H_1\}, H_1\} + u_2\{\{H_0, H_1\}, H_2\} = 0 \\ \{\{H_0, H_2\}, H_0\} + u_1\{\{H_0, H_2\}, H_1\} + u_2\{\{H_0, H_2\}, H_2\} = 0 \end{cases} \tag{3.30}$$

This leads in general to *three* relations to compute *two* control components, and for a generic system such conditions are not satisfied [28], but in our case, according to Lie brackets computations, we have:

Lemma 3.3. *If* $H_1 = H_2 = 0$*, one has*

$$\{\{H_1, H_2\}, H_0\} = \{\{H_1, H_2\}, H_1\} = \{\{H_1, H_2\}, H_2\} = 0$$

and (3.29) *is satisfied.*

The equation (3.30) are then written: $\widetilde{A} + \widetilde{B}u$ and if $\det(\widetilde{B}) \neq 0$, the corresponding singular control is given by:

$$u_s'(z) = -\widetilde{B}^{-1}(z)\widetilde{A}(z) \tag{3.31}$$

Using the relations:

$$H_1 = H_2 = \{H_1, H_2\} = \{H_0, H_1\} = \{H_0, H_2\} = 0,$$

the vector p is orthogonal to F_1, F_2, $[F_1,F_2]$, $[F_0,F_1]$, $[F_0,F_2]$. Introducing:

$$A=\begin{pmatrix}A_1\\A_2\end{pmatrix},\quad B=\begin{pmatrix}B_1\ B_3\\B_2\ B_4\end{pmatrix},\quad C=(F_1,F_2,[F_1,F_2],[F_0,F_1],[F_0,F_2]),$$

with

$$A_1=\det(C,[[F_0,F_1],F_0]),\quad A_2=\det(C,[[F_0,F_2],F_0]),$$

and

$$\begin{aligned}B_1&=\det(C,[[F_0,F_1],F_1]),\quad B_2=\det(C,[[F_0,F_2],F_1]),\\B_3&=\det(C,[[F_0,F_1],F_2]),\quad B_4=\det(C,[[F_0,F_2],F_2]),\end{aligned}$$

the relation (3.30) leads to:

$$A+Bu=0,$$

and if $\det B\neq 0$, one gets the singular control given by the feedback:

$$u_s'(q)=-B^{-1}(q)A(q) \tag{3.32}$$

and the associated vector field:

$$Q_s'=F_0+u_{s,1}'F_1+u_{s,2}'F_2.$$

Moreover, the singular control has to be admissible: $|u_s'|\leq 1$. We introduce the stratum:

$$\Sigma_2: H_1=H_2=\{H_1,H_2\}=\{H_0,H_1\}=\{H_0,H_2\}\setminus\det\widetilde{B}=0.$$

Hence we have:

Lemma 3.4. *1. On the stratum Σ_2, there exists singular extremals satisfying Goh condition where the singular control is given by the feedback* (3.31)*.*
2. For the contrast problem:

$$\begin{aligned}\det B=&(x_1y_2-x_2y_1)^4(\delta_1-\delta_2)(2\delta_1z_1-\gamma_1)(2\delta_2z_2-\gamma_2)\\&\left(2(\delta_1^2\gamma_2z_1-\delta_2^2\gamma_1z_2)-\gamma_1\gamma_2(\delta_1-\delta_2)-2\delta_1\delta_2(\gamma_1z_2-\gamma_2z_1)\right),\end{aligned} \tag{3.33}$$

The behaviors of the extremals of order zero near a point $z_0\in\Sigma_2$ is a complicated problem. Additional singular extremals can be contained in the surface:

$$\Sigma_3: H_1=H_2=\{H_1,H_2\}=\{H_0,H_1\}=\{H_0,H_2\}=\det\widetilde{B}=0,$$

and they can be computed using the property that the corresponding control has to force the surface $\det B=0$ to be invariant. *Some have an important meaning, due to the symmetry of revolution of the Bloch equations*. They correspond to control the system, imposing $u_2=0$. In this case, one can restrict the system to

$$\mathbf{Q}=\{q=(q_1,q_2)\in\mathbb{R}^n:\ |q_1|\leq 1,\ |q_2|\leq 1,\ x_1=x_2=0\}.$$

The computations of the corresponding extremals amount to replace in the relations; H_2 by εH_2 and to impose $\varepsilon = 0$. The remaining relations are then:

$$H_1 = \{H_0, H_1\} = 0$$

and from (3.30) one gets the relations:

$$\{\{H_0, H_1\}, H_0\} + u_{1,s}\{\{H_0, H_1\}, H_1\} = 0, \tag{3.34}$$

and thus, this defines the singular control:

$$u_{1,s} = -\frac{\{\{H_0, H_1\}, H_0\}}{\{\{H_0, H_1\}, H_1\}} \tag{3.35}$$

and the associated Hamiltonian $H_{1,s} = H_0 + u_{1,s}H_1$. We have the following result:

Proposition 3.3. *The singular extremals of the single-input case with $u_2 \equiv 0$ are extremals of the bi-input case with the additional condition: $x_1 = p_{x_1} = x_2 = p_{x_2} = 0$.*

Moreover from the geometric interpretation of the maximum principle for a Mayer problem, in order to be optimal the generalized Legendre-Clebsch condition has to be satisfied:

$$\frac{\partial}{\partial u_1}\frac{\mathrm{d}^2}{\mathrm{d}t^2}\frac{\partial H}{\partial u_1} = \{H_1, \{H_1, H_0\}\}(z) \leq 0 \tag{3.36}$$

Observe that if we impose $u_2 = 0$, the classification of the extremals near the switching surface, which reduces to $H_1 = 0$, is a standard problem [43].

Finally, another important property of the extremal flow, again a consequence of the symmetry of revolution is given next, in relation with Goh condition. It is a consequence of Noether integrability theorem.

Proposition 3.4. *In the contrast problem, for the Hamiltonian vector field $\overrightarrow{H}_n$ whose solutions are extremals of order zero, the Hamiltonian lift $H(z) = \{H_1, H_2\}(z) = (p_{x_1}y_1 - p_{y_1}x_1) + (p_{x_2}y_2 - p_{y_2}x_2)$ is a first integral.*

Exercise 3.2 (Generalization to the case of B_1 and B_0 inhomogeneities). It is interesting to compare to the case of an ensemble of two spins of the same spin particle with B_0 and B_1 inhomogeneities which is left to the reader. More precisely:

- *B_1-inhomogeneities.*
  In this case, the control directions of the second spin are relaxed by a factor and the Lie brackets computations can be used to stratified. It can be applied to the multisaturation problem.
- *B_0-inhomogeneities.*
  In this case the vector field F_0 of the second spin contains a non-zero detuning. Clearly this introduces modifications in the Lie brackets computations. Again it can be applied to multisaturation problem. It explains the following phenomenon: *in the precense of detuning both controls (u_1, u_2) have to be used.*

Next, motivating by the fact that due to the symmetry of revolution and the observed numerical experiments, we shall restrict our study to the single-input case. It is an important theoretical step since we can reduce the analysis of the singular flow for a 4-dimensional system with one input vs a 6-dimensional system. This complexity will be illustrated by the computations presented next.

3.3.6 The classification of the singular extremals and the action of the feedback group

Preliminairies

Restricting to the single input case, the research program concerning the contrast problem or the multisaturation problem for an ensemble of two spins is clear.

Saturation problem for a single spin and bridge phenomenon

In the case of a single spin the complete geometric analysis requires the computations of the two singular line and the understanding of the singularity associated with their intersection, which causes the saturation of the singular control and the occurrence of a bang arc called a bridge to connect both singular arcs. This phenomenon generalizes to higher dimension and it tells you that the analysis of the singular flow codes all the information of the optimal solution which is a sequence of arcs of the form $\delta_{\pm}\delta_S\delta_{\pm}...\delta_S$, where $\delta_{\pm}$ denotes bang arcs with $u=\pm 1$, while δ_S are singular arcs.

This will be presented in details next, in relation with the action of the feedback group.

Computations of the singular flow

Consider a control system of the form:

$$\frac{\mathrm{d}q}{\mathrm{d}t} = F(q) + uG(q),\ q \in \mathbb{R}^n$$

and relaxing the control constraints: $u \in \mathbb{R}$. Denoting H_F and H_G the Hamiltonian lifts of F and G, if the denominator is not vanishing, a singular control is given by:

$$u_S(z) = -\frac{\{\{H_G, H_F\}, H_F\}(z)}{\{\{H_G, H_F\}, H_G\}(z)} \tag{3.37}$$

Plugging such u_S into the pseudo-Hamiltonian one gets the true Hamiltonian: $H_S = H_F + u_S H_G$ and the singular extremals are solutions of the *constrained Hamiltonian*

equation:

$$\frac{\mathrm{d}z}{\mathrm{d}t} = \overrightarrow{H}_S(z),\ \Sigma' \ :\ H_G = \{H_G, H_F\} = 0.$$

This set of equations defines a Hamiltonian vector field on the surface $\Sigma' \setminus \{\{H_G, H_F\}, H_G\} = 0$, restricting the standard symplectic from $\omega = \mathrm{d}p \wedge \mathrm{d}q$.

We use the notation $\mathscr{D} = \{\{H_G, H_F\}, H_G\}$ and $\mathscr{D}' = \{\{H_G, H_F\}, H_F\}$. The differential equation (3.37) can be desingularized using the time reparametrization

$$\mathrm{d}s = \mathrm{d}t/\mathscr{D}(z(t))$$

which amounts to analyze the one dimensional foliation.

We get the system:

$$\frac{\mathrm{d}q}{\mathrm{d}s} - \mathscr{D}F - \mathscr{D}'F,\ \frac{\mathrm{d}p}{\mathrm{d}s} = -p\left(\mathscr{D}\frac{\partial F}{\partial q} - \mathscr{D}'\frac{\partial G}{\partial q}\right).$$

restricted to the surface Σ'.

In the contrast problem, since the state space is of dimension four, using the two constraints $H_G = \{H_G, H_F\} = 0$ and the homogeneity with respect to p, equation (3.37) can be reduced to the explicit form:

$$\frac{\mathrm{d}q}{\mathrm{d}t} = F(q) - \frac{\mathscr{D}'(q,\lambda)}{\mathscr{D}(q,\lambda)}G(q)$$

where λ is a one-dimension time-dependant parameter whose dynamics is deduced from the adjoint equation.

Using the previous remark, the optimal problem can be analyzed by understanding the behavior of the corresponding trajectories and the singularities of the flow near the set $\mathscr{D} = 0$, which codes the switching sequence.

This is a very complicated task, in particular because the system is depending upon four parameters and simplifications have to be introduced to simplify this task. Two simplifications can be introduced. First, we can restrict to some specific parameters corresponding to some experimental cases. For instance, in the water case, saturation of a single spin amounts to the standard inversion sequence. Second, a projection of the singular flow which is physically relevant can be introduced. A natural choice is to consider the case where the transfer time t is not fixed. Then according to the maximum principle this leads to the additional constraint: $M = \underset{u(.)}{\mathrm{Max}}\, H_F + uH_G = 0$, which gives in the singular case the additional constraint: $H_F(z) = 0$. This case is called the *exceptional case* using the terminology of [22].

With this constraint, the adjoint vector can be eliminated and the singular control in this exceptional case is the feedback:

$$u_S^e = -\frac{D'(q)}{D(q)},$$

where $D = \det(F,G,[G,F],[[G,F],G])$, $D' = \det(F,G,[G,F],[[G,F],F])$ with the corresponding vector field X^e defined by

$$\frac{\mathrm{d}q}{\mathrm{d}t} = F(q) - \frac{D'(q)}{D(q)}G(q)$$

which can again be desingularized using the reparametrization $\mathrm{d}s = \mathrm{d}t/D(q(t))$ and this gives the smooth vector field

$$X_r^e = DF - D'G.$$

Feedback classification

Definition 3.1. Let E and F be two $\mathbb{R}$-vector spaces and let $\mathfrak{G}$ be a group acting linearly on E and F. A homomorphism $\mathfrak{X} : \mathfrak{G} \to \mathbb{R}\setminus\{0\}$ is called a *character*. A *semi-invariant of weight* $\mathfrak{X}$ is a map $\lambda : E \to \mathbb{R}$ such that for all $g \in \mathfrak{G}$ and all $x \in E$, $\lambda(g,x) = \mathfrak{X}(g)\lambda(x)$; it is an *invariant* if $\mathfrak{X} = 1$. A map $\lambda : E \to F$ is a *semi-covariant of weight* $\mathfrak{X}$ if for all $g \in \mathfrak{G}$ and for all $x \in E$, $\lambda(g.x) = \mathfrak{X}(g)g.\lambda(x)$; it is called a *covariant* if $\mathfrak{X} = 1$.

More about invariant theory can be found in [30].

The key concept in analyzing the role of relaxation parameters in the control problem is the action of the *feedback group* $\mathfrak{G}$ on the set of systems. We shall restrict our presentation to the single-input case and we denote $\mathscr{C} = \{F,G\}$ the set of such (smooth) systems on the state space $Q \simeq \mathbb{R}^n$, see [12] for the details.

Definition 3.2. Let $(F,G),(F',G')$ be two elements of $\mathscr{C}$. They are called feedback equivalent if there exist a smooth diffeomorphism φ of $\mathbb{R}^n$ and a feedback $u = \alpha(q) + \beta(q)v$, β invertible such that:

- $F' = \varphi * F + \varphi * (G\alpha)$, $G' = \varphi * (G\beta)$.

where $\varphi * z$ denotes the image of the vector field.

Definition 3.3. Let $(F,G) \in \mathscr{C}$ and let λ_1 be the map which associated the constrained Hamiltonian vector field $(\overrightarrow{H}_S, \Sigma')$ (see (3.37)) to (F,G). We define the action of (φ,α,β) of $\mathfrak{G}$ on $(\overrightarrow{H}_S, \Sigma')$ to be the action of the symplectic change of coordinates:

$$\overrightarrow{\varphi} : \; q = \varphi(Q), \quad p = P\frac{\partial \varphi}{\partial x}^{-1}$$

in particular the feedback acts trivially.

Theorem 3.2 ([12]). *The mapping λ_1 is a covariant.*

Next, we detail the induced action restricting to exceptional singular trajectories when $\dim Q = 4$.

The exceptional singular trajectories and the feedback classification

Notation. Let φ be a diffeomorphism of Q. Then φ acts on the mapping $F : Q \to R$ according to $\varphi.F = Fo\varphi$ and on vector fields X as $\varphi.X = \varphi * X$ (image of X): this corresponds to the action on tensors.

The feedback group acts on the vector field X^e by change of coordinates only and this can be checked as a consequence of the following lemma.

Lemma 3.5. •
- $D^{F+\alpha G,\beta G} = \beta^4 D^{F,G}$
- $D'^{F+\alpha G,\beta G} = \beta^3 \left(D'^{F,G} + \alpha D^{F,G}\right)$
- $D^{\varphi * F,\varphi * G}(q) = \det\left(\frac{\partial \varphi}{\partial q}^{-1}\right) D^{F,G}(\varphi(q))$
- $D'^{\varphi * F,\varphi * G}(q) = \det\left(\frac{\partial \varphi}{\partial q}^{-1}\right) D'^{F,G}(\varphi(q))$

From which we deduce the following crucial result in our analysis.

Theorem 3.3. *We have the following:*

- $\lambda_2 : (F,G) \to X^e$ *is a covariant*
- $\lambda_3 : (F,G) \to D$ *is a semi-covariant*
- $\lambda_4 : (F,G) \to X_r^e = DF - D'G$ *is a semi-covariant*

The classification program. Having introduced the concepts and results, the contrast problem is related to the following classification program (up to change of coordinates)

- Classification of the vector fields $X_r^e = DF - DF'$ and the surfaces: $D = 0$, $D = D' = 0$.

Interpretation.

- The singular control is $u_S^e = -\frac{D'}{D}$ and will explode at $D = 0$ except if $D' = 0$, taking into account the (non isolated) singularities of X_r^e (if $D = D' = 0$, $X_r^e = 0$).

Collinear set. The collinear set of F, G is a feedback invariant which has also an important meaning in our classification.

Remark 3.1. In our classification program we use semi-covariants and in the set of parameters $\Lambda = (\gamma_1, \Gamma_1, \gamma_2, \Gamma_2)$ it amounts to work in the projective space. It is also clear from our reparametrization of time.

Now, the problem is to test the computational limits of our program which is clearly:

- Compute the surfaces $D = 0$, $D = D' = 0$,
- Compute the equilibrium points of X_r^e.

Clearly, in the framework of computational methods in real algebraic geometry it is a complicated task which has been achieved in two cases.

- The multisaturation problem of two spins taking into account B_1-inhomogeneity.

- The contrast problem when the first spin system corresponds to water ($\gamma_1 = \Gamma_1$). The second problem has application in in vivo, where the parameters are varying, in particular in the brain.

We shall present the results in details in the first case.

3.3.7 Algebraic classification in the multisaturation of two spins with B_1-inhomogeneity

The point $N = ((0,1),(0,1))$ is a singular point of X_e^r and under a translation N is taken as the origin of the coordinates. We have:

$$F_0 = (-\Gamma y_1, -\gamma z_1, -\Gamma y_2, -\gamma z_2),$$
$$F_1 = ((-(z_1+1), y_1), (1-\varepsilon)(-(z_2+1), y_2))$$

where $(1-\varepsilon)$ denotes the control rescaling of the second spin.

We have $D = (1-\varepsilon)\widetilde{D}$, where $\widetilde{D}$ is a quadric which decomposes into $h_2+h_3+h_4$ where h_i are the homogeneous part of degree i:

$$h_2 = (2\Gamma-\gamma)\bar{h}_2$$
$$\bar{h}_2 = \Gamma\,(2\Gamma-\gamma)\,((\varepsilon-1)\,y_1+y_2)^2+\gamma^2\,(\varepsilon-1)^2\,z_1^2-\gamma^2\left(2-2\,\varepsilon+\varepsilon^2\right)z_2\,z_1+\gamma^2 z_2^2$$
$$h_3 = 2(\gamma-\Gamma)\bar{h}_3$$
$$\bar{h}_3 = (\gamma-2\Gamma)\left(\gamma+2\Gamma\,(\varepsilon-1)^2\right)z_2\,y_1^2+(\gamma-2\Gamma)\,(\gamma+2\Gamma)\,(\varepsilon-1)\,(y_2\,z_1+z_2\,y_2)\,y_1-$$
$$\gamma^2\varepsilon\,(\varepsilon-2)\,z_2\,z_1^2+\left((\gamma-2\Gamma)\left(2\Gamma+(\varepsilon-1)^2\,\gamma\right)y_2^2+\gamma^2\varepsilon\,(\varepsilon-2)\,z_2^2\right)z_1$$
$$h_4 = 4(\gamma-\Gamma)^2\bar{h}_4$$
$$\bar{h}_4 = 2\left(\gamma+(\varepsilon-1)^2\,\Gamma\right)z_2^2y_1^2+4\,(\varepsilon-1)\,(\gamma+\Gamma)\,z_2\,y_2\,z_1\,y_1+2\left(\Gamma+(\varepsilon-1)^2\,\gamma\right)y_2^2z_1^2$$
$$D' = 2\gamma^2(\Gamma-\gamma)(2\Gamma-\gamma)(1-\varepsilon)(z_1-z_2)((\varepsilon-1)\,z_1y_2+z_2y_1).$$

In particular we deduce (compare with [16] in the contrast problem):

Proposition 3.5. *The quadric D' reduces to a cubic form which is factorized into a linear and a quadratic (homogeneous) forms.*

Singular analysis

We assume $\gamma > 0$ and $2\Gamma > 3\gamma$. It implies $\gamma \neq \Gamma$ and $\gamma \neq 2\Gamma$. The main result is the following:

Theorem 3.4. *Provided $\varepsilon \neq 1$ the equilibrium points of $X_e^r = DF_0 - D'F_1$ are all contained in $\{D = D' = 0\}$.*

Proof. Obviously, every point of $\{D=0\}\cap\{D'=0\}$ is a singularity of X_e^r.

Conversely, let us assume $\varepsilon\neq 1$. We first divide X_e^r by $1-\varepsilon$. We still assume that $\Gamma\neq 0$. We consider the equations $\{(X_e^r)_{y_1}=0,(X_e^r)_{z_1}=0,(X_e^r)_{y_2}=0,(X_e^r)_{z_2}=0\}$ and remark that the last third are dividable by γ. By homogeneity, changing γ into $\gamma\Gamma$, we get rid of Γ. So we may assume $\Gamma=1$. The resulting system is denoted Σ_r. We add the two polynomials $((\varepsilon-1)\,z_1\,y_2+z_2\,y_1)\,a_1-1$ and $(z_1-z_2)\,a_2-1$, and the polynomials $\gamma g-1$, $(\gamma-1)g_1-1$, $(\gamma-2)g_2-1$. We denote $\widetilde{\Sigma}_r$ this new system, involving four new variables g_1,g_2,a_1,a_2. We compute a Gröbner basis with total degree with reverse lexicographic order on $(y_1,y_2,z_1,z_2,\varepsilon,g,g_1,g_2,a_1,a_2)$ and get $\{1\}$. Hence, provided γ is different from $0,1,2$, there is no singular point of X_e^r outside of $\{D=0\}\cap\{D'=0\}$.

The remaining of the section is devoted to the singularity resolution. From the factorized form of D' (Proposition 3.5) we get:

Proposition 3.6. *$\{D=0\}\cap\{D'=0\}$ is an algebraic variety of algebraic dimension 2 whose components are located in the hyperplane $z_1=z_2$ and in the hypersurface $(\varepsilon-1)\,z_1y_2+z_2y_1=0$.*

These components are studied in the following analysis, and explicitly expressed in Lemmas 3.6, 3.7, 3.8, 3.9.

- Case A: components of $\{D=0\}\cap\{D'=0\}$ in $z_1=z_2$.
  Under the constraint $z_1=z_2$, we have a factorization $\widetilde{D}=p_1\,p_2$ with:

$$p_1=2\,(\gamma-\Gamma)\,z_1+\gamma-2\Gamma$$

and:

$$\begin{aligned}p_2=&\left(2\,(\gamma-\Gamma)\left(\gamma+(\varepsilon-1)^2\,\Gamma\right)z_1+\Gamma\,(\varepsilon-1)^2\,(\gamma-2\Gamma)\right)y_1^2+\\&(4\,(\gamma-\Gamma)\,(\gamma+\Gamma)\,(\varepsilon-1)\,z_1+2\Gamma\,(\varepsilon-1)\,(\gamma-2\Gamma))\,y_2\,y_1+\\&\left(2\,(\gamma-\Gamma)\left(\Gamma+(\varepsilon-1)^2\,\gamma\right)z_1+\Gamma\,(\gamma-2\Gamma)\right)y_2^2\end{aligned}$$

The first polynomial has one root $z_1=z_{\gamma,\Gamma}$

$$z_{\gamma,\Gamma}=\frac{1}{2}\,\frac{2\Gamma-\gamma}{\gamma-\Gamma}$$

which corresponds to the plane-solution $\{(y_1,z_{\gamma,\Gamma},y_2,z_{\gamma,\Gamma}),\ (y_1,y_2)\in\mathbb{R}^2\}$.
We put:

$$d_2(y_1,y_2)=\left(\gamma+(\varepsilon-1)^2\,\Gamma\right)y_1^2+2\,(\varepsilon-1)\,(\gamma+\Gamma)\,y_2\,y_1+\left(\Gamma+(\varepsilon-1)^2\,\gamma\right)y_2^2$$

The discriminant of d_2 with respect to y_1 is $-4\,(\varepsilon-2)^2\,\gamma\Gamma\,\varepsilon^2\,y_2^2$ which is strictly negative provided $\varepsilon\neq 0$. So d_2 is non-zero outside $y_1=y_2=0$.
So, provided $y_1^2+y_2^2\neq 0$, $d_2\neq 0$, and $p_2=0$ is solved with respect to z_1. We get $z_1=r_2(y_1,y_2)$ with

$$r_2(y_1,y_2)=\frac{\Gamma\,(2\Gamma-\gamma)\,((\varepsilon-1)\,y_1+y_2)^2}{2\,(\gamma-\Gamma)\,d_2(y_1,y_2)}$$

and $(y_1,r_2(y_1,y_2),y_2,r_2(y_1,y_2))$ (defined for $(y_1,y_2)\neq(0,0)$) vanishes both D and D'.
Finally, if $y_1=y_2=0$, we have the solution $(0,z,0,z),\quad z\in\mathbb{R}$.
We summarize the case $z_1=z_2$ in:

Lemma 3.6. *$\{D=0\}\cap\{D'=0\}\cap\{z_1=z_2\}$ is the union of an affine plane $z_1=z_2=z_{\gamma,\Gamma}$, a rational surface $z_1=z_2=r_2(y_1,y_2)$ (defined for $(y_1,y_2)\neq(0,0)$), and the line $\{(0,z,0,z),\ z\in\mathbb{R}\}$.*

- Case B: components of $\{D=0\}\cap\{D'=0\}$ in $(\varepsilon-1)\,z_1y_2+z_2y_1=0$.
  - Assume first that $y_1=0$ and $z_1\neq z_2$. We have $z_1y_2=0$.
    - If $y_1=z_1=0$, then:

      $$\widetilde{D}=(\gamma-2\Gamma)\left(\Gamma\,(\gamma-2\Gamma)\,y_2^2+\gamma^2z_2^2\right)$$

      Since $2\Gamma>\gamma$, $\{\widetilde{D}=0\}\cap\{y_1=z_1=0\}$ corresponds to two lines intersecting at N.
    - If $y_1=y_2=0$, then let us put

      $$d_1(z_1)=2\,\varepsilon\,(\varepsilon-2)\,(\gamma-\Gamma)\,z_1+2\Gamma-\gamma.$$

      We have:

      $$\widetilde{D}=\gamma^2(z_2-z-1)(d_1(z_1)z_2-(\varepsilon-1)^2\,(2\Gamma-\gamma)\,z_1$$

      Observe that the polynomial d_1 vanishes if and only if z_1 equals $\widetilde{z}_{\gamma,\Gamma}$ with

      $$\widetilde{z}_{\gamma,\Gamma}=\frac{1}{2}\,\frac{\gamma-2\Gamma}{\varepsilon\,(\varepsilon-2)\,(\gamma-\Gamma)}$$

      and in this case, there is no solution such that $z_2\neq z_1$.
      Provided $d_1(z_1)\neq 0$, one gets $z_2=r_1(z_1)$:

      $$r_1(z_1)=\frac{(\varepsilon-1)^2\,(2\Gamma-\gamma)\,z_1}{d_1(z_1)}$$

      which is a rational function of z_1. And the intersection with $\{D=0\}\cap\{D'=0\}$ is the curve $\{(0,z_1,0,r_1(z_1))\ z_1\in\mathbb{R}\setminus\{\widetilde{z}_{\gamma,\Gamma}\}\}$.

      Lemma 3.7. *$\{D=0\}\cap\{D'=0\}\cap\{y_1=0\}\cap\{(z_1-z_2)\neq 0\}$ is the union of two lines of $\{y_1=z_1=0\}$ intersecting at N and a rational curve $\{(0,z_1,0,r_1(z_1))\ z_1\in\mathbb{R}\setminus\{\widetilde{z}_{\gamma,\Gamma}\}\}$.*

  - Let us assume $y_1\neq 0$.
    We can eliminate z_2 using:

$$z_2 = \frac{z_1\, y_2\, (1-\varepsilon)}{y_1}$$

and, substituting in $y_1^2\widetilde{D}$ we get the factorization $y_1^2\widetilde{D} = q_1\, q_2$, with:

$$\begin{aligned} q_1 = {} & \Gamma\,(\varepsilon-1)\,(2\Gamma-\gamma)\,y_1^3 + \gamma^2\,(\varepsilon-1)\,z_1^2 y_1 + \gamma^2\,(\varepsilon-1)^2\,z_1^2 y_2 \\ & + (2\Gamma\,\varepsilon\,(\varepsilon-2)\,(\gamma-\Gamma)\,z_1 - \Gamma\,(\gamma-2\Gamma))\,y_2\,y_1^2 \end{aligned}$$

and:

$$\begin{aligned} q_2 &= (\varepsilon-1)\,(\gamma-2\Gamma)\,y_1 + (2\,\varepsilon\,(2-\varepsilon)\,(\gamma-\Gamma)\,z_1 + \gamma - 2\Gamma)\,y_2 \\ &= (\varepsilon-1)\,(\gamma-2\Gamma)\,y_1 + d_1(z_1)y_2 \end{aligned}$$

Provided $d_1 \neq 0$ (that is $z_1 \neq \widetilde{z}_{\gamma,\Gamma}$), we solve $q_2 = 0$ with respect to y_2, and then we get the value of (y_2, z_2):

$$\left(\frac{(\varepsilon-1)\,(\gamma-2\Gamma)\,y_1}{d_1(z_1)}, \frac{(\varepsilon-1)^2\,(2\Gamma-\gamma)\,z_1}{d_1(z_1)} \right)$$

Lemma 3.8. *$\{D=0\} \cap \{D'=0\} \cap \{(z_1-z_2)\,y_1 d_1(z_1) \neq 0\}$ is a rational surface $(y_2 = \rho_2(y_1,z_1), z_2 = \rho_1(z_1) y_1 \neq 0 z_1 \neq \widetilde{z}_{\gamma,\Gamma})$.*

We put d_3

$$d_3 = (2\Gamma\,\varepsilon\,(\varepsilon-2)\,(\gamma-\Gamma)\,z_1 - \Gamma\,(\gamma-2\Gamma))\,y_1^2 + \gamma^2\,(\varepsilon-1)^2\,z_1^2$$

Its discriminant with respect to y_1 is:

$$-4\,\left(2\Gamma - 4\,\gamma z_1\,\varepsilon + 2\,\gamma z_1\,\varepsilon^2 - \gamma + 4\Gamma\,z_1\,\varepsilon - 2\Gamma\,z_1\,\varepsilon^2\right)\Gamma\,\gamma^2 z_1^2\,(\varepsilon-1)^2$$

$$-4\,(2\Gamma - \gamma + 2\,\varepsilon\,(2-\varepsilon)\,(\Gamma-\gamma)\,z_1)\,\Gamma\,\gamma^2 z_1^2\,(\varepsilon-1)^2$$

and its sign changes when z_1 reaches $\widetilde{z}_{\gamma,\Gamma}$.
Provided $d_3(y_1,z_1) \neq 0$, we solve q_1 with respect to y_2, and then we get the value of (y_2, z_2):

$$\left(\frac{\left(\Gamma\,(2\Gamma-\gamma)\,y_1^2 + \gamma^2 z_1^2\right)(1-\varepsilon)\,y_1}{d_3(y_1,z_1)}, \frac{\left(\Gamma\,(2\Gamma-\gamma)\,y_1^2 + \gamma^2 z_1^2\right)(\varepsilon-1)^2\,z_1}{d_3(y_1,z_1)} \right)$$

Lemma 3.9. *$\{D=0\} \cap \{D'=0\} \cap \{(z_1-z_2)\,y_1 d_3(z_1) \neq 0\}$ is a rational surface with parameterization $(y_2 = \rho_3(y_1,z_1), z_2 = \rho_4(y_1,z_1))$.*

- Analysis of the behaviors of the solutions of X_e^r near O.
  We set $\widetilde{z}_i = 1 + z_i$ and we have the following approximations:
  - $D = (1-\varepsilon)\widetilde{D}$, $\widetilde{D} = h_1 + h_2$,

$$
\begin{aligned}
h_1 &= \gamma^2\varepsilon\,(\varepsilon-2)\,(\gamma-2\Gamma)\,(\widetilde{z}_1-\widetilde{z}_2)\\
h_2 &= \Gamma\,(\varepsilon-1)^2\,(\gamma-2\Gamma)^2\,y_1^2+2\Gamma\,(\gamma-2\Gamma)^2\,(\varepsilon-1)\,y_2\,y_1\\
&\quad+\Gamma\,(\gamma-2\Gamma)^2\,y_2^2-\gamma^2\,(\varepsilon-1)^2\,(\gamma-2\Gamma)\,\widetilde{z}_1^2\\
&\quad-\gamma^2\,(\gamma-2\Gamma)\,\widetilde{z}_2^2+\gamma^2\left(\varepsilon^2+2-2\varepsilon\right)(\gamma-2\Gamma)\,\widetilde{z}_1\widetilde{z}_2
\end{aligned}
$$

– $D' = 2\gamma^2(\Gamma-\gamma)(2\Gamma-\gamma)(1-\varepsilon)(\widetilde{z}_2-\widetilde{z}_1)[(-1+\widetilde{z}_1)y_2(\varepsilon-1)+(-1+\widetilde{z}_2)y_1]$.

Conclusion: these computations allow to evaluate the equilibrium points and the behaviors of the solutions near such point, using linearization methods. A first step towards the global behavior is the following result.

Lemma 3.10. *The surface $y_1 = y_2 = 0$ is foliated by lines solutions connecting O to the north pole N, the singular control being zero.*

3.3.8 Numerical simulations, the ideal contrast problem

This section is devoted to numerical simulation in the ideal control problem using three complementary softwares:

- `Bocop`: direct method,
- `HamPath`: indirect method,
- `GloptiPoly`: Lmi technique to estimate the global optimum.

The algorithms based on the softwares are presented in details in [19].

The ideal contrast problem by saturation in the single-input case, can be summarized this way:

$$
\begin{cases}
c(q(t_f)) &= -|q_2(t_f)|^2 \longrightarrow \min_{u(\cdot)},\ \text{fixed } t_f\\
\dot{q} &= F_0(q)+u_1F_1(q),\\
q(0) &= q_0\\
q_1(t_f) &= 0
\end{cases}
\tag{ICPS}
$$

where $q=(q_1,q_2)$, $q_i=(y_i,z_i)\in\mathbb{R}^2$, $|q_i|\leq 1$, $i=1,2$. The initial condition for each spin is $q_i(0)=(0,1)$. The vector fields F_0 and F_1 are given by:

$$
\begin{aligned}
F_0(q) &= \sum_{i=1,2}(-\Gamma_i y_i)\frac{\partial}{\partial y_i}+(\gamma_i(1-z_i))\frac{\partial}{\partial z_i},\\
F_1(q) &= \sum_{i=1,2}-z_i\frac{\partial}{\partial y_i}+y_i\frac{\partial}{\partial z_i},
\end{aligned}
$$

where $\Lambda_i=(\gamma_i,\Gamma_i)$ are the physical parameters representing each spin.

We present the simulations using the numerical methods (see [19] for a complete description of the algorithms).

The simulations correspond to the two following sets of experimental data, with the relaxation times in seconds and $T_{\min}$ the solution of the time minimal saturation problem for a single spin, from section 3.3.3.

P_1: **Fluid case.**
Spin 1: Cerebrospinal fluid: $T_1 = 2$, $T_2 = 0.3$;
Spin 2: Water: $T_1 = 2.5 = T_2$.
$T_{\min} = 26.17040$.

P_2: **Blood case.**
Spin 1: Deoxygenated blood: $T_1 = 1.35$, $T_2 = 0.05$;
Spin 2: Oxygenated blood: $T_1 = 1.35$, $T_2 = 0.2$.
$T_{\min} = 6.7981$.

Optimal solutions of the contrast problem are concatenations of bang and singular extremals. For the following sections, we introduce some notations. We note BS the sequence composed by one bang arc (δ_+ or δ_-) followed by one singular arc (δ_s), and nBS, $n > 1$, the concatenation of n BS-sequences.

First results with fixed final time

The first difficulty comes from the discontinuities of the optimal control structure. We need to know the control structure (meaning the number of Bang-Singular sequences) before calling the multiple shooting method. The indirect method also typically requires a reasonable estimate for the control switching times, as well as the states and costates values at the initial and switching times. We use the `Bocop` software based upon direct methods to obtain approximate optimal solutions in order to initialize the indirect shooting, within the `HamPath` code. We recall that the costate (or adjoint state) for Pontryagin's Principle corresponds to the Lagrange multipliers for the dynamics constraints in the discretized problem, and can therefore be extracted from the solution of the direct method.

The only a priori information is the value of the minimum time transfer $T_{\min}$, used to set the final time t_f in the $[T_{\min}, 3T_{\min}]$ range. We note $t_f = \lambda T_{\min}$ with λ in $[1,3]$. The state variables are initialized as constant functions equal to the initial state, *i.e.* $y_1(\cdot) = y_2(\cdot) = 0$, $z_1(\cdot) = z_2(\cdot) = 1$. For the control variables we use the three constant initializations $u_1(\cdot) \in \{0.1, 0.25, 0.5\}$. The discretization method used is implicit midpoint (2nd order) with a number of time steps set to $\lambda \times 100$. In order to improve convergence, we add a small regularization term to the objective to be minimized, $\varepsilon_{reg} \int_0^{t_f} |u(t)|^2 \mathrm{d}t$, with $\varepsilon_{reg} = 10^{-3}$.

We repeat the optimizations for λ in $\{1.1, 1.5, 1.8, 2.0, 3.0\}$ with the three control initializations, see Table. 3.1. The solutions from `Bocop` are used to initialize the continuations in `HamPath`, and we discuss in the following sections the results obtained with the indirect method. Both methods confirm the existence of many

local solutions, as illustrated on Fig. 3.2 for $\lambda = 1.5$, due in particular to symmetry reasons.

λ	1.1	1.5	1.8	2	3
u_{init} : 0.1	0.636 (++)	0.678 (+−+)	0.688 (+−+)	0.702 (−+)	0.683 (−+−+)
u_{init} : 0.25	FAIL	0.661 (++−+)	0.673 (++−+)	0.691 (−++)	0.694 (+−+)
u_{init} : 0.5	0.636 (++)	0.684 (++)	0.699 (−+)	0.697 (++)	0.698 (++)

Table 3.1 Fluid case: Batch optimizations (Direct method). For each value of λ we test the three initializations for the control u, and record the value of the objective (*i.e.* the contrast), as well as the control structure (*i.e.* the signs of bang arcs). CPU times for a single optimization are less than one minute on a Intel Xeon 3.2GHz.

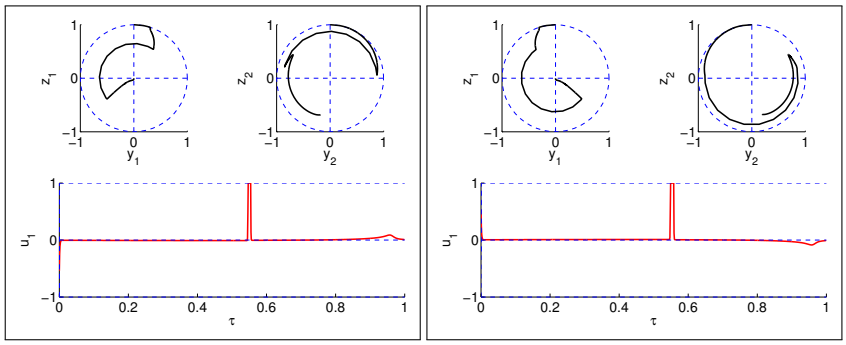

Fig. 3.2 Fluid case: Two local solutions for $\lambda = 2.0$. Trajectories for spin 1 and 2 in the (y,z)-plane are portrayed in the first two subgraphs of each subplot. The corresponding control is drawn in the bottom subgraph. The two bang arcs have the same sign for the left solution, whereas for the right solution, the two bang arcs are of opposite sign.

Second order conditions

According to proposition 3.2 from [20], the non-existence of conjugate points on each singular arc of a candidate solution is a necessary condition of local optimality. See [20] for details about conjugate points in the contrast problem. Here, we compute for each singular arc of all the solutions from subsection 3.3.8, the first conjugate point along the arc, applying the algorithm presented in subsection 4.3 from [20]. None of the solutions has a conjugate point on a singular arc. Hence all the solutions satisfy the second order necessary condition of local optimality. Fig. 3.3 represents the computations of the two conjugate points (since the structure is 2BS) of the best solution with $\lambda = 2.0$ from subsection 3.3.8.

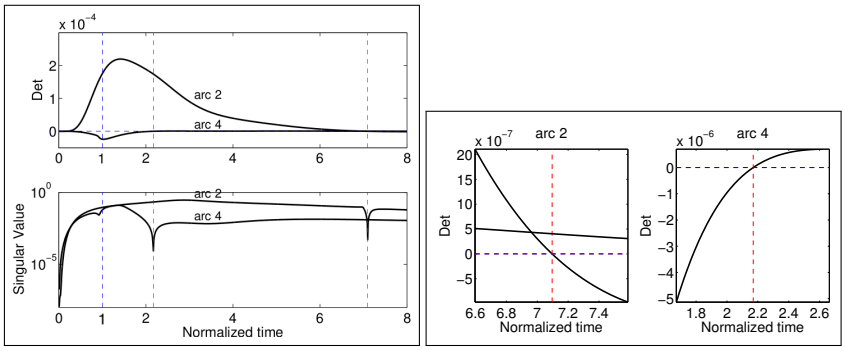

Fig. 3.3 Fluid case: second order conditions. Second order necessary condition checked on the best solution with $\lambda = 2.0$ from subsection 3.3.8. The rank condition from the algorithm presented in subsection 4.3 from [20] is evaluated along the two singular arcs. See [14] for details on the concept of conjugate times. On the left subplot, for each singular arc, the curve is reparameterized so that the final time corresponds to the abscissa 1 (vertical blue dashed line); the determinant associated with the rank condition is plotted (top subgraph), so there is a conjugate time whenever it vanishes (vertical red dashed lines). One observes that conjugate times on each arc are located after the (normalized to 1) final time, satisfying necessary condition of local optimality of the trajectory. At the bottom, the smallest singular value of the matrix whose rank we test is plotted, extracting only the relevant information to detect the rank drops. On the right subplot is presented a zoom of top-left subgraph near the two conjugate times.

Influence of the final time

Given that the initial point (the North pole) is a stationary point, the constrast is an increasing function of t_f acting as a parameter. Indeed, applying a zero control at $t = 0$ leaves the system in its initial state so there is an inclusion of admissible controls between problems when the final time is increased (and the bigger the set of controls, the larger the maximum contrast). Having increasing bounded (by one, which is the maximum possible contrast given the final condition on spin no. 1) functions, it is natural to expect asymptotes on each branch.

In both cases P_1 and P_2, the contrast problem has many local solutions, possibly with different control structures. Besides, the structure of the best policy can change depending on the final time. The possible change of structure along a single path of zeros is emphasized in Fig. 3.4. In this figure, the branch made of 2BS solutions is represented in blue, whereas the 3BS branch is the dashed red line. We also show a crossing between two value functions of two different paths of zeros in Fig. 3.5.

Then for each solution of each branch the second order necessary condition is checked as in subsection 3.3.8: the first conjugate point of each singular extremal is computed. There is no failure in this test, hence all the solutions satisfy the necessary second order condition of local optimality. Fig. 3.6 presents the second order conditions along the extended path from Fig. 3.4.

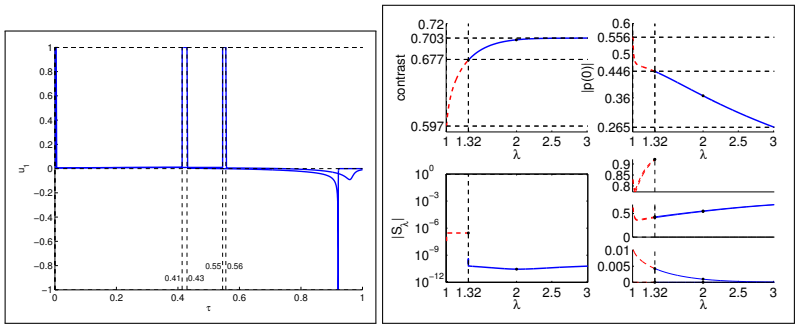

Fig. 3.4 Fluid case: influence of the final time. On the left subgraph are shown the control laws of solutions at $\lambda = 2$ and $\lambda = 1.32$ from path from the right subplot. For $\lambda = 1.32$, we can see the saturating singular arc around the normalized time $\tau = 0.92$ (the time is normalized to be between 0 and 1 for each solution). The 2BS solution at $\lambda = 1.32$ is used to initialize a multiple shooting with a 3BS structure and then to perform a new homotopy from $\lambda = 1.32$ to $\lambda = 1$. On the right subgraph is portrayed the two homotopies: the first from $\lambda = 2$ to $\lambda = 1.32$ and the second to $\lambda = 1$, with one more BS sequence. The value function, the norm of the initial adjoint vector, the norm of the shooting function and the switching times along the path are given. The blue color represents 2BS solutions while the red color is for 3BS structures. The dashed red lines come from the extended path after the change of structure detected around $\lambda = 1.32$.

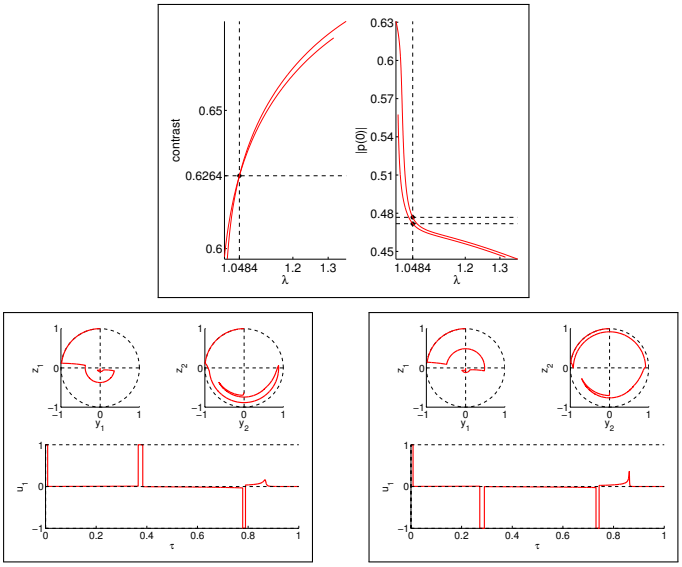

Fig. 3.5 Fluid case: influence of the final time. Crossing between two branches with 3BS solutions. The crossing is around $\lambda = 1.0484$, see top subgraph. Thus for $\lambda \leq 1.0484$, the best solution, locally, has a 3BS structure of the form $\delta_+\delta_s\delta_+\delta_s\delta_-\delta_s$ (bottom-left subgraph) while for $\lambda \in [1.0484, 1.351]$ the best solution is of the form $\delta_+\delta_s\delta_-\delta_s\delta_-\delta_s$ (bottom-right subgraph). On the two bottom subgraphs, the trajectories for spin 1 and 2 in the (y,z)-plane are portrayed with the corresponding control, both for $\lambda = 1.0484$.

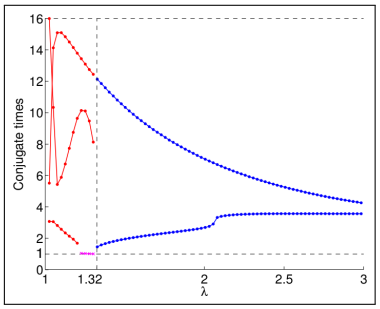

Fig. 3.6 Fluid case: influence of the final time. Second order necessary condition checked along the extended path from Fig. 3.4. For all solutions from $\lambda = 1$ to $\lambda = 3$ are computed the first conjugate times along each singular arc. For $\lambda \in [1, 1.32]$, the structure is 3BS and there are 3 singular arcs. For $\lambda \in [1.32, 3]$, there are 2 singular arcs. Each singular interval is normalized in such a way the initial time is 0 and the final time is 1. The lower dashed horizontal line represents the final time 1. There is no conjugate time before the normalized final time 1 which means that all solutions satisfy the second order necessary condition of local optimality. Note that at a magenta cross, around $(1.32, 1)$, the control of the first singular arc saturates the constraint $|u| = 1$, and so no conjugate time is computed after this time.

Sub-optimal syntheses in fluid and blood cases

We give the syntheses of locally optimal solutions obtained in the blood and fluid cases. Note that in the special case $t_f = T_{\min}$, for both cases the solution is 2BS and of the form $\delta_+\delta_s\delta_+\delta_s$.

For the fluid case, the left subplot of Fig. 3.7 represents all the different branches we obtained by homotopy on λ. The greatest two value functions intersect around $t_f = 1.048 T_{\min}$. The right subplot shows the sub-optimal synthesis. The best policy is:

$$\begin{array}{ll} \delta_+\delta_s\delta_+\delta_s & \text{for } \lambda \in [1.000, 1.006], \\ \delta_+\delta_s\delta_+\delta_s\delta_-\delta_s & \text{for } \lambda \in [1.006, 1.048], \\ \delta_+\delta_s\delta_-\delta_s\delta_-\delta_s & \text{for } \lambda \in [1.048, 1.351], \\ \delta_+\delta_s\delta_-\delta_s & \text{for } \lambda \in [1.351, 3.000]. \end{array} \tag{3.38}$$

For the blood case, the results are excerpted from [29]. The left subplot of Fig. 3.8 shows the contrast for five different components of $\{h = 0\}$, for final times $t_f \in [1, 2] T_{\min}$. The three black branches are made only of BS solutions whereas the two others are made of 2BS and 3BS solutions. To maximize the contrast, the best policy, drawn as solid lines, is:

$$\begin{array}{ll} \delta_+\delta_s\delta_+\delta_s & \text{for } \lambda \in [1.000, 1+\varepsilon],\ \varepsilon > 0 \text{ small} \\ \delta_+\delta_s & \text{for } \lambda \in [1+\varepsilon, 1.294], \\ \delta_+\delta_s\delta_-\delta_s\delta_-\delta_s & \text{for } \lambda \in [1.294, 2.000]. \end{array} \tag{3.39}$$

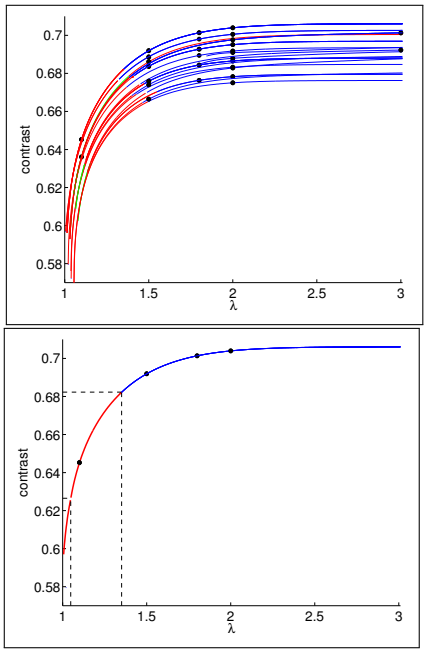

Fig. 3.7 Fluid case, sub-optimal synthesis. Illustration on the left subplot, of local solutions (each branch corresponds to a control structure). The suboptimal synthesis is plotted on right subplot. The colors are blue for 2BS structure, red for 3BS and green for 4BS. The best policy is $\delta_+\delta_s\delta_+\delta_s\delta_-\delta_s$ for $\lambda \leq 1.0484$, and $\delta_+\delta_s\delta_-\delta_s\delta_-\delta_s$ for $\lambda \in [1.0484, 1.351]$. Then, for $\lambda \in [1.351, 3]$, the best policy is 2BS and of the form $\delta_+\delta_s\delta_-\delta_s$.

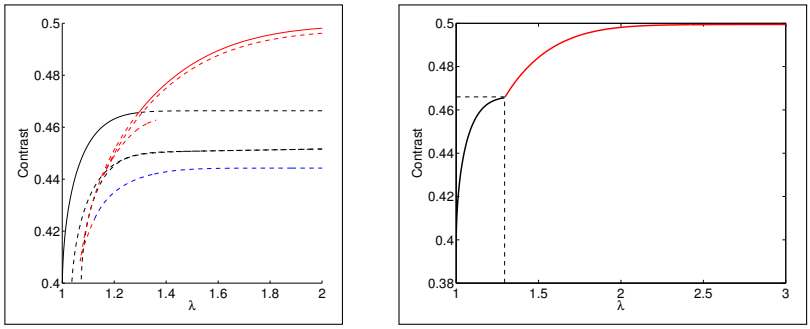

Fig. 3.8 Blood case, sub-optimal synthesis. Illustration on the left subplot, of local solutions (each branch corresponds to a control structure). Best policy as solid lines, local solutions as dashed lines. The suboptimal synthesis is plotted on right subplot. The colors are black for BS structure, blue for 2BS and red for 3BS. The best policy is BS for $t_f \in (1, 1.294)T_{\min}$ and 3BS of the form $\delta_+\delta_s\delta_-\delta_s\delta_-\delta_s$ for $t_f \in (1.294, 2]T_{\min}$. In the special case $t_f = T_{\min}$, the solution is 2BS and of the form $\delta_+\delta_s\delta_+\delta_s$

Sub-optimal syntheses compared to global results

We now apply the `lmi` method to the contrast problem, described in [19], in order to obtain upper bounds on the true contrast. Comparing these bounds to the contrast of our solutions then gives an insight about their global optimality.

Table 3.2 shows the evolution of the upper bound on the contrast in function of `lmi` relaxation order, for the fluid case with $t_f = T_{\min}$. As expected, the method yields a monotonically non-increasing sequence of sharper bounds. Relaxations of orders 4 and 5 yield very similar bounds, but this should not be interpreted as a termination criterion for the `lmi` method.

r	$\sqrt{-J_M^r}$	N_r	t_r
1	0.8474	63	0.7
2	0.7552	378	3
3	0.6226	1386	14
4	0.6069	3861	332
5	0.6040	9009	8400

Table 3.2 Fluid case, $t_f = T_{\min}$: upper bounds on contrast $\sqrt{-J_M^r}$, numbers of moments N_r and CPU times t_r in function of relaxation order r.

Figs. 3.9 and 3.10 compare the tightest upper bounds found by the `lmi` method with the best candidate solutions found by `Bocop` and `HamPath`, in both the blood and fluid cases. The figures also represent the relative gap between the methods defined as $(C_{LMI} - C_H)/C_H$, where C_{LMI} is the `lmi` upper bound and C_H is the contrast found with `HamPath`. As such, this measure characterizes the optimality gap between the methods. It does not, however, specify which of the method(s) could be further improved. At the fifth relaxation, the average gap is around 11% in the blood case, which, given the application, is satisfactory on the experimental level. For the fluid case, the average gap on the contrast is about 2% at the fifth relaxation, which strongly suggest that the solution is actually a global optimum. The gap is even below the 1% mark for $t_f \leq 2\,T_{\min}$.

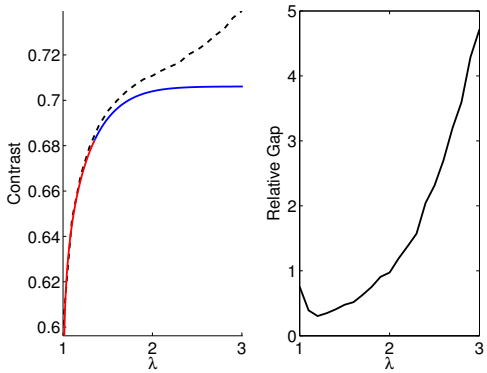

Fig. 3.9 Fluid case. Best upper bounds (dashed line) by the `lmi` method compared with best solutions by `HamPath` (solid line), and relative gap between the two.

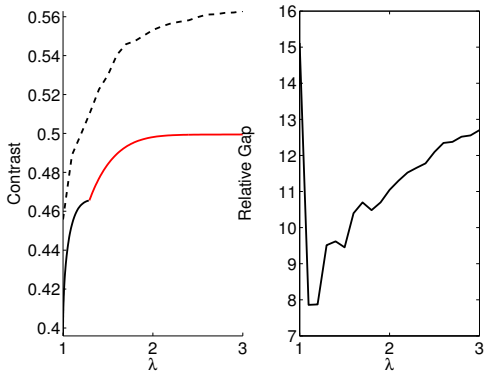

Fig. 3.10 Blood case. Best upper bounds (dashed line) by the `lmi` method compared with best solutions by `HamPath` (solid line), and relative gap between the two.

References

1. Alouges, F., DeSimone, A., Lefebvre, A.: Optimal strokes for low Reynolds number swimmers: an example. J. Nonlinear Sci. **18**, 277–302 (2008).
2. Agrachev, A., Sarychev, A.: Abnormal sub-Reimannian geodesics: Morse index and rigidity. Ann. Inst. H. Poincaré Anal. Non Linéaire **13**, 6 635-690 (1996)
3. Aleexev, V., Tikhomirov, V., Fomine, S.: Commande Optimale. Mir, Moscow (1982)
4. Arnol˜d, V. I., Guseĭn-Zade, S.M., Varchenko, A.N.: Singularities of differentiable maps. Birkhäuser Boston, Inc., Boston MA. (1985)
5. Batchelor, G.K.: Slender-body theory for particles of arbitrary cross-section in Stokes flow. J. Fluid Mech. **44**, 419–440 (1970)
6. Becker, L.E., Stephan, A.K., Howard, A.S.: On self-propulsion of micro-machines at low Reynolds number: Purcell's three-link swimmer. J. Fluid Mech. **490**, 15–35 (2003)
7. Bellaïche, A.: The tangent space in sub-Riemannian geometry. J. Math. Sci. (New York) **35**, 461–476 (1997)
8. Berger, M.: La taxonomie des courbes. Pour la science, 297 56–63 (2002)
9. Bettiol, P., Bonnard, B., Giraldi, L., Martinon, P., Rouot, J.: The Purcell Three-link swimmer: some geometric and numerical aspects related to periodic optimal controls. *to appear* (2015)
10. Bloch, F.: Nuclear induction. Physical review, 7-8 460 (1946)
11. Bonnans, F., Giorgi, D., Maindrault, S., Martinon, P., Grélard, V.: Bocop - A collection of examples, Inria Research Report, Project-Team Commands. **8053** (2014)
12. Bonnard, B.: Feedback equivalence for nonlinear systems and the time optimal control problem. SIAM J. Control Optim. **29**, 6 pp 1300–1321 (1991)
13. Bonnard, B., Caillau, J.-B., Trélat, E.: Geometric optimal control of elliptic Keplerian orbits. Discrete Contin. Dyn. Syst. Ser. B 5, 4 929–956 (2005)
14. Bonnard, B., Caillau, J.-B., Trélat, E.: Second order optimality conditions in the smooth case and applications in optimal control. ESAIM Control Optim. Calc. Var. **13**, 2 207–236 (2007)
15. Bonnard, B., Chyba, M.: Singular trajectories and their role in control theory. Springer-Verlag, Berlin (2003)
16. Bonnard, B., Chyba, M., Jacquemard, A., Marriott, J.: Algebraic geometric classification of the singular flow in the contrast imaging problem in nuclear magnetic resonance. Math. Control Relat. Fields **3**, 4 397–432 (2013)
17. Bonnard, B., Chyba, M., Marriott, J.: Singular Trajectories and the Contrast Imaging Problem in Nuclear Magnetic resonance. SIAM J. Control Optim. **51**, 2 1325–1349 (2013)
18. Bonnard, B., Chyba, M., Rouot, J., Takagi, D., Zou, R.: A note about the geometric optimal control of the copepod swimmer. *Submitted Math. Control and Related Fields* (2015)
19. Bonnard, B., Claeys, M., Cots, O., Martinon, P.: Geometric and numerical methods in the contrast imaging problem in nuclear magnetic resonance. Acta Appl. Math. (2013)
20. Bonnard, B., Cots, O.: Geometric numerical methods and results in the control imaging problem in nuclear magnetic resonance. Math. Models Methods Appl. Sci. **24**, 1 187–212 (2014)
21. Bonnard, B., Faubourg, L., Trélat, E.: Mécanique céleste et contrôle des véhicules spatiaux. Mathématiques & Applications, Springer-Verlag **51**, Berlin (2006)
22. Bonnard, B., Kupka, I.: Théorie des singularités de l'application entrée/sortie et optimalité des trajectoires singulières dans le problème du temps minimal. Forum Math. **5**, 2 111–159 (1993)
23. Bliss, G.A.: Lectures on the Calculus of Variations. Univ. of Chicago Press, Chicago (1946)
24. Brockett, R.W.: Control theory and singular Riemannian geometry. Springer, New York-Berlin, 11–27 (1982)
25. Caillau, J.B., Daoud, .B.: Minimum time control of the circular restricted three-body problem. SIAM J. Control Optim. **50**, 6 3178–3202 (2011)
26. Cartan, E.: Les systèmes de Pfaff a cinq variables et les équations aux derivées partielles du second ordre. Ann. Sci. École Normale **27**, 109–192 (1910)
27. Chambrion, T., Giraldi, L., Munnier, A.: Optimal Strokes for Driftless Swimmers: A General Geometric Approach. *Submitted* (2014)

28. Chitour, Y., Jean, F., Trélat, E.: Genericity results for singular curves. J. Diff. Geom. **73**, 1 45–73 (2006)
29. Cots, O.: Contrôle optimal géométrique: méthodes homotopiques et applications. PhD thesis, Université de Bourgogne (2012)
30. Dieudonné, J.A., Carrell, J.B.: Invariant theory, old and new. Academic Press, New York-London (1971)
31. Gamkrelidze, R.V.: Discovery of the maximum principle. J. Dynam. Control Systems **5**, 4 437–451 (1977)
32. Gelfand, I.M., Fomin, S.V.: Calculus of Variations. Prentice Hall Inc., Englewood Cliffs, New Jersey (1963)
33. Godbillon, C.: Geométrie différentielle et mécanique analytic. Hermann, Paris (1969)
34. Gregory, J.: Quadratic form theory and differential equations. Mathematics in Science and Engineering **152**, New York-London (1980)
35. Hancock, G.J.: The self-propulsion of microscopic organisms through liquids. Proc. R. Soc. Lond. A **217**, 96–121 (1953)
36. Happel, J., Brenner, H.: Low Reynolds number hydrodynamics with special applications to particulate media. Prentice-Hall, Inc., Englewood Cliffs, N.J. (1965)
37. Hermes, H.: Lie algebras of vector fields and local approximation of attainable sets. SIAM J Control Optim. **16**, 5 715-727 (1978)
38. Jean, F.: Control of Nonholonomic Systems: from Sub-Riemannian Geometry to Motion Planning. Springer International Publishing, SpringerBriefs in Mathematics (2014)
39. John, F.: Partial differential equations, reprint of 4th edition. Applied Mathematical Sciences **1**, Springer-Verlag, New York (1991)
40. Jurdjevic, V.: Geometric control theory. Cambridge Studies in Advanced Mathematics **52**, Cambridge University Press, Cambridge (1997)
41. Klingenberg, W.: Riemannian geometry. de Gruyter Studies in Mathematics, Walter de Gruyter and Co., Berlin-New York (1982)
42. Krener, A.J.: The high order maximum principle and its application to singular extremals. SIAM J Control Optim. **15**, 2 256–293 (1977)
43. Kupka, I.: Geometric theory of extremals in optimal control problems. i. the fold and Maxwell case. Trans. Amer. Math. Soc. **299**, 1 225–243 (1987)
44. Kupka, I.: Géométrie sous-riemannienne. Astérisque, Séminaire Bourbaki **1995/96**, 351–380 (1997)
45. Landau, L., Lipschitz, E.: Physique théorique. Ed. Mir (1975)
46. Lapert, M.: Développement de nouvelles techniques de contrôle optimal en dynamique quantique : de la Résonance Magnétique Nucléaire à la physique moléculaire. Phd thesis, Laboratoire Interdisciplinaire Carnot de Bourgogne, Dijon (2011)
47. Lapert, M., Zhang, Y., Glaser, S.J., Sugny, D.: Towards the time-optimal control of dissipative spin-1/2 particles in nuclear magnetic resonance. J. Phys. B: At. Mol. Opt. Phys. **44**, 15 (2011)
48. Lauga, E., Powers, T.R.: The hydrodynamics of swimming microorganisms. Rep. Progr. Phys. **72**, 9 (2009)
49. Lawden, D.F.: Elliptic functions and applications. Applied Mathematical Sciences, Springer-Verlag, New York **80** (1989)
50. Lee, E.B., Markus, L.: Foundations of optimal control theory, Second edition. Robert E. Kreiger Publishing Co., Inc., Melbourne (1986)
51. Levitt, M.H.: Spin dynamics: basics of nuclear magnetic resonance. John Wiley and Sons (2001)
52. Liberzon, D.: Calculus of Variations and Optimal Control Theory: A Concise Introduction. Princeton University Press, (2011)
53. Maciejewski, A.J., Respondek, W.: The nilpotent tangent 3-dimensional sub-Riemannian problem is nonintegrable. 2004 43rd IEEE Conference on Decision and Control, (2004)
54. Milnor, J.: Morse theory. Annals of Mathematics Studies **51**, Princeton University Press, Princeton (1963)
55. Mishchenko, A.S., Shatalov, V.E., Sternin, B.Y.: Lagrangian manifolds and the Maslov operator. Springer Series in Soviet Mathematics, Springer-Verlag, Berlin (1990)

56. Or, Y., Zhang, S., Murray, R.M.: Dynamics and stability of low-Reynolds-number swimming near a wall. SIAM J. Appl. Dyn. Syst. **10**, 1013–1041 (2011)
57. Passov, E., Or, Y.: Supplementary document to the paper: Dynamics of Purcell's three-link microswimmer with a passive elastic tail. Supplementary Notes.
58. Pontryagin,L.S., Boltyanskii, V.G., Gamkrelidze, R.V.: The Mathematical Theory of Optimal Processes. John Wiley and Sons, New York (1962)
59. Purcell, E.M.: Life at low Reynolds number. Am. J. Phys. **45**, 3–11 (1977)
60. Sachkov, Y.L.: Symmetries of flat rank two distributions and sub-Riemannian structures. Trans. Amer. Math. Soc. **356**, 457–494 (2004)
61. Sontag, E.D.: Mathematical control theory. Deterministic finite-dimensional systems, second edition. Texts in Applied Mathematics **6**, Springer-Verlag, New York (1998)
62. Sussmann, H.J.: Orbits of families of vector fields and integrability of distributions. Trans. Am. Math. Soc. **180**, 171-188 (1973)
63. Sussmann, H.J., Jurdjevic, V.: Controllability of non-linear systems. J Differential Equations **12**, 95-116 (1972)
64. Takagi, D.: Swimming with stiff legs at low Reynolds number. Submitted (2015)
65. Zakaljukin, V.M.: Lagrangian and Legendre singularities. Funkcional. Anal. i Priložen. **10**, 26–36 (1976)
66. Zhitomirskiĭ, M.: Typical singularities of differential 1-forms and Pfaffian equations. American Mathematical Society, Providence, RI. **113**, 176 (1992)